

**Master of Sciences in Bioengineering**

***Immobilization of Peroxidase on Functionalized  
Carbon Nanotubes for Synthesis of Biocatalysts  
with High Performance***

**Master's Thesis**

by

**Renato Alexandre Moreira Azevedo**

**Dissertation for Master degree in Biological Engineering**

performed in

**Associate Laboratory LSRE-LCM,  
Department of Chemical Engineering  
Faculdade de Engenharia, Universidade do Porto**



**Supervisors: Dr<sup>a</sup>. Ana Paula Tavares and**

**Dr<sup>a</sup>. Cláudia Gomes Silva**



**Universidade do Porto  
Faculdade de Engenharia  
FEUP**

**July, 2014**







## Declaration

It is declared on oath that this work is original and that all non-original contributions have been properly referenced with the identification of the source.

---

*Renato Alexandre Moreira Azevedo*

DEPARTMENT OF CHEMICAL ENGINEERING

Tel. +351-22-508 1884

Fax +351-22 508 1449

***Published by***

FACULTY OF ENGINEERING OF THE UNIVERSITY OF PORTO

Rua Dr. Roberto Frias

4200-465 PORTO

Portugal

Tel. +351-22-508 1400

Fax +351-22-508 1440

feup@fe.up.pt

<http://www.fe.up.pt>

***Author's information:***

Renato Alexandre Moreira Azevedo

200905207

[bio09083@fe.up.pt](mailto:bio09083@fe.up.pt)

---

*This page intentionally left empty*

---

*“The only source of knowledge is experience.”*

*Albert Einstein*

---

*This page intentionally left empty*

---



## **Acknowledgements**

A project results invariably of a conjoined set of efforts. The present work fits this rule. Although this is a document for which I assume total responsibility, the reality is that its merit is not entirely mine. I, therefore, dedicate this first segment to those that, in a way or another, have fostered my academic growth and have guided me in this master thesis.

Firstly, the continuous guidance of my supervisors, Dr<sup>a</sup>. Ana Paula Tavares and Dr<sup>a</sup>. Cláudia Gomes Silva must be highlighted. Their knowledge, experience and motivation made this work possible.

Evidently, my close relatives, friends and girlfriend were, likewise, an import pillar. I could always count with their unconditional support, without which this project couldn't be done.

---

*This page intentionally left empty*

---

## **Abstract**

Carbon nanotubes (CNTs) have been used in nanotechnology field to create new functional nanostructures, due to its exceptional mechanical, electrical and chemical properties. Consequently, there is now an increasing interest in understanding and controlling the interactions of this nanomaterial with biological molecules, such as enzymes. Peroxidases have been attached in CNTs for various applications, such as sensing, drug delivery and biocatalysis. However, very few studies have elucidated the influence of the nanoscale environment on the structure and function of this enzyme. This present work describes the effect of multi-walled carbon nanotubes (MWCNTs) surface functionalization through oxidation and selective removal of O<sub>2</sub>-containing surface groups at different temperatures, on the immobilization efficiency, catalytic activity and thermal stability of peroxidase, with the overall goal of design optimized MWCNT-Perox conjugates for applications to biocatalysis.

The oxidation treatment increases the pore volume and diameter of MWCNTs and also introduces carboxylic acid, anhydride, lactone and quinone groups on the MWCNTs surface, which was confirmed through characterization tests. Electrostatic interactions and hydrogen bonding are the main mechanisms involved in the immobilization process. In an identical mode, for the MWCNTox-400, which mainly presents hydroxyl surface groups, peroxidase is immobilized by the formation of hydrogen bonds between OH groups at the surface of the MWCNTs and peroxidase's amine terminal groups and, thus, it is thermally more stable when it is immobilized on this support. The optimal conditions for commercial peroxidase immobilization on MWCNTs are acidic pH (4.5), peroxidase concentration of 8  $\mu\text{L}/\text{mL}_{\text{buffer}}$  and contact time of 30 min. Peroxidase was completely adsorbed on purified MWCNTs with an immobilization yield of 100%, where hydrophobic interactions between the support and the enzyme are the main driving forces. The highest enzymatic activity value obtained was 327.4  $\text{U}\cdot\text{g}^{-1}$ , at pH 6, for a MWCNTs treated at 900 °C. This immobilization process increases the storage stability of peroxidase and protects it to the thermal denaturation, with a  $t_{1/2}$  4.5 times higher than the free form; however it decreases the affinity of peroxidase with the substrate. Additionally, magnetic nanoparticles constituted by magnetite (Fe<sub>3</sub>O<sub>4</sub>) were successfully covalently attached on MWCNTs surface. By immobilizing peroxidase onto the magnetic MWCNTs, it was demonstrated its recovery by a magnet, and subsequently reuse of the mMWCNT-peroxidase complex several times. Regarding the biocatalyst application, peroxidase was used for dye discoloration, in both free and immobilized form; however, further testing to optimize the reaction conditions is needed. It has been demonstrated that MWCNTs have an outstanding affinity to adsorb peroxidase, which makes them excellent supports for the immobilization of this enzyme and constitutes a great advantage for industrial applications

---

## Graphical Abstract

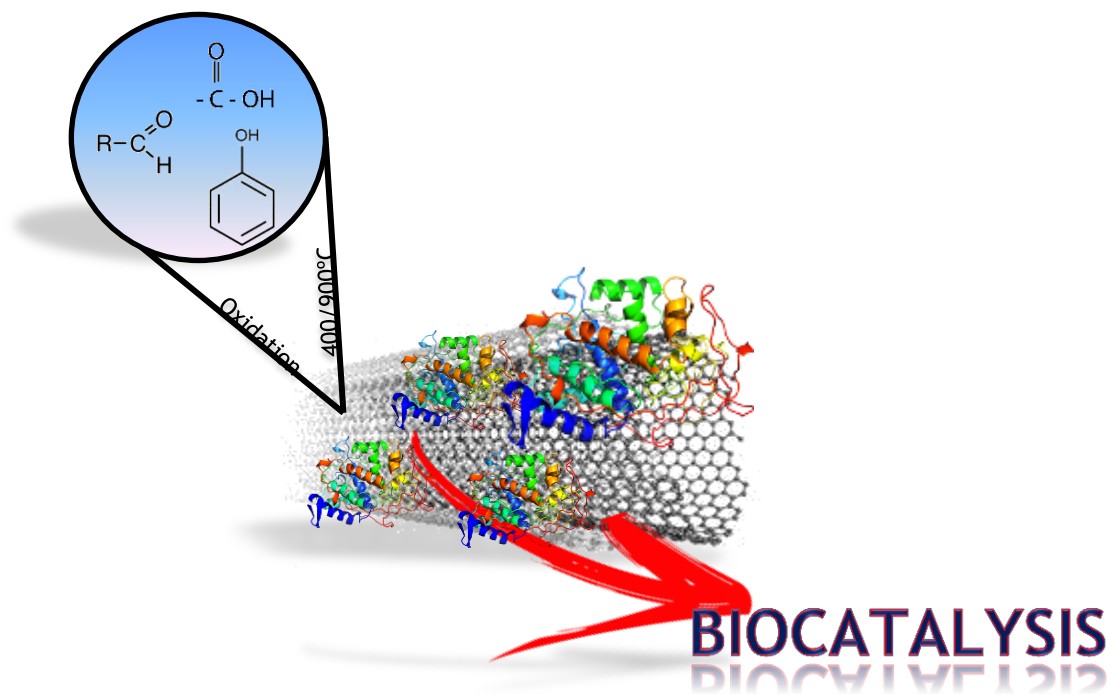


# Table of Contents

Table of Contents.....	i
Figures List.....	iii
Tables List.....	v
Glossary.....	vi
<b>1 Introduction.....</b>	<b>1</b>
1.1 Background and Project Presentation .....	1
1.2 Main Objectives .....	2
1.3 Thesis organization .....	3
<b>2 Literature Review .....</b>	<b>5</b>
2.1 Carbon Nanotubes .....	5
2.2 Enzyme Immobilization .....	12
2.2.1 General overview .....	12
2.2.2 Immobilization Methods.....	16
2.3 Peroxidase: origin, structure, function and applications .....	18
2.3.1 Immobilization of Peroxidase on Carbon Nanotubes.....	23
<b>3 Experimental Section .....</b>	<b>25</b>
3.1 Materials and Chemicals .....	25
3.2 Functionalization of MWCNT.....	25
3.3 Production of magnetic MWCNT.....	25
3.4 Characterization of MWCNT.....	27
3.5 Immobilization Technique.....	28
3.6 Enzymatic activity measurement .....	29
3.7 Optimization of the conditions for peroxidase immobilization on MWCNT .....	29
3.8 Thermal stability of free and immobilized peroxidase .....	30
3.9 Determination of kinetic parameters of free and immobilized peroxidase .....	31
3.10 Storage and operational stability of immobilized peroxidase .....	32

3.11	Protein determination .....	32
3.12	Gel electrophoresis.....	32
3.13	Discoloration of textile dyes.....	33
4	Results and Discussion .....	35
4.1	Characterization of MWCNT.....	35
4.1.1	N <sub>2</sub> adsorption-desorption isotherms .....	35
4.1.2	Temperature programmed desorption (TPD).....	36
4.1.3	Fourier transform infrared (FTIR).....	38
4.1.4	Scanning electron microscope (SEM) .....	39
4.1.5	X-ray diffraction (XDR).....	39
4.1.6	Transmission electron microscopy (TEM) .....	39
4.2	Optimization of peroxidase immobilization on MWCNTs .....	40
4.3	Effect of MWCNT surface chemistry on peroxidase immobilization.....	41
4.4	Thermal stability of free and immobilized peroxidase .....	46
4.5	Kinetic parameters of free and immobilized peroxidase.....	51
4.6	Storage and operational stability of immobilized peroxidase .....	53
4.7	Discoloration of textile dyes.....	56
5	Concluding remarks and research needs .....	59
5.1	General conclusions .....	59
5.2	Perspectives for further research .....	61
5.3	Final appreciation .....	62
6	References .....	63
	Appendix 1 .....	77

## Figures List

Fig. 1 - Molecular representation of MWCNT left and SWCNT right .....	5
Fig. 2 - Strategies for covalent functionalization of CNTs (A) direct sidewall functionalization; (B) defect functionalization .....	9
Fig. 3 - Classification of immobilization methods.....	16
Fig. 4 - Enzyme immobilization strategies: entrapment (a), encapsulation (b), support based (c) and self immobilization (d). Enzymes are represented by green circles .....	16
Fig. 5 - Peroxidase classes .....	19
Fig. 6 - Conserved amino acid residues of different origin peroxidases .....	21
Fig. 7 - Crystal structure of the CN-bound form of <i>Arthromyces ramosus</i> peroxidase at 1.3 Angstroms resolution .....	22
Fig. 8 - Scheme of enzyme immobilization on functionalize CNTs through covalent linking.....	24
Fig. 9 - Covalent attachment of magnetite nanoparticles (MNPs) on the carbon nanotube (MWCNT) surface to form MWCNT-MNP nanohybrids. ....	27
Fig. 10 - CO <sub>2</sub> (a) and CO (b) TPD profiles of pristine and functionalized MWCNTs.....	37
Fig. 11 - Enzymatic activity registered in the catalysis using MWCNT with immobilized peroxidase when immobilization was performed with peroxidase solutions of different concentrations (a) and for different periods of contact time (b).....	41
Fig. 12 - Immobilized peroxidase activity on treated MWCNTs at different pH values .....	42
Fig. 13 - Thermal inactivation of (a) free peroxidase and (b) immobilized on MWCNTox-400.....	47
Fig. 14 - Michaelis-Menten plot for peroxidase catalysis. Effect of substrate concentration on the initial rate of oxidation of ABTS catalyzed by (a) free peroxidase and (b) MWCNT-peroxidase. ....	52
Fig. 15 - Storage stability of the free (dashed line) and immobilized (solid line) peroxidase by physical adsorption at 4 °C over 40 days. ....	54
Fig. 16 - Reusability of complex mMWCNT-Peroxidase .....	55
<u>Appendix</u>	
Fig. A1 - Nitrogen adsorption-desorption isotherm of obtained samples. ....	78
Fig. A2 - Schematic representation of the main chemical features in a graphene sheet, whit its typical surface functionalities .....	79
Fig. A3 - FTIR-ATR spectra of MWCNT, MWCNTox, MWCNTox-400 and MWCNTox-900, before (dash line) and after peroxidase immobilization (solid line).....	81
Fig. A4 - SEM images of peroxidase adsorbed in MWCNTox-900 on different resolution. ....	82

*Fig. A5 - XRD diffractogram of magnetite (Fe<sub>3</sub>O<sub>4</sub>) and CNT-Fe<sub>3</sub>O<sub>4</sub> hybrid materials. .... 83*

*Fig. A6 - mMWCNT attracted by a simple magnet..... 84*

*Fig. A7 - TEM images of Fe<sub>3</sub>O<sub>4</sub> (a) and mMWCNTs (b, c and d). .... 85*

*Fig. A8 - Arrhenius plot for free and immobilized peroxidase on MWCNTox-400. .... 87*

*Fig. A9 - Thermal deactivation of free peroxidase and immobilized on purified and functionalized MWCNT at 40 °C ..... 88*

*Fig. A10 - Thermal deactivation of free and immobilized peroxidase on purified and functionalized MWCNT at 50 °C ..... 89*

*Fig. A11 - Effect of H<sub>2</sub>O<sub>2</sub> concentration on the initial rate of oxidation of ABTS (0.4 mM) catalyzed by free peroxidase ..... 90*

*Fig. A12 - Lineweaver-Burk representation of free peroxidase..... 91*

*Fig. A13 - Lineweaver-Burk representation of immobilized peroxidase ..... 91*

*Fig. A14 - Reusability of peroxidase immobilized on MWCNTox-400 ..... 93*

*Fig. A15 - Reusability of peroxidase immobilized on a MWCNTs membrane ..... 93*

*Fig. A16 - Standard curves for Bradford protein assay ..... 98*

*Fig. A17 - Isoelectric point focusing. Lac (Laccase), Std. (Standard) and Perox (Peroxidase), pH 4-6. .... 100*

*Fig. A18 - SDS-Page image for peroxidase (~31 kDa) and for laccase (~80 kDa) ..... 103*



## Tables List

<i>Table 1 - A summary of the major CNTs production methods and their efficiency.....</i>	<i>6</i>
<i>Table 2 - Application of enzymes immobilized on carbon nanotubes.....</i>	<i>11</i>
<i>Table 3 - Technological properties of immobilized enzyme systems .....</i>	<i>13</i>
<i>Table 4 - Classification of supports .....</i>	<i>14</i>
<i>Table 5 - Selected characteristic parameters of immobilized enzymes.....</i>	<i>15</i>
<i>Table 6 - Molecular properties of a fungal peroxidase ARP .....</i>	<i>20</i>
<i>Table 7 - Specific surface area <math>S_{BET}</math>, pore volume <math>V_p</math> and pore diameter <math>d_p</math> for the different MWCNT samples.....</i>	<i>35</i>
<i>Table 8 - Peroxidase immobilization yield on the MWCNT materials for the different pH .....</i>	<i>44</i>
<i>Table 9 - Recovered activity of the immobilization process for the different pH of the medium used to perform immobilization.....</i>	<i>44</i>
<i>Table 10 - Thermal parameters and thermal stabilities obtained for the thermal inactivation of free and immobilized peroxidase.....</i>	<i>48</i>
<i>Table 11 - Thermal parameters (50 °C) for free and immobilized peroxidase on purified and functionalized MWCNT .....</i>	<i>50</i>
<i>Table 12 - Kinetic parameters of ABTS oxidation for free and immobilized peroxidase on purified MWCNTs .....</i>	<i>53</i>
<i>Table 13 - Dye discoloration % of RB5, RB and BR by free and immobilized peroxidase on mMWCNTs .</i>	<i>56</i>
<u>Appendix</u>	
<i>Table A1 - Desorption temperature of oxygen functional groups in carbon materials.....</i>	<i>79</i>
<i>Table A2 - Characterization of <math>Fe_3O_4</math> and CNT-<math>Fe_3O_4</math> hybrid material.....</i>	<i>83</i>
<i>Table A3 - Summary table for test at pH range 4.5-9 .....</i>	<i>86</i>
<i>Table A4 - Thermal parameters (40 °C) for free and immobilized peroxidase on purified and functionalized MWCNT .....</i>	<i>88</i>
<i>Table A5 - Comparison of Michaelis-Menten parameters obtained for free peroxidase .....</i>	<i>91</i>
<i>Table A6 - Comparison of Michaelis-Menten parameters obtained for immobilized peroxidase .....</i>	<i>92</i>
<i>Table A7 - Properties of Reactive Black 5 .....</i>	<i>94</i>
<i>Table A8 - Properties of Reactive Blue 4.....</i>	<i>95</i>
<i>Table A9 - Properties of Bromophenol Blue .....</i>	<i>96</i>
<i>Table A10 - Protein quantification for the immobilization process .....</i>	<i>99</i>

# Glossary

## Abbreviations

ABTS	2,2'-azino-bis(3-ethylbenzathiazoline-6-sulfonic) acid
AMG	Amyloglucosidase
APTS	(3-Aminopropyl)triethoxysilane
APX	Pea ascorbate peroxidase
Arg	Arginine
ARP	<i>Arthromyces ramosus</i> peroxidase
BAP	Lignin peroxidase from <i>Bjerkandera adusta</i>
BCA	Bicinchoninic acid
BET	Brunauer-Emmett-Teller
BJH	Barrett-Joyner-Halenda
BR	Bromophenol Blue
CcP	Cytochrome-c peroxidase
CD	Circular dichroism spectroscopy
CFX	Ciprofloxacin
CNT	Carbon nanotube
Cys	Cysteine
EDC	N-ethyl-N'-(3-dimethylaminopropyl)carbodiimide hydrochloride
ELISA	Enzyme-linked immunosorbent assay
FTIR	Fourier transform infrared
His	Histidine
HRP	Horseradish peroxidase
LiP	Lignin peroxidase
MnP	Manganese peroxidase
MNP	Magnetite nanoparticle
MWCNT	Multi-walled carbon nanotube
NHS	N-hydroxysuccinimide
PCP	Lignin peroxidase of <i>P. chrysosporium</i>
pI	Isoelectric point
RB	Reactive blue 4
RB5	Reactive black 5
Rz	Reinheitszahl value
SBP	Soybean peroxidase
SDS	Sodium dodecyl sulfate

SDS-PAGE	Sodium dodecyl sulfate polyacrylamide gel electrophoresis
SEM	Scanning electron microscope
SWCNT	Single-walled carbon nanotube
TEM	Transmission electron microscopy
TH	Thionine
THF	Tetrahydrofuran
TPD	Temperature programmed desorption
UV	Ultraviolet
XRD	X-ray diffraction
<i>S</i>	Substrate

### Variables

$D_p$	Pore diameter	nm
$K_M$	Michaelis-Menten constant	mM
$S_{BET}$	Specific surface area	$m^2 \cdot g^{-1}$
$V_p$	Pore volume	$cm^3 \cdot g^{-1}$
$pH_{PZC}$	pH value at the point of zero charge	
$v_{max}$	Maximum rate of the reaction	$mM \cdot min^{-1}$
Abs	Absorbance	$m^2$
$E_a$	Arrhenius activation energy	$kJ \cdot mol^{-1}$
$h$	Planck constant	J.h
$k$	Thermal inactivation rate constant	$h^{-1}$
$K$	Boltzmann constant	$J \cdot K^{-1}$
$t_{1/2}$	Half-life time	h
$\alpha$	Ratio of specific activity	
$\epsilon$	Molar extinction coefficient	$M^{-1} \cdot cm^{-1}$
$v$	Catalytic reaction rate	$mM \cdot min^{-1}$
$\Delta G$	Standard free energy for the thermal inactivation	$J \cdot mol^{-1}$
$\Delta H$	Activation enthalpy	$kJ \cdot mol^{-1}$
$\Delta S$	Activation entropy	$kJ \cdot mol^{-1}$



# 1 Introduction

## 1.1 Background and Project Presentation

Nanotechnology is the ability to understand, create, and use material structures devices and systems with fundamentally new properties and functions at the atomic, molecular, and supramolecular levels (Drexler, 1996). In addition to physical and chemical sciences, one of the most interesting objectives of nanotechnology might be described by the ability to assemble biological molecules into nanostructured materials, i.e., the relationship with biology field. The ability to understand the structure and function of biological systems at the nanoscale, along with the controlled production (geometries, dimensions, surface properties) of nanomaterials, has led to a new field: nanobiotechnology. It is defined as the application of the tools and techniques developed by nanotechnology to understand and transform biosystems and which uses biological principles and materials to create new functional nanostructures (Roco, 2003). Thus, there is now an increasing interest in understanding and controlling the interactions of nanomaterials with biological molecules, such as proteins

With unique chemical, electronic, mechanical and biocompatibility properties (Balasubramanian, 2006), carbon nanotubes (CNTs) have been extensively investigated for various applications during the last decade, especially in biomedical imaging, drug delivery, biosensing, biocatalyst and in the design of functional nanocomposites. These robust nanoscaffolds have an inherently large surface area, which leads to high enzyme loading and consequently high enzyme activity (Silva et al., 2014).

In general, free enzymes are less stable and prone to denaturation in extreme conditions of pH, temperature and organic solvents. To improve their stability, enzymes have generally been immobilized on a solid carrier, which is expected to enhance catalytic stability, selectivity and reusability of the enzymes. The most used strategies for enzyme immobilization on CNTs described in the literature include adsorption and covalent bonding. Adsorption is a relatively simple method as it is a chemical free enzyme binding process. However, leaching of the enzyme from the immobilized enzyme preparation after a certain number of reuses has limited its application at a commercial scale. On the other hand, covalent binding methods produce relatively stable immobilized enzyme preparations with more reusability as compared to the physical adsorption method. Therefore, the investigation on the structure and function of enzymes immobilized on CNTs is fundamental in order to understand the interactions between the enzyme and the support, with the aim at developing very stable biocatalysts. Additionally, CNTs offer the possibility of being functionalized, thus modifying their properties and improving their efficiency as supports or catalysts.

The surface functionalization of nanomaterials involves grafting of desirable functional groups onto their surface to obtain nanomaterials with desired properties (Shim et al., 2002). This functionalization can change their dispersibility and interactions with enzymes and consequently affect the catalytic activity of the immobilized enzyme. It has been demonstrated that biological and bioactive species such as proteins, carbohydrates and nucleic acids can be conjugated with carbon nanotubes, either by covalent and noncovalent conjugations (Thordarson et al., 2006; Wei et al., 2007). It is important to study the behavior of the immobilized enzyme under different conditions, such as pH, temperature and enzyme concentration. Investigating the structure and function of enzymes immobilized on nanomaterials will be crucial for developing a better understanding of enzyme-nanomaterial interactions, as well as for designing functional protein-nanomaterial conjugates.

Peroxidases are attractive and industrially relevant enzymes that belong to the group of oxidoreductases which catalyse the reduction of peroxides to form water and the oxidation of a variety of organic and inorganic compounds (Johannes Everse et al., 1990). Peroxidase has been immobilized on CNTs through adsorption or covalent bonding for various applications, such as bioelectrochemical sensor, fuel cells, glucose and H<sub>2</sub>O<sub>2</sub> biosensor and, as in this work, the use in biocatalysts. However, information about the relationship between surface properties of this type of supports and its immobilization capacity and thermal stability have been to the date scarcely explored.

## **1.2 Main Objectives**

All biological systems have the first level of organization at the nanoscale where their fundamental properties and functions are defined. A variety of enzymes, including peroxidases, have been attached to a suite of nanomaterials, in particular carbon nanotubes, for various applications, such as sensing, drug delivery and biocatalysis. However, very few studies have elucidated the influence of the nanoscale environment on structure and function of this enzyme. This present work describes the effect of MWCNTs surface functionalization through oxidation and selective removal of oxygen-containing surface groups at different temperatures, on the immobilization efficiency, catalytic activity and thermal stability of peroxidase, with the main goal to design optimal MWCNT-peroxidase conjugates for applications relevant to biocatalysis. Therefore, the objectives of this work are:

- To produce and to characterize functionalized MWCNTs through selectively introduction or removing of oxygen containing groups.
- To evaluate the structure, function, and stability of peroxidase on different MWCNTs with the overall aim of synthesis of biocatalysts with high performance.

- To study the biocatalytic capacity of free and immobilized peroxidase for degradation of textile dyes.

### **1.3 Thesis organization**

This thesis work is divided into 7 chapters, with the last two being the chapter of references and appendix, respectively.

Chapter 1 describes the main goals of this work, background and motivations for its developments. It serves as a guideline to the overall work presented in the further chapters.

In Chapter 2 a brief review of the literature is provided, situating the work within the context of existing published reports. This chapter is divided into three parts: in the first one, a theoretical introduction to carbon nanotubes is made, referring its main features and advantages as well as production methods. The different functionalization techniques are also discussed, ending with the various applications of enzyme immobilization on this material. Continuing, in the second part, a general overview of enzyme immobilization is made. Their advantages and disadvantages and immobilization techniques are presented as well as the importance of the enzyme-carrier relationship. The last part is related to the enzyme used in this work peroxidase. Information about its structure and composition as well as its properties and potential applications are described. Finally, a revision of literature on immobilization of peroxidase on carbon nanotubes is presented.

Chapter 3 refers to materials and methods of experimental work of this thesis. The first part focuses on the production and characterization of the CNTs used. The second part presents the methodology used for the immobilization of peroxidase and for all tests associated with MWCNT-peroxidase conjugates. At the end, this complex was applied to degradation of dyes.

In chapter 4, a presentation of results with discussion is made, following the same pattern of the previous chapter. Firstly, the changes on the surface of carbon nanotubes caused by oxidation and thermal treatment were discussed, as well as the possibility of CNT magnetization. The effect of functionalization on the immobilization of peroxidase was evaluated by comparing the results of activity and immobilization yield. After analyzing the optimal immobilization conditions, the stability and kinetic constants of the immobilized enzyme with the enzyme in its free state is compared. Finally, the discoloration yield of 3 textile dyes was assessed using free and immobilized peroxidase.

Finally, chapter 5 gives an overview of the work presented, describing the main conclusions and showing proposals for future research with the possible limitations or possibilities for further studies.





## 2 Literature Review

### 2.1 Carbon Nanotubes

Among the huge amount of nanomaterials, carbon nanotubes (CNTs), discovered in 1991 by Iijima (Iijima, 1991) have been extensively investigated for various applications during the last decade owing to their unique chemical, electronic and mechanical properties (Balasubramanian and Burghard, 2005; Gong K.P., 2005; Trojanowicz, 2006). CNTs consist of graphitic sheets rolled up into a cylindrical shape with lengths in the micrometers range, and diameters up to 100 nm (Aqel et al., 2012). CNTs can be classified in terms of the number of walls as multi-walled carbon nanotubes (MWCNT) and single-walled carbon nanotubes (SWCNT). MWCNT is comprised of several layers of graphite surrounding a central tubule, whereas a SWCNT only has the central graphitic tubule.

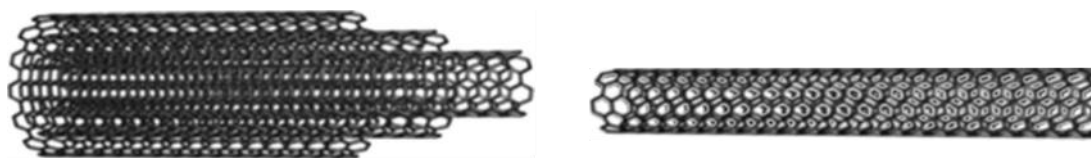


*Fig. 1 - Molecular representation of MWCNT left and SWCNT right (Saifuddin et al., 2013)*

These two types of CNTs have been used to immobilize enzymes. SWCNTs are attractive for their higher surface area for enzyme interaction, but MWCNTs are desirable for their easier dispersibility and lower cost.

Referring to their properties, carbon nanotubes generally have a large length-to-diameter aspect ratio of about 1000, so they can be considered as nearly one-dimensional structures (Dresselhaus et al., 2004). The strength of the  $sp^2$  carbon-carbon bonds gives carbon nanotubes amazing mechanical properties. Their densities can be as low as  $1.3 \text{ g.cm}^{-3}$  one-sixth of that of stainless steel (Saifuddin et al., 2013). CNTs Young's moduli are superior to all carbon fibers with values greater than 1 TPa which is approximately 5x higher than steel (Yu et al., 2000). The highest measured tensile strength was up to 63 GPa which is around 50 times higher than steel (Yu et al., 2000). Besides that, CNTs have good chemical and environmental stability and high thermal conductivity ( $3000 \text{ W.m}^{-1}.\text{K}^{-1}$ ).

High-quality carbon nanotube materials are desired for both fundamental and technological applications. However there are four main challenges regarding synthesis of CNT: i) mass production, that is, the development of low-cost and large-scale processes; ii) selective production, that is, control over the structure and electronic properties; iii) organization, that is, control over location and orientation of the produced nanotubes on a flat substrate;

and iv) mechanism, that is, the development of a thorough understating of the processes of nanotube growth (Saifuddin et al., 2013).

Three methods are commonly used to synthesize CNTs: arc discharge (Journet et al., 1997), laser ablation (Thess et al., 1996) and chemical vapor deposition (Kong et al., 1998; Fan et al., 1999; Bower et al., 2000). The basic elements for the formation of nanotubes are a catalyst, a source of carbon and sufficient energy electricity, heat or high-intensity light. In Table 1, a short summary of the three most common techniques used is given.

*Table 1 - A summary of the major CNTs production methods and their efficiency (Joselevich et al., 2008)*

Method	Arc discharge	Laser ablation	Chemical vapour deposition
<b>Process</b>	Connect two graphite rods to a power supply, place the a few millimeters apart. At 100 amps, carbon vaporizes and forms hot plasma	Blast graphite with intense laser pulses; use the laser pulses rather than electricity to generate carbon gas from which the CNTs form; try various conditions until hit on one that produces prodigious amounts of SWNTs	Place substrate in oven, heat to high temperature, and slowly add a carbon-bearing gas such as methane. As gas decomposes it frees up carbon atoms which recombine in the form of NTs
<b>Condition</b>	Low-pressure inert gas Helium	Argon or Nitrogen gas at 500 Torr	High temperatures within 500 to 1000 °C at atmospheric pressure
<b>Typical yield</b>	30-90%	Up to 70%	20-100%
<b>SWCNT</b>	Short tubes with diameters of 0.6-1.4 nm	Long bundles of tubes 5-20 microns, with individual diameter from 1-2 nm	Long tubes with diameters ranging from 0.6 to 4 nm
<b>MWCNT</b>	Short tubes with inner diameter of 1-3 nm and outer diameter of approximately 10 nm	Not very much interest in this technique, as it is too expensive, but MWCNT synthesis is possible	Long tubes with diameter ranging from 10 to 240 nm

<b>Carbon source</b>	Pure graphite	Graphite	Fossil-based hydrocarbon and botanical hydrocarbon
<b>Cost</b>	High	High	Low
<b>Advantage</b>	Can easily produce SWCNT, MWCNTs. SWCNTs have few structural defects; MWCNTs without catalyst, not too expensive, open air synthesis possible	Good quality, higher yield, and narrower distribution of SWCNT than arc-discharge	Easiest to scale up to industrial production; long length, simple process, SWCNT diameter controllable, and quite pure
<b>Disadvantage</b>	Tubes tend to be short with random sizes and directions often needs a lot of purification	Costly technique, because it requires expensive lasers and high power requirement, but is improving	Often riddled with defects

Beyond the different techniques, it appears immediately clear that CNTs need processing after their synthesis. To address this issue, purification methods and, above all, functionalization approaches are essential to allow manipulation and further application of this material. Usually, metal nanoparticles and amorphous carbon are present as a synthetic residue. In general, CNTs are a fluffy powder difficult to manage, while chemical functionalization contributes to prepare more homogenous and soluble material (Toma, 2009). Moreover, beyond their interesting size, shape, structure, electrical and mechanical properties, CNTs may have, with all atoms exposed on the surface, ultrahigh surface area ( $1300 \text{ m}^2.\text{g}^{-1}$ ) that permits efficient loading of multiple molecules along the length of the nanotube sidewall. These carbon atoms on CNT walls are chemically stable because of the aromatic nature of the bond. As a result, the reinforcing CNTs are inert and can interact with the surrounding matrix mainly through van der Waals interactions, unable to provide an efficient load transfer across the CNT/matrix interface (Ma et al., 2010). Therefore, significant efforts have been made to modify surface properties of CNTs and to understand the reaction mechanisms between the CNTs and functional groups (Hirsch, 2002; Balasubramanian and Burghard, 2005; Tasis et al., 2006; Hirsch and Vostrowsky, 2007). These functionalizations can be chemical or physical, based on interactions between the active

molecules and carbon atoms on the CNTs. Strategies for covalent functionalization of CNTs are summarized in Fig. 2.

While there are many studies relating to the modification of the surface characteristics of CNTs, these processes are not fully optimized. Furthermore, there is some concern about the structural changes resulting from the chemical functionalization and other effects caused, for example, during sonication.

Chemical functionalization can be performed at the termini of the tubes or at their walls. It is based on the covalent linkage of functional entities onto CNTs with a change of hybridization from  $sp^2$  to  $sp^3$  and a simultaneous loss of  $\pi$ -conjugation system on graphene layer (Ma et al., 2010). This process can be made by reaction with some highly reactive. A lot of methods have been employed in recent years, such as, fluorination (Mickelson et al., 1998), carbene and nitrene addition (Chen et al., 1998; Hu et al., 2003; Holzinger et al., 2004), chlorination, bromination (Unger et al., 2002), hydrogenation (Kim et al., 2002), among others Fig. 2A.

Another method for covalent functionalization of CNTs is defect functionalization. This process takes advantage of chemical transformation of defect sites on CNTs, for example, the open ends and/or holes in the sidewalls or oxygenated sites. These defects can be created by an oxidative process with strong acids such as  $HNO_3$  (Silva et al., 2014),  $H_2SO_4$  or a mixture of them (Esumi et al., 1996), or with strong oxidants such as  $KMnO_4$  (Yu et al., 1998) or ozone (Sham and Kim, 2006). These processes leads to the introduction of carboxylic acid, hydroxyl, phenol, carbonyl and quinone groups on the nanotube's surface, changing the hydrophobic nature of CNTs to hydrophilic. These functional groups have rich chemistry and the CNTs can be used as precursors for further chemical reactions, such as silanation (Ma et al., 2006), polymer grafting (Liu et al., 2006), esterification (Hamon et al., 2002), thiolation (Liu et al., 1998), alkylation and arylation (Stephenson et al., 2006) and even some biomolecules (Coleman et al., 2006).

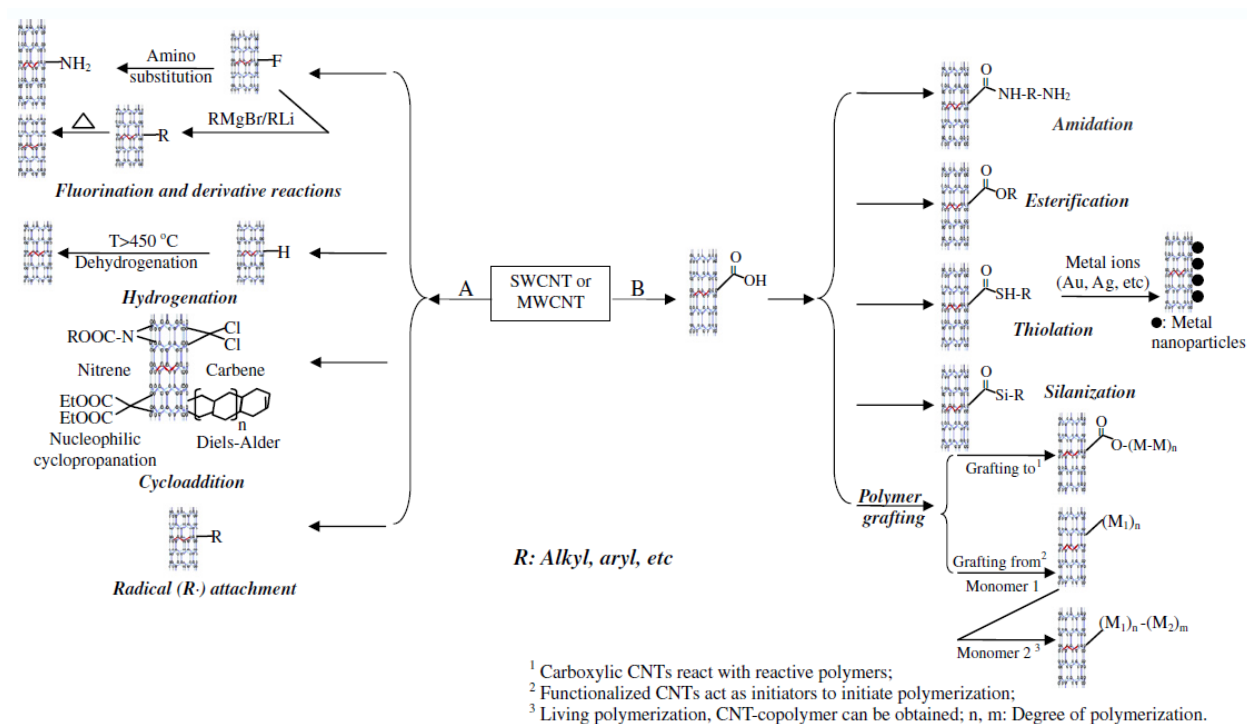


Fig. 2 - Strategies for covalent functionalization of CNTs (A) direct sidewall functionalization; (B) defect functionalization. Adapted from (Ma et al., 2010)

Functionalization of CNTs using covalent methods can provide useful functional groups onto the CNT surface. However, these methods have two major drawbacks. Firstly, during the functionalization reaction, especially along with damaging ultra sonication process, a large number of defects are inevitably created on the CNT sidewalls, and in some extreme cases, CNTs are fragmented into smaller pieces. These damaging effects result in severe degradation in mechanical properties of CNTs as well as disruption of  $\pi$  electron system in nanotubes. Secondly, concentrated acids or strong oxidants are often used for CNT functionalization, which are environmentally unfriendly. Therefore, many efforts have been put forward to developing methods that are convenient to use, of low cost and less damaging to CNT structure.

An alternative method is noncovalent functionalization. In this case, the CNTs surface is modified with polymers, such as polyphenylene vinylene (McCarthy et al., 2001) or polystyrene (Hill et al., 2002). The polymer wrapping process is achieved through the van der Waals interactions and  $\pi$ - $\pi$  stacking between CNTs and polymer chains contain aromatic rings (Ma et al., 2010). Besides polymers, surfactants have also been employed to functionalize CNTs. Several works have been contributed to studying the effects of surfactant on dispersibility and other property of CNTs (Gong et al., 2000; Kim et al., 2007; Yu et al., 2007).

Finally, endohedral method is another noncovalent method which consists on insertion of atoms or molecules at defect sites localized at the ends or on the sidewalls of CNTs, through the capillary effect (Ma et al., 2010). A typical example is the insertion of inorganic nanoparticles (Georgakilas et al., 2007). Furthermore, many studies have been focused on depositing metal or metal oxide nanoparticles on the nanotubes surface (Dresselhaus et al., 2004). Magnetic nanoparticles have received great attention due to their size-dependent magnetic properties (Won et al., 2005; Chu et al., 2006). Magnetite particles are widely studied for their applications in biology and medicine such as enzyme and protein immobilization (Pan et al., 2005), magnetic resonance imaging MRI (Lee et al., 2006), RNA and DNA purification (Yoza et al., 2003), magnetic cell separation and purification (Zhang and Zhang, 2005) and magnetically controlled transport of anticancer drugs (Ito et al., 2005). One of the practical advantages of using magnetite in enzyme immobilization using CNTs as carrier, is to allow easy recovery and reuse of mMWCNT-enzyme conjugates by a simply applying an external magnetic field (Qu et al., 2008). The magnetization of the nanotubes may also be achieved by covalent attachment of magnetite as described by (Xu et al., 2008). They used a pretreatment to form functional groups such as carboxylic, carbonylic and amine groups on the nanotubes surface allowing the covalent attachment of magnetite on CNTs. This strategy may be superior to those with noncovalent ways due to its ability to maintain the electrical and structural properties of CNTs (Xu et al., 2008).

In the same way, small biomolecules, such as proteins, DNA, can also be entrapped in the inner hollow channel of nanotubes by simple adsorption, forming natural nano-test tubes (Tsang et al., 1997). It has been demonstrated that biological and bioactive species such as proteins, carbohydrates and nucleic acids can be conjugated with CNTs, either by covalent and noncovalent conjugations (Thordarson et al., 2006; Wei et al., 2007). The combination of these two materials i.e. CNTs and guest molecules is particularly useful to integrate the properties of the two components in hybrid materials for use in catalysis, energy storage, nanotechnology and molecular scale devices (Georgakilas et al., 2007). It should be noted that, noncovalent attachment preserves the unique properties of both enzymes and CNTs, but the immobilized protein can be gradually lost during the use of the CNT-enzyme complex (Gao and Kyratzis, 2008) and covalent conjugation provides durable attachment, but the enzyme structure may be more disrupted. The main challenge on this type of immobilization is promoting the stable attachment of enzymes while maintaining their activity and function as closely as possible to their native state, so it is important to study the behavior of the immobilized enzyme under different conditions such as, pH, temperature and concentration.

CNTs, by virtue of these advantages, have a lot of potential biotechnological applications, which have captured the imagination of many researchers Table 2.

Table 2 - Application of enzymes immobilized on carbon nanotubes. Adapted from (Saifuddin et al., 2013)

Protein	Carbon nanotube nanomaterials	Application	Reference
<b>B-Glucosidase</b>	MWCNT-COOH	Biocatalysis	(Gómez et al., 2005)
<b><i>Candida rugosa</i> Lipase</b>	MWCNTs or MWCNTs-COOH	Biocatalysis	(Shi et al., 2007)
<b>Horseradish peroxidase</b>	SWCNT/chitosan modified glassy carbon electrode GCE	Bioelectrochemical sensor	(Jiang et al., 2009)
<b><i>Trametes hirsute</i> Laccase</b>	MWCNT modified GCE	Biofuel cells	(Smolander et al., 2008)
<b>Horseradish peroxidase</b>	SWNT/ionic liquid modified GCE	Biofuel cells, biosensors	(Du et al., 2007)
<b><i>Cerrena unicolors</i> Laccase</b>	CNT modified boron-doped diamond electrode	Biofuels cells, biosensors	(Stolarczyk et al., 2008)
<b>Alcohol dehydrogenase</b>	SWCNT/PDDA modified GCE	Ethanol biosensor	(Liu and Cai, 2007)
<b>Glucose oxidase</b>	SWCNT/silica modified GCE	Glucose biosensor	(Ivnitski et al., 2008)
<b>Glucose oxidase, Horseradish peroxidase</b>	MWCNT-toluidine blue/nafion modified GCE	Glucose biosensor	(Jeykumari and Narayanan, 2009)
<b>Cytochrome c</b>	MWCNT/chitosan/ionic liquid modified GCE	H <sub>2</sub> O <sub>2</sub> detector	(Zhang and Zheng, 2008)
<b>Horseradish peroxidase</b>	MWCNT/chitosan/sol-gel modified GCE	H <sub>2</sub> O <sub>2</sub> detector	(Kang et al., 2009)
<b>Cytochrome c</b>	MWCNT/polyamidoamine/chitosan modified GCE	Nitrite biosensor	(Chen et al., 2009)
<b><i>Trametes versicolor</i> Hemoglobin</b>	MWCNT/chitosan	Oxygen biosensor, Biofuel cells	(Liu et al., 2006)

Amyloglucosidase	Magnetic-SWCNTs	Biofuel production	(Goh et al., 2012)
Horseradish peroxidase	Maize-tassel-MWCNTs	Metal ions biosensor	(Moyo et al., 2014)
Horseradish peroxidase	MWCNTs	H <sub>2</sub> O <sub>2</sub> detector	(Yamamoto et al., 2003)
Horseradish peroxidase	MWCNT/alumina-coated silica	H <sub>2</sub> O <sub>2</sub> detector	(Huang and Tsai, 2009)
Laccase	Magnetic-MWCNTs	Catechol biosensor	(Pang et al., 2011)
Laccase	MWCNT-COOH	Laccase-based biocatalysts	(Silva et al., 2014)
<i>Thermomyces lanuginosus</i> lipase	Amino-MWCNTs	Biocatalytic characterization	(Verma et al., 2013)

## 2.2 Enzyme Immobilization

### 2.2.1 General overview

Enzymes can catalyze reactions in different states: as individual molecules in solution, in aggregates with other entities, and as attached to surfaces. The attached—or “immobilized”—state has been of particular interest for technical purposes. The term “immobilized enzymes” refers to “enzymes physically confined or localized in a certain defined region of space with retention of their catalytic activities, and which can be used repeatedly and continuously” (Katchalski-Katzir, 1993). The introduction of immobilized catalysts has, in some cases, greatly improved both the technical performance of the industrial processes and their economy (Table 3).



*Table 3 - Technological properties of immobilized enzyme systems*

<b>Advantages</b>	<b>Disadvantages</b>
Catalyst reuse	Loss or reduction in activity
Easier reactor operation	Diffusional limitation
Easier product separation	Additional cost
Wider choice of reactor	Changes on enzyme properties
Continuous process	Interaction enzyme-substrate
Enzyme stability	No general method of immobilization

During the past decades, immobilized enzyme technology has advanced into an ever-expanding and multidisciplinary field focused on analyzing clinical, industrial, and environmental samples. Enzyme immobilization has been used in various fields such as in medicine diagnosis and treatment of various diseases, antibiotic production, drug metabolism, food industry, biodiesel production, bioremediation, etc. (Khan and Alzohairy, 2010)

The major components of an immobilized enzyme system are the enzyme, the matrix, and the mode of attachment of the enzyme to the matrix. The terms solid phase support, carrier, and matrix are used synonymously.

The choice of the type of support influences the performance of the immobilized enzyme system. Ideal support properties include physical resistance to compression, hydrophilicity, inertness toward enzymes, ease of derivatization, biocompatibility, resistance to microbial attack, and availability at low cost (Brena and Batista-Viera, 2006). Table 4 presents the different types of supports, which can be classified as inorganic and organic according to their chemical composition. The organic supports can be further subdivided into natural and synthetic polymers (Cabral and Kennedy, 1991).

*Table 4 - Classification of supports (Brena and Batista-Viera, 2006)*

Organic
<p>Natural materials</p> <ul style="list-style-type: none"> <li>• Polysaccharides: cellulose, dextrans, agar, agarose, chitin, alginate</li> <li>• Proteins: collagen, albumin</li> <li>• Carbon</li> </ul> <p>Synthetic materials</p> <ul style="list-style-type: none"> <li>• Polystyrene</li> <li>• Other polymers: polyacrylate polymethacrylates, polyacrylamide, polyamides and vinyl</li> </ul>
Inorganic
<p>Natural minerals: bentonite, silica</p> <p>Processed materials: glass nonporous and controlled pore, metals, controlled pore metal oxides</p>

The properties of immobilized enzyme preparations are governed by the properties of both the enzyme and the carrier material. The specific interaction between the latter provides an immobilized enzyme with distinct chemical, biochemical, mechanical and kinetic properties. Among the numerous parameters that have to be taken into account, the most important are outlined in Table 5.

Table 5 - Selected characteristic parameters of immobilized enzymes (Tischer and Wedekind, 1999)

<p><b>Enzyme</b></p>	<p><b>Biochemical properties</b></p> <p>molecular mass, prosthetic groups, functional groups on protein surface, purity inactivating/protective function of impurities</p> <p><b>Enzyme parameters</b></p> <p>specific activity, pH-, temperature profiles, kinetic parameters for activity and inhibition, enzyme stability against pH, temperature, solvents, contaminants, impurities</p>
<p><b>Carrier</b></p>	<p><b>Chemical characteristics</b></p> <p>chemical basis and composition, functional groups, swelling behavior, accessible volume of matrix and pore size, chemical stability of carrier</p> <p><b>Mechanical properties</b></p> <p>mean wet particle diameter, single particle compression behavior, flow resistance for fixed bed application, sedimentation velocity for fluidized bed, abrasion for stirred tanks</p>
<p><b>Immobilized enzyme</b></p>	<p><b>Immobilization method</b></p> <p>bound protein, yield of active enzyme, intrinsic kinetic parameters properties free of mass transfer effects</p> <p><b>Mass transfer effects</b></p> <p>consisting of partitioning different concentrations of solutes inside and outside the catalyst particles, external and internal porous diffusion; this gives the effectiveness in relation to free enzyme determined under appropriate reaction conditions</p> <p><b>Stability</b></p> <p>operational stability expressed as activity decay under working conditions, storage stability</p> <p><b>Performance</b></p> <p>productivity amount of formed product per unit or mass of enzyme enzyme consumption e.g. units kg<sup>-1</sup> product, until half-life</p>

### 2.2.2 Immobilization Methods

Immobilization of macromolecules can be generally defined as a procedure leading to their restricted mobility. A classification of immobilization methods according to different chemical and physical principles is shown in Fig. 3. The most used enzyme immobilization strategies are also outlined in Fig. 4.

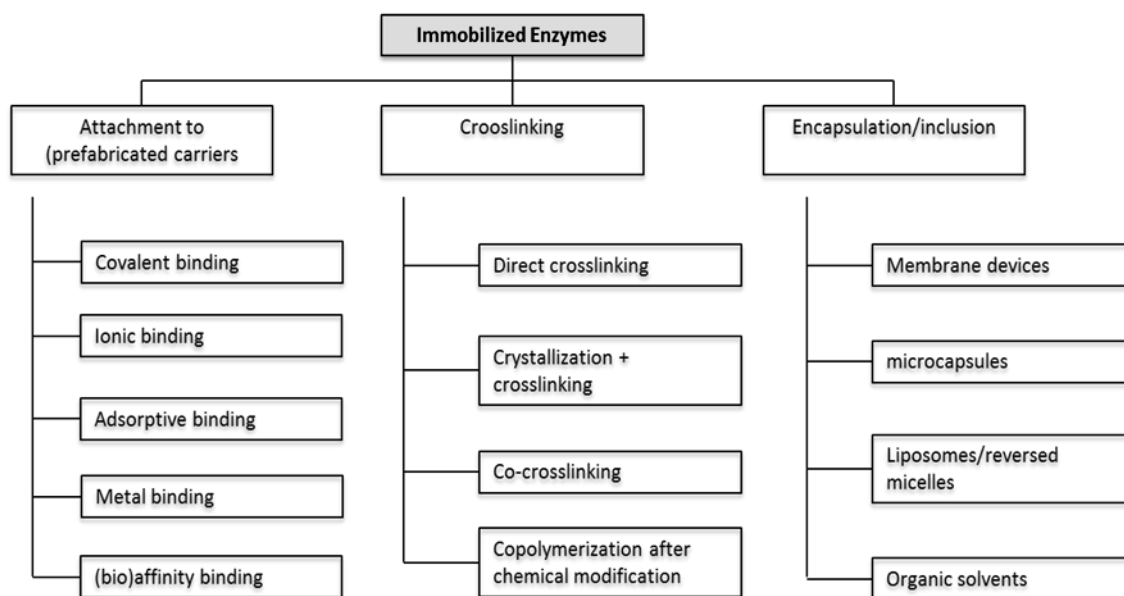


Fig. 3 - Classification of immobilization methods (Tischer and Wedekind, 1999)

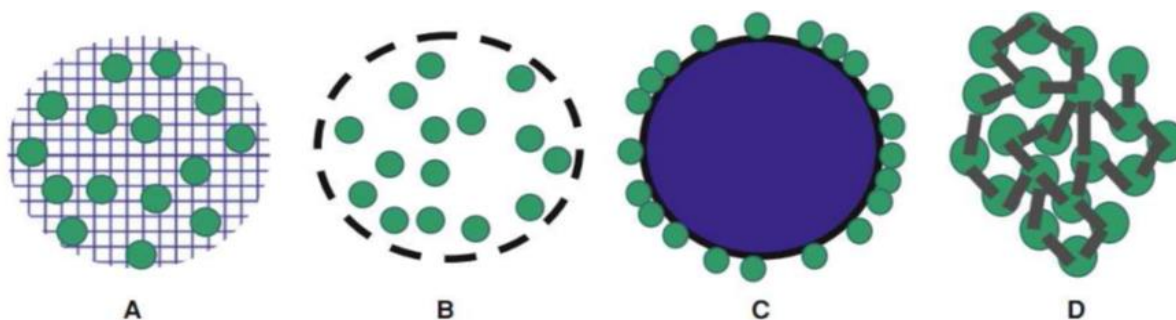


Fig. 4 - Enzyme immobilization strategies: entrapment (a), encapsulation (b), support based (c) and self immobilization (d). Enzymes are represented by green circles (Brady and Jordaan, 2009)

Enzyme entrapment (Fig. 4a) is typically achieved using a polymer network such as an organic polymer or sol-gel and is usually performed in situ. This technique has the advantage of protecting the enzyme thus preventing direct contact with the environment, minimizing the effects of gas bubbles, mechanical shear and hydrophobic solvents. However, it has the disadvantage of mass transfer limitations and low enzyme loading (Lalonde and Margolin, 2008). A common method of entrapment is through use of silica sol-gel matrices formed by

hydrolytic polymerization. Bruns and Tiller, (2004) used this type of immobilization to immobilize horseradish peroxidase and chloroperoxidase in a polymer network. They have obtained an enzyme-complex network suitable for biocatalytic application in organic solvents.

Encapsulation (Fig. 4b) is similar to entrapment. This technique protects the enzyme from the external environment but requires the use of large amounts of substrate, due to mass transfer limitations (Brady and Jordaan, 2009).

Support based immobilization (Fig. 4c) consists on the immobilization of the enzymes on the surface of the different supports. According to the binding mode of the enzyme, the carrier-binding method can be further sub-classified into: physical adsorption; ionic binding and covalent binding (Goel, 1994). In other way, carrier-free enzyme immobilization (Fig. 4d) is possible using bifunctional cross-linkers, such as glutaraldehyde, to bind enzymes to each other without resorting to a support.

Briefly, the physical adsorption mode is based on the adsorption of enzyme on the surface of water-insoluble carriers, mainly through Van der Waals interactions and hydrogen bonding. Hence, the method causes little or no conformational change of the enzyme or destruction of its active center. If a suitable carrier is found, this method can be both simple and cheap. However, it has the disadvantage that the adsorbed enzyme may leak from the carrier during use due to a weak binding force between the enzyme and the carrier (Goel, 1994).

Another way to achieve immobilization at the carrier surface is by ionic binding. This method relies on the ionic binding of the enzyme protein to water-insoluble carriers containing ion-exchange residues. Polysaccharides and synthetic polymers having ion-exchange centers are usually used as carriers. The binding of an enzyme to the carrier is easily carried out, and the conditions are much milder than those needed for the covalent binding method. Hence, the ionic binding method causes little changes in the conformation and the active site of the enzyme. Therefore, this method yields immobilized enzymes with high activity in most cases (Goel, 1994). The main difference between ionic binding and physical adsorption is that the enzyme-to-carrier linkages are much stronger for ionic binding although weaker than in covalent binding

Finally, the covalent binding mode is based on the formation of covalent bonds between the enzyme and the support matrix. The functional groups that may take part in this binding are, for example, amino, carboxylic, phenolic, hydroxyl, etc. The conditions for immobilization by covalent binding are much more complicated and less mild than in the cases of physical adsorption and ionic binding. Therefore, covalent binding may alter the conformational structure and active center of the enzyme, resulting in major loss of activity and/or changes of the enzyme. However, the binding force between enzyme and carrier is so strong that no

leakage of the enzymes occurs, even in the presence of substrate or solution of high ionic strength (Goel, 1994).

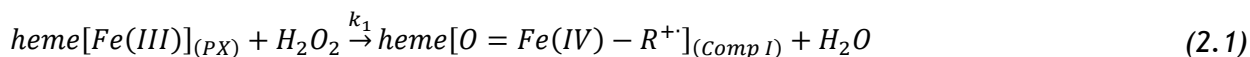
As shown before in Table 5 the choice of the most suitable carrier to perform immobilization is influenced by its chemical properties, mechanical stability and geometric properties. Hereupon, a wide range of synthetic carriers, organic or inorganic, can be created to encounter the optimal characteristics to perform immobilization of the desired enzyme. Thus, currently, there is an increasingly interest on using nano-dimensional materials as a support for the enzymatic immobilization, e.g. nanoparticles, nanofibres and, as used in this study, carbon nanotubes.

## **2.3 Peroxidase: origin, structure, function and applications**

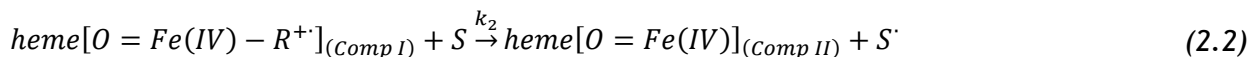
Peroxidase (EC 1.11.1.7) is one of a number of enzymes that act as catalyst to allow a variety of biological processes. Peroxidases are a group of oxidoreductases that catalyze the reduction of peroxides, such as hydrogen peroxide, and the oxidation of a variety of organic and inorganic compounds (Johannes Everse et al., 1990). The term peroxidase represents a group of specific enzymes, such as NADH peroxidase (EC 1.11.1.1), glutathione peroxidase (EC 1.11.1.9), iodide peroxidase (EC 1.11.1.8), among others as well as a group of nonspecific enzymes that are simply known as peroxidases. They had attracted industrial attention because of its usefulness as a catalyst in clinical examinations and other applications.

Peroxides are produced as byproducts of various biochemical reactions within organisms, but can cause damage as they are oxidizing agents. These enzymes break these compounds down in to harmless substances by adding hydrogen, obtained from another molecule – known as a donor molecule – in a reduction-oxidation (redox) reaction in which the peroxide is reduced to form water, and the other molecule is oxidized. There are a large number of peroxidases, and they are found in plants and animals, including humans. Perhaps, the best-known peroxidase is that from horseradish root (HRP) which, due to its broad specificity for hydrogen donors and its high catalytic efficiency, has been used widely in spectrophotometric determinations of biological materials. But currently, fungi (*A. ramosus*, *C. cinereus*) are known as new practical sources of peroxidase for industrial purposes (Shinmen et al., 1986; Morita et al., 1988).

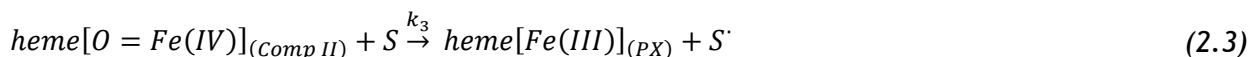
The peroxidase catalytic cycle involves distinct intermediate enzyme forms (Chung et al., 1997; Mantha et al., 2002). In the initial step, the native ferric enzyme is oxidized by hydrogen peroxide to form an unstable intermediate called compound I, which has a hem structure of Fe IV = O-porphyrin  $\pi$ -cation radical, with consequent reduction of peroxide to water (Eq. (2.1)).



Then, Comp I oxidizes electron donor substrate (S) to give compound II, releasing a free radical (S<sup>•</sup>) (Eq. (2.2)). Compounds I and II differ by only one electron on the porphyrin ring.



Comp II is further reduced by a second substrate molecule, regenerating the iron III state and producing another free radical, according to the following equation:



Several peroxidases have been isolated, sequenced and characterized. They have been classified essentially in three classes, depending on the organism: Class I, intracellular prokaryotic peroxidases, Class II extracellular fungal peroxidases and Class III secretory plant peroxidases. It has been proposed, from an extensive comparison among the amino acid sequences, that heme peroxidases from plants, fungi and bacteria are evolutionary related (Welinder, 1992). Production of peroxidase has also been achieved by genetic engineering approaches in *Saccharomyces cerevisiae* (Sawai-Hatanaka et al., 1995) and *Aspergillus oryzae* (Dalboge H. et al., 1992). It can be observed in Fig. 5 the main peroxidases superfamilies.

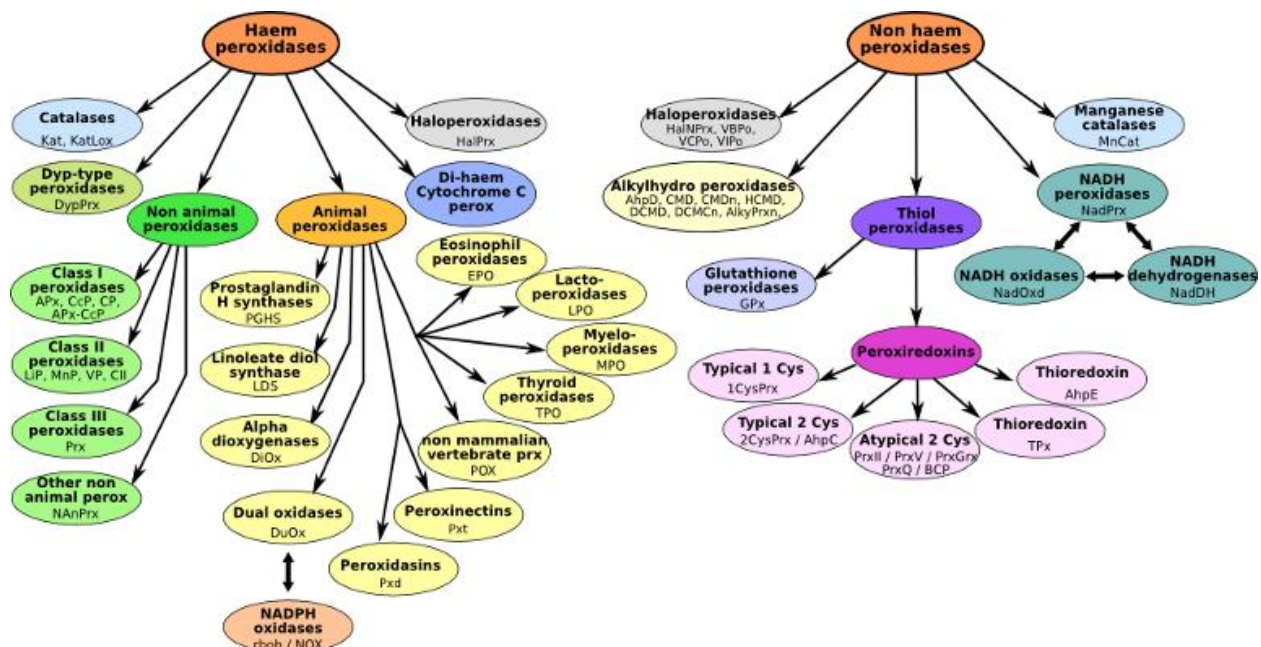


Fig. 5 - Peroxidase classes (Fawal et al., 2013)

In humans, and other mammals, a group of these enzymes called glutathiones, which contain the element selenium, are found both within and outside cells (Maier, 2014). Some of these catalyze reactions involving H<sub>2</sub>O<sub>2</sub>, while others use peroxide compounds of lipids fats and oils. Their main role seems to be to remove these potentially harmful oxidizing agents.

Peroxidases in the saliva also enable redox reactions between H<sub>2</sub>O<sub>2</sub> and chemicals called thiocyanates, producing compounds that can kill potentially harmful microorganisms (Maier, 2014). Thyroid peroxidase releases iodine from nutrients to form essential thyroid hormones.

Like all enzymes, peroxidases are very large complex molecules with complicated shapes involving multiple folds. They come in a variety of types, some of which can use a wide variety of donor molecules and reduce a wide range of peroxides, and some of which are much more specific. Enzymes have an “active site,” which is the part of the molecule where the reaction takes place. This may be in an easily accessible part of the molecule, or it may be tucked away in a fold, where it can only be reached by a molecule of exactly the right shape. Fungal peroxidase is an example of an enzyme that can use a wide variety of donor molecules and peroxides. Molecular properties of the purified *Arthromyces ramosus* peroxidase (ARP) are summarized in Table 6.

*Table 6 - Molecular properties of a fungal peroxidase ARP (Nakayama and Amachi, 1999)*

Molecular weight (Da)	41,000 (Shinmen et al., 1986); 38,000 SDS-PAGE (Welinder and Gajhede, 1993)
Number of subunits	1 (Shinmen et al., 1986)
Amino acids/subunit	344 <sup>a,b</sup> (Kunishima et al., 1994)
Disulfide bonds	4 <sup>b</sup>
pI	3,4-3,5
Optimum pH	6,0-7,0 <sup>c</sup> , 5,0-8,0, 8,8-9,0 <sup>d</sup>
K <sub>m</sub> (μM)	52,6; 71,4 (Heinzkill et al., 1998)
Optimum temperature	40 °C <sup>c</sup>
pH stability	pH 5,0-9,0 at 30 °C for 16 h
Thermal stability	Up to 50 °C at pH 7.0 for 30 min
Cofactor	One protoheme IX/enzyme
Absorption maxima	280, 415, 540, 640 nm oxidized form; 280, 438, 557, 585 nm reduced form
Rz value <sup>e</sup>	2,7
Sugar content and glycosylation sites	5%, Asn143 and Ser339 <sup>b</sup>
Metal ion requirement	Two endogenous Ca <sup>2+</sup> ions <sup>b</sup>
Cellular localization	extracellular



<sup>a</sup> From primary structure analysis.

<sup>b</sup> From X-ray crystallography.

<sup>c</sup> Oxidative coupling of phenols with 4-aminoantipyrine.

<sup>d</sup> Chemiluminescent reaction with luminol.

<sup>e</sup>RZ Reinheitszahl. value is the absorbance ratio with absorption at  $\lambda_{\max}$  of Soret band/absorption at 280 nm.

In the past few years, several X-ray structures of peroxidases from different sources were reported: cytochrome-c peroxidase (CcP), reported more than 30 years ago (Finzel et al., 1984); lignin peroxidase (Piontek et al., 1993; Poulos et al., 1993; Neves, 2007); *Arthromyces ramosus peroxidase* (Kunishima et al., 1994); *Coprinus cinereus peroxidase* (CiP); (Petersen et al., 1994); manganese peroxidase (MnP); (Poulos et al., 1995) and pea ascorbate peroxidase (APX); (Patterson and Poulos, 1995).

From a comparison among them, it was noted that, despite the low level of sequence homology (often <20%), the overall folding and the organization of the secondary structure is conserved (Poulos et al., 1995); In Fig. 6 it can be observed conservation of amino acids in peroxidase from different species.

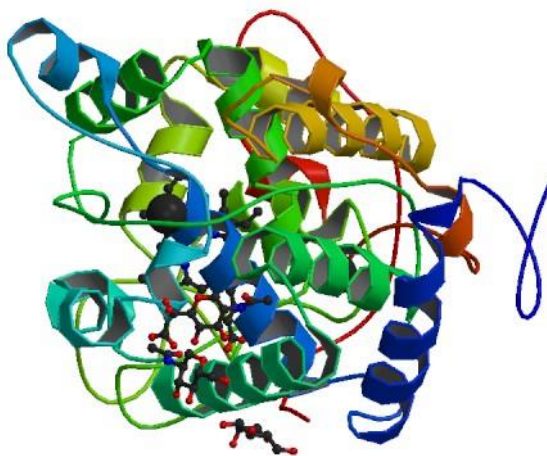
			□		○				▽																						
ARP	47	V	R	K	I	L	R	I	V	F	H	D	A	I	59	-----	175	D	E	V	V	D	L	L	A	A	H	S	L	A	187
BAP	39	A	H	Q	A	I	R	L	T	F	H	D	A	V	51	-----	168	L	E	T	V	W	G	L	I	A	H	T	V	G	180
PCP	38	A	H	E	S	I	R	L	V	F	H	D	S	I	50	-----	167	L	E	L	V	W	M	L	S	A	H	S	V	A	179
MnP	37	A	H	E	V	I	R	L	T	F	H	D	A	I	49	-----	164	F	E	V	V	S	L	L	A	S	H	T	V	A	176
Turnip	33	G	A	S	I	L	R	L	F	F	H	D	C	F	45	-----	159	R	D	M	V	A	L	S	G	A	H	T	I	G	171
CCP	43	G	P	V	L	V	R	L	A	W	H	T	S	G	55	-----	165	R	E	V	V	A	L	M	G	A	H	A	L	G	177
HRP	33	A	A	S	I	I	R	L	H	F	H	D	C	F	45	-----	161	S	D	L	V	A	L	S	G	G	H	T	F	G	173

Fig. 6 - Conserved amino acid residues. The amino acid sequences near the invariant His and Arg residues of several peroxidases are aligned with each other. The proximal and distal His and essential Arg residues of ARP are indicated by Δ, o and □, respectively, above the sequences. The enzymes are as follows: ARP, *A. ramosus peroxidase* (Sawai-Hatanaka et al., 1995); BAP, lignin peroxidase of *Bjerkandera adusta* (Kimura et al., 1991); PCP, lignin peroxidase of *P. chrysosporium* (Tien and Tu, 1987); MnP, manganese peroxidase of *P. chrysosporium* (Tien and Tu, 1987); Turnip, turnip peroxidase (Welinder and Mazza, 1977); CCP, *S. cerevisiae cytochrome c peroxidase* (Kaput et al., 1982); and HRP, horseradish peroxidase (Welinder, 1976).

The enzyme is divided in two different structural domains, enveloping the heme moiety. It has been proposed that the two domains originate from an early gene duplication event (Welinder and Gajhede, 1993). The structures of peroxidases are constituted by 10-11  $\alpha$ -helices, linked by loops and turns, while  $\beta$ -structures are essentially absent or are a minor

component. Some glycine and proline residues are conserved, which determine the correct backbone bending, and a buried salt bridge, involving residues Asp107 and Arg132. The latter fixes the long loop connecting the two structural domains.

Class I peroxidases do not contain any disulphide bridge; they do not contain any carbohydrate and any calcium ions. On the other hand, Cys bridges are present in Class II and III, even if differently located; all the Cys residues present in the proteins around 8-10 form disulphide bridges which provide an high degree of rigidity to the protein. Finally, Class II and III are glycosylated on the protein surface. Tyrosine residues are absent in fungal peroxidases (Class II), except for one residue in one isoenzyme of LiP. This makes the reduction potential of the protein matrix for this class higher than in the other and could explain why Compound I is not able to oxidize the protein itself (Welinder, 1992). However, despite these differences within the peroxidase families, the proteins present a similar folding. A crystal structures 1.3 Å of the cyanide, nitric oxide and hydroxylamine complexes of *Arthromyces ramosus* peroxidase (ARP), a class II peroxidase belonging to the fungal peroxidase superfamily are demonstrated in Fig. 7.



*Fig. 7 - Crystal structure of the CN-bound form of Arthromyces ramosus peroxidase at 1.3 Angstroms resolution Protein chains are colored from the N-terminal to the C-terminal using a rainbow spectral color gradient (Fukuyama and Okada, 2007)*

Peroxidases are widely used in clinical biochemistry and enzyme immunoassays (Vámos-Vigyázó and Haard, 1981; Lin et al., 1996). Quoting some of the main applications, such as, removal of phenolic contaminants and related compounds; decolorization of synthetic dyes; organic and polymer synthesis; deodorization of swine manure; paper pulp industry; biosensors; diagnostic kits; enzyme immunoassays; biofuel production and biofuel cells; and

oxidation of pharmaceutically active compounds. These potential applications of peroxidase are reported in a review by (Hamid and Khalil ur, 2009). Horseradish root tubers are commonly employed as a commercial source for peroxidase production. However, other cultivated species may provide peroxidases exhibiting similar or better properties, especially recombinant species. The use of fungal peroxidases would be of more practical advantage because their production on an industrial scale is more feasible.

Reduction of peroxides at the expense of electron-donating substrates makes peroxidases useful in a number of industrial and analytical applications. Peroxidase is probably the most well-suited enzyme for the preparation of enzyme-conjugated antibodies, which are used in enzyme-linked immunosorbent assay (ELISA), due to its ability to yield chromogenic products at low concentrations (H.W., 1991). Peroxidase coupled with other enzymes in polyenzymatic systems producing hydrogen peroxide is also used in the determination of many compounds, such as glucose in blood (Hamid and Khalil ur, 2009). Because of the oxidative nature of peroxidase there are several areas where it could replace current chemical oxidant techniques.

### **2.3.1 Immobilization of peroxidase on carbon nanotubes**

Practical use of enzymes is being expanded in new fields, such as fine-chemical synthesis, pharmaceuticals, biosensors, and biofuel cells (Kim et al., 2006). As mentioned in a previous section, CNTs can serve as excellent supporting materials for enzyme immobilization because they offer the ideal characteristics that determine the efficiency of biocatalysts. Both multi-walled and single-walled CNTs have been demonstrated to have the ability to adsorb many types of enzymes. This adsorption involves both hydrophobic and electrostatic interaction (Karajanagi et al., 2004). Apart from these two types of interactions, hydrogen bonds and nonspecific adsorption can also play a role for enzyme adsorption onto CNTs (Matsuura et al., 2006).

Studies with horseradish peroxidase (HRP), mainly, adsorbed on the MWCNTs surface indicated that the enzyme activity was not inactivated during its immobilization onto the carbon nanomaterials. It has been reported that the specific activity of HRP adsorbed onto CNTs was 33% (Asuri et al., 2006) and 49 % (Asuri et al., 2007), respectively.

Adsorption capacity and activity of bound protein could be affected by the structure, density and length of carbon nanotubes. The activity of immobilized HRP is proportional to the initial concentration of HRP in immobilization buffer. As the increase in HRP concentration in solution, the activity of MWCNT adsorbed HRP was also increased until reaching the optimum concentration (Kim et al., 2009).

Jeykumari and Narayanan, (2008) presents a novel approach to fabricate nanobiocomposite bienzymatic glucose oxidase and HRP biosensor based on functionalized MWCNTs. The enzyme immobilization with TH-functionalized MWCNTs was achieved by mixing thoroughly with the enzyme mixture. Due to the ability of MWNTs to bind biomolecules, the two enzymes became electrostatically and hydrophobically adsorbed onto the surface of TH-functionalized MWNTs during mixing (Jeykumari and Narayanan, 2008). In another study, a complex chitosan-SWCNT was used for the noncovalent immobilization of HRP to construct an electrode for direct bioelectrochemical sensing without an electron mediator, allowing, specifically, the detection of trace levels of nitric oxide (Jiang et al., 2009).

In other studies, peroxidase was immobilized through covalent linking, e.g., using a glutaraldehyde cross linker or carbodiimide chemistry (EDC/NHS) (Asuri et al., 2006; Neves, 2007). In the latter, a suspension of oxidized nanotubes  $H_2SO_4/HNO_3$  was added to N-hydroxysuccinimide (NHS). The mixture was sonicated and N-ethyl-N'-3-dimethylaminopropylcarbodiimide hydrochloride (EDC) was then added to initiate the coupling of NHS to the carboxylic groups on the oxidized nanotubes. Finally, this nanotube film was transferred to a solution of enzyme. Fig. 8 illustrates an example of procedure for the covalent immobilization of peroxidase on CNTs.

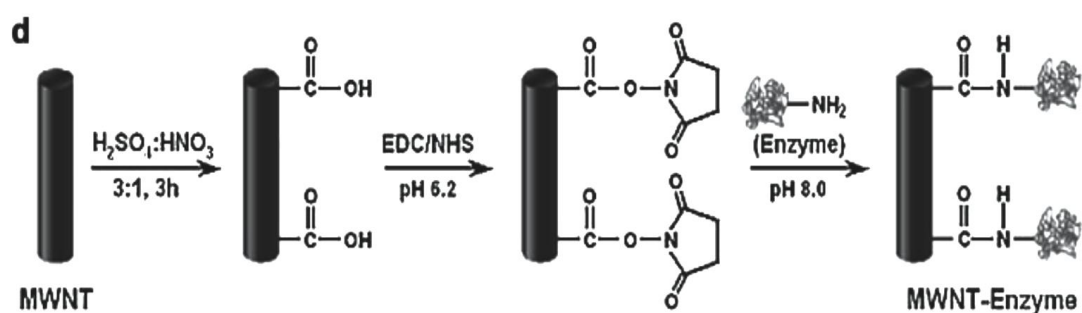


*Fig. 8 - Scheme of enzyme immobilization on functionalize carbon nanotubes through covalent linking (Asuri et al., 2006)*

As shown in Table 2, peroxidase has been immobilized either covalently or noncovalently on CNTs for various applications. Highlighting its use as bioelectrochemical sensor, fuel cells, glucose and  $H_2O_2$  biosensor and, as in this work, the use in a biocatalytic reaction.

## 3 Experimental Section

### 3.1 Materials and Chemicals

All studies were performed using pure commercial fungal peroxidase (EC 1.11.1.7; NS 51004) supplied by Novozymes, Denmark. Multi-walled carbon nanotubes with external diameter c.a. 20 nm, synthesized by chemical vapor deposition (CVD) using a Fe catalyst, were kindly provided by *Laboratoire de Chimie de Coordination* Toulouse, France. For peroxidase activity assays, 2,2'-azino-bis(3-ethylbenzothiazoline-6-sulfonic acid) - (ABTS) and H<sub>2</sub>O<sub>2</sub> (30%) were supplied by AppliChem Germany and Sigma-Aldrich, respectively. For MWCNTs magnetization, nitric acid (HNO<sub>3</sub>), thionyl chloride (SOCl<sub>2</sub>), anhydrous tetrahydrofuran (THF), iron(II) chloride, iron (III) chloride and ammonium hydroxide were all reagent grade and purchased from Sigma-Aldrich. Reactive Black 5 (RB5), Bromophenol blue (BPB) and Reactive Blue 4 (RB) supplied by Ciba, Portugal, were used in dye oxidation reactions without any further purification.

### 3.2 Functionalization of MWCNT

Multi-walled carbon nanotubes were prepared from ethylene gas by chemical vapor deposition using Fe nanoparticles supported on alumina as catalyst. Details on the reactor configuration and preparation of the catalyst can be found elsewhere (Morançais et al., 2007). The catalyst was removed by boiling with diluted sulfuric acid (50%) at 140 °C for 3 h after which the nanotubes were filtered when hot by a glass frit followed by washing with hot water and drying at 120 °C. This sample was designated as MWCNT.

MWCNTox were prepared by liquid-phase oxidation of MWCNT. For oxidative functionalization, 1 g of purified nanotubes was mixed with 50 mL of HNO<sub>3</sub> 7 M and refluxed for 3 h at 130 °C under stirring. The nanotubes were filtered on a glass frit, washed with water until the filtrate reached neutral pH, and dried overnight at 120 °C.

MWCNTox material was heat-treated under inert atmosphere N<sub>2</sub> at 400 °C for 1 h, sample MWCNTox-400, and at 900 °C for 1 h, sample MWCNTox-900, to selectively remove functional surface groups.

### 3.3 Production of magnetic MWCNT

MWCNTs were coupled with Fe<sub>3</sub>O<sub>4</sub> using a simple method adapted from Xu et al., (2008). First, 75 mL of a HNO<sub>3</sub> 0.3 M solution was transferred to a Teflon liner with 200 mg of pristine MWCNT and then placed into a autoclave at 200 °C for 2 h. The oxidized MWCNTs were

filtered and washed several times with distilled water till the filtrate was neutral. This sample, MWCNT-COOH was dried overnight at 120 °C (Fig. 9).

Then, to produce MWCNT-COCl, dried MWCNT-COOH was suspended in SOCl<sub>2</sub> 30 mL and stirred for 24 h at 70 °C. The solution was filtered, washed with anhydrous THF, and dried under vacuum at room temperature for 24 h, generating MWCNT-COCl.

For preparation of magnetite nanoparticles (MNPs), 1.0 g ferrous chloride was dissolved in 3 mL of a 2 M HCl solution and 1.6 g ferric chloride in 10 mL of a 2 M HCl solution. Ferrous chloride and ferric chloride solutions were mixed in a beaker under vigorously stirring (Pan et al., 2005). At the same time, 25 mL ammonium hydroxide solution was added slowly into the beaker by a pipette and magnetite in the form of a black precipitate was formed immediately. Stirring was continued for 15 min after adding ammonia hydroxide. The resulting precipitate was washed with water (6 x 200 mL) until the pH of the wash supernatant was reduced to 7. The final total volume for the suspension was adjusted to 300 mL using water.

The magnetite solution prepared above was diluted to 150 mL with ethanol. The solution was then sonicated for 30 min. 10 mL of 3-aminopropyltriethoxysilane (NH<sub>2</sub>CH<sub>2</sub>-Si-OCH<sub>2</sub>CH<sub>3</sub>, APTS) was added into the magnetite suspension under rapid stirring for 7 h. The resulting solution was washed with methanol five times by magnetic separation. APTS-coated magnetite nanoparticles were dried under vacuum at room temperature for 24 h, generating amine-terminated MNP-NH<sub>2</sub> (Yoza et al., 2003).

Finally, to fabricate the MWCNT-MNP nanohybrid, 10 mg MNP-NH<sub>2</sub> and 50 mg CNT-COCl were added to 25 mL THF solution and the mixture was placed in an ultrasonic bath (40 kHz for 60 min.) and then stirred for 24 h at room temperature. The resulting solution was washed magnetically with water for five times, and the precipitate was dissolved into 20 mL of water, obtaining a black solution.

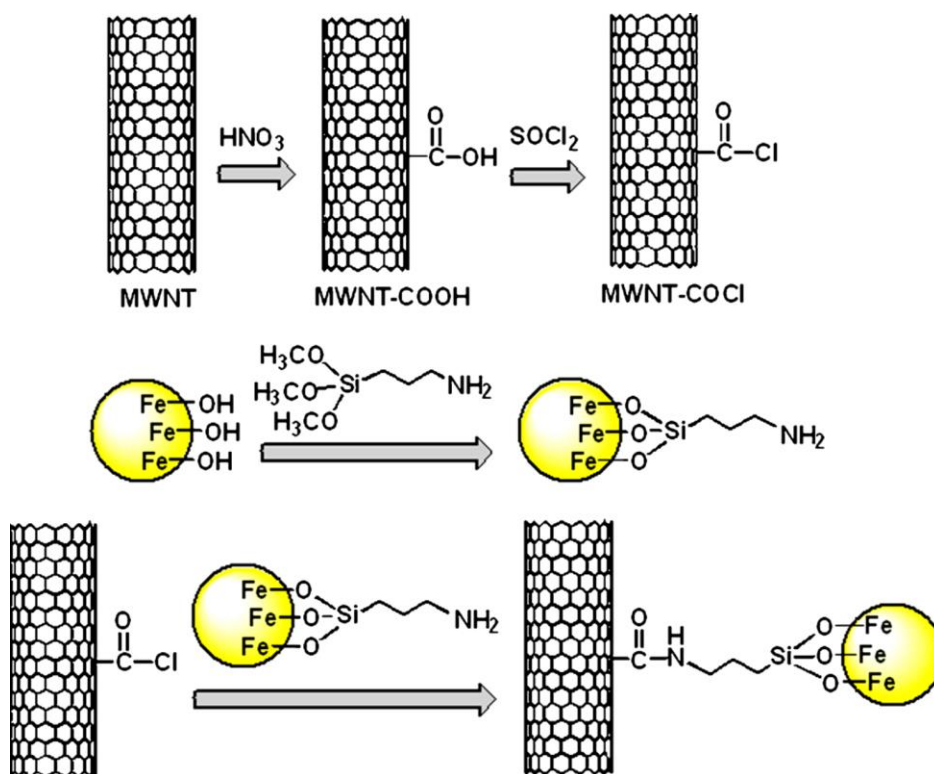


Fig. 9 - Covalent attachment of magnetite nanoparticles (MNPs) on the carbon nanotube (MWCNT) surface to form MWCNT-MNP nanohybrids (Xu et al., 2008).

### 3.4 Characterization of MWCNT

The obtained samples were characterized by  $\text{N}_2$  adsorption-desorption isotherms at  $-196\text{ }^\circ\text{C}$  using a Quantachrome NOVA 4200e multi-station apparatus. Brunauer-Emmett-Teller (BET) specific surface area was calculated from nitrogen adsorption in the relative pressure range from 0,05 to 0,15. The Barrett-Joyner-Halenda (BJH) method was applied to the desorption branch of the  $\text{N}_2$  adsorption isotherms to obtain the pore size distributions curves and cumulative volume of pores.

Surface chemical groups were characterized and quantified by temperature programmed desorption (TPD) using an AMI-300 Catalyst Characterization Instrument Altamira Instruments equipped with a quadruple mass spectrometer (Ametek, Mod. Dymaxion). The sample (0.1 g) was placed in a U-shaped quartz tube and heated at  $5\text{ K}\cdot\text{min}^{-1}$  in an electrical furnace under a constant flow of  $25\text{ cm}^3\cdot\text{min}^{-1}$  (STP) of helium, used as carrier gas. The total amounts of CO and  $\text{CO}_2$  evolved from the samples were obtained by integration of the TPD spectra.

Fourier transform infrared (FTIR) measurements were performed on a FT-IR Nicolet 510-P spectrometer (Thermo Fisher Scientific, USA) equipped with a MIRacle™ Single Reflection ATR Attenuated Total Reflectance ZnSe crystal plate accessory (PIKE Technologies, USA). Transmission electron microscopy (TEM) was performed in a LEO 906E instrument operating at

120 kV, equipped with a 4 M pixel 28×28 mm CCD camera from TRS at Centro de Química - Universidade de Trás-os-Montes e Alto Douro (UTAD).

The morphology of the materials was observed using a high resolution (Schottky) environmental scanning electron microscope (SEM) with X-ray microanalysis and electron backscattered diffraction analysis (Quanta 400 FEG ESEM/EDAX Genesis X4M; secondary electron detector, 20 000×, 15,00 kV) at the Materials Centre of the University of Porto (CEMUP).

X-ray diffraction (XRD) analysis of selected samples was carried out at UTAD in a PANalytical X'Pert MPD equipped with a X'Celerator detector and secondary monochromator (Cu Ka  $\lambda = 0,154$  nm, 50 kV, 40 mA; data recorded at a 0,0178 step size, 100 s/step). Rietveld refinement with PowderCell software was used to identify the crystallographic phases present and to calculate the crystallite size from the XRD diffraction patterns.

### 3.5 Immobilization Technique

In all experiments 4 mg of MWCNT were added to 1,2 mL of peroxidase solution ( $8 \mu\text{L}_{\text{peroxidase}}/\text{mL}_{\text{buffer solution}}$ ) under orbital stirring for 1h. After immobilization, MWCNT were washed several times with appropriated buffer.

The immobilization yield (%) and the activity recovered (%) after immobilization are defined as:

$$\text{Immobilization yield (\%)} = \frac{\text{activity}_{\text{initial}} - \text{activity}_{\text{final}}}{\text{activity}_{\text{initial}}} \times 100 \quad (3.1)$$

$$\text{Activity Recovered (\%)} = \frac{\text{activity}_{\text{immobilized}} \times m_{\text{carrier}}}{(\text{activity}_{\text{initial}} - \text{activity}_{\text{final}}) \times V_{\text{reaction}}} \times 100 \quad (3.2)$$

Where  $\text{activity}_{\text{initial}}$  ( $\text{U}\cdot\text{L}^{-1}$ ) is the enzymatic activity registered with a sample of solution of peroxidase prepared to perform immobilization,  $\text{activity}_{\text{final}}$  ( $\text{U}\cdot\text{L}^{-1}$ ) the enzymatic activity registered with a sample of the supernatant recovered after performing immobilization,  $\text{activity}_{\text{immobilized}}$  ( $\text{U}\cdot\text{g}^{-1}$ ) the enzymatic activity registered with the MWCNTs onto which peroxidase was immobilized,  $m_{\text{carrier}}$  (g) the mass of MWCNTs with enzyme immobilized and  $V_{\text{reaction}}$  (L) the volume of reaction.

In this work, the immobilization yield represents the yield of the immobilization process in terms of the quantity of active peroxidase adsorbed onto the carrier, while the activity recovered represents the yield of the immobilization process in terms of the capacity of the enzymes immobilized onto the carrier to perform catalysis.



### 3.6 Enzymatic activity measurement

The free and immobilized peroxidase activity were assayed spectrophotometrically (JASCO V-560 UV-Vis spectrophotometer) with ABTS as substrate (0,4 mM) and H<sub>2</sub>O<sub>2</sub> (0,33 mM) in 50 mM citrate/100 mM phosphate buffer at pH 4,5. To measure the free peroxidase activity, 100 µL of enzyme solution were mixed with 0,4 mL of ABTS and 1,4 mL of citrate/phosphate buffer (50/100 mM, pH 4,5, 40 °C). The reaction was started by adding 100 µL of H<sub>2</sub>O<sub>2</sub>. The change in absorbance at 420 nm ( $\epsilon = 36000 \text{ M}^{-1} \text{ cm}^{-1}$ ) was recorded automatically by the spectrophotometer and the catalytic activity was determined by measuring the slope of the initial linear portion of the kinetic curve. The free peroxidase activity is defined as:

$$\frac{U}{L} = \frac{abs/min \times f_{dilution} \times 10^6}{\epsilon} \quad (3.3)$$

Where  $U/L$  is the quantity of enzyme capable of breaking down 1 µmol of ABTS per minute and per volume unit of enzymatic solution,  $abs/min$  the absorbance per minute determined by linear regression,  $f_{dilution}$  the dilution factor of the sample,  $10^6$  the conversion factor from M to µM; and  $\epsilon$  the molar extinction coefficient ( $36000 \text{ M}^{-1} \text{ cm}^{-1}$  at 420 nm).

To measure peroxidase activity when using immobilized enzyme, MWCNT were mixed with 21 mL of citrate/phosphate buffer (50/100 mM, pH 4,5) at 40 °C and 6 mL of ABTS, under magnetic stirring for 2 min. The reaction was started after adding 1,5 mL of H<sub>2</sub>O<sub>2</sub> solution. Samples were taken every 20 seconds and absorbance was measured spectrophotometrically at 420 nm (Silva et al., 2014). After linear regression of the data obtained, enzyme activity was determined using Eq.(3.4:

$$\frac{U}{g} = \frac{abs/min \times f_{dilution} \times V_{reaction} \times 10^6}{\epsilon \times m_{carrier}} \quad (3.4)$$

Where  $U/g$  is the quantity of enzyme capable of breaking down 1µmol of ABTS per minute and per mass unit of carrier,  $abs/min$  the absorbance per minute determined by linear regression,  $f_{dilution}$  the dilution factor of the sample,  $V_{reaction}$  (L) the volume of reaction,  $10^6$  the conversion factor from M to µM,  $\epsilon$  the molar extinction coefficient ( $36000 \text{ M}^{-1} \text{ cm}^{-1}$  at 420 nm) and  $m_{carrier}$  g the mass of MWCNTs with enzyme immobilized.

### 3.7 Optimization of the conditions for peroxidase immobilization on MWCNT

Assays to determine the optimal peroxidase concentration were performed immobilizing the peroxidase solution in citrate/phosphate buffer (50/100 mM, pH 4,5) on 4 mg of MWCNTox-900 at different concentrations of peroxidase: 3-11 µL<sub>peroxidase</sub>/mL<sub>buffer</sub> for 1 h.

To evaluate the influence of pH on peroxidase immobilization in 4 different carbon nanotubes, different buffers were used: citrate/phosphate 50 mM for pH 4,5; phosphate buffer 50 mM for pH 6,0, 7,0 and 8,0 and carbonate buffer 50 mM for pH 9,0. Measurements of enzymatic activity, according to the method described above, were performed for: i) initial peroxidase solution, ii) supernatants recovered after immobilization and iii) immobilized enzyme.

To determine the optimum contact time, peroxidase immobilization was carried out several time laps ranging from 15 min to 4 h at the optimum conditions for this carrier (pH 4,5; 8  $\mu\text{L}_{\text{peroxidase}}/\text{mL}_{\text{buffer}}$ ).

### 3.8 Thermal stability of free and immobilized peroxidase

The thermal stabilities of the free and immobilized peroxidase were investigated by incubating the free and immobilized enzymes in citrate/phosphate buffer (50/100 mM, pH 4,5) and phosphate buffer (50 mM, pH 6,0), respectively, at different temperatures (30-50 °C). Immobilized peroxidase was suspended in 500  $\mu\text{L}$  of the immobilization buffer. In both cases samples were removed regularly from the water bath and enzymatic activity was quickly determined according to the methods described above.

The thermal parameters were calculated according to a simplified deactivation model described in the literature (Henley and Sadana, 1985):



$$A = \left[ 100 + \frac{\alpha_1 k_1}{k_2 - k_1} - \frac{\alpha_2 k_2}{k_2 - k_1} \right] e^{-k_1 t} + \left[ \frac{\alpha_2 k_1}{k_2 - k_1} - \frac{\alpha_2 k_2}{k_2 - k_1} \right] e^{-k_2 t} + \alpha_2 \quad (3.6)$$

Where  $A$  (%) is the residual enzyme activity,  $\alpha_1$  and  $\alpha_2$  ratios of specific activities (remaining activities), respectively to the different states  $E_1/E$  and  $E_2/E$  (see Eq. 3.5),  $k_1$  ( $\text{h}^{-1}$ ) and  $k_2$  ( $\text{h}^{-1}$ ) the thermal inactivation rate constants and  $t$  (h) the time.

Analyzing the data obtained, it was considered that peroxidase undergoes a conformational transition due to the increase in temperature according to the model of Eq. (3.5). This implies that inactivation follows a single exponential decay, in which  $\alpha_2 = 0$  and  $k_2 = 0$ , leading to:

$$A = [100 - \alpha] \times e^{-kt} + \alpha \quad (3.7)$$

The thermal parameters  $\alpha$  and  $k$  of the model described in Eq. (3.7) were estimated by a non-linear fitting of the experimental data, using CurveExpert v 2.0.4 © 2011-2014.

Biocatalyst half-life ( $t_{1/2}$ ) was calculated from Eq. 3.7, using the estimated parameters  $k$  and  $\alpha$  and making  $A$  equal to 50.

The energetic barrier (activation energy,  $Ea$ ) for the thermal deactivation process was calculated by nonlinear regression considering the Arrhenius equation, defined as:

$$k = k_0 e^{-\frac{Ea}{RT}} \quad (3.8)$$

Where  $k_0$  ( $h^{-1}$ ) is the pre-exponential factor,  $Ea$  ( $J mol^{-1}$ ) the energy of activation,  $T$  (K) the temperature and  $R$  the universal gas constant ( $8,314 J mol^{-1} K^{-1}$ ).

The standard free energy for the thermal inactivation ( $\Delta G^0$ ) was calculated from the first-order rate constant of inactivation process,  $k$  at different temperatures, using the following equation (Longo and Combes, 1999):

$$\Delta G^0 = -RT \ln \left( \frac{kh}{KT} \right) \quad (3.9)$$

Where  $h$  (J h) is the Planck constant ( $1,84E-37$ ) and  $K$  ( $J.K^{-1}$ ) the Boltzmann constant ( $1,3807E-23$ )

The activation enthalpy ( $\Delta H$ ) was calculated from the activation energy:

$$\Delta H = Ea - RT \quad (3.10)$$

And the activation entropy ( $\Delta S$ ) was calculated from the enthalpy and standard free energy as follow:

$$\Delta S = \frac{\Delta H - \Delta G}{T} \quad (3.11)$$

### **3.9 Determination of kinetic parameters of free and immobilized peroxidase**

To determine the kinetic parameters of free peroxidase, enzymatic activity was measured for concentrations of ABTS ranging from 3 to 120  $\mu M$ , according to the method described previously. Similarly, the kinetic parameters of immobilized peroxidase were determined measuring the enzymatic activity, for the catalysis of ABTS at concentrations ranging from 0,01 to 0,9 mM. The hydrogen peroxide concentration was kept at 0,33 mM.

Since the data obtained followed the pattern predicted by the Michaelis-Menten model (Eq. 3.12), CurveExpert (v2.0.4 © 2011-2014) was used to perform a non-linear fit of the experimental values in order to determine  $K_M$  and  $v_{max}$ .

$$v = \frac{v_{max}[S]}{K_M + [S]} \quad (3.12)$$

Where  $v$  ( $\text{mM}\cdot\text{min}^{-1}$ ) is the catalytic reaction rate,  $v_{max}$  ( $\text{mM}\cdot\text{min}^{-1}$ ) the maximum rate of the reaction,  $[S]$  the concentration of substrate ( $\text{mM}$ ) and  $K_M$  the Michaelis-Menten constant. (Steevensz et al., 2009).

### **3.10 Storage and operational stability of immobilized peroxidase**

The stability of free and immobilized peroxidase was evaluated at 4 °C, for one month. Peroxidase was immobilized on MWCNT in phosphate buffer (50 mM, pH 6,0), according to the method described above.

The operational stability was determined by reacting peroxidase immobilized on mMWCNT with 6 mL of ABTS (0,4 mM) in 21 mL of citrate-phosphate buffer pH 4,5 at 40 °C. The reaction was started by adding 1,5 mL of  $\text{H}_2\text{O}_2$  (0,35 mM). At each cycle, a sample was withdrawn in 30 sec intervals over 4 minute period and the absorbance was measured at 420 nm. The mMWCNT-Peroxidase conjugates were then removed by a simple magnet, washed once with phosphate buffer (50 mM, pH 6,0), and re-immersed in a fresh ABTS solution to begin the next cycle. A total of 9 cycles were performed.

The operation stability of the immobilized peroxidase on a MWCNT membrane and on MWCNTox-400 was also analyzed, as described as Appendix information.

### **3.11 Protein determination**

The supernatants from the immobilization method were collected and used in the Bradford protein assay (Appendix 1) to determine the mass of peroxidase on 4 mg of MWCNTs. This was done by measuring the difference in the amount of enzyme in the supernatant and the total amount of enzyme added to the carbon nanotubes. This mass balance was also estimated for the second wash and thermal incubation (50 °C) supernatants.

### **3.12 Gel electrophoresis**

Sodium dodecyl sulfate polyacrylamide gel electrophoresis (SDS-PAGE) was performed in order to evaluate the purity of commercial peroxidase solution. The gel was then stained with Coomassie Blue stain for 24 h and destained using acetic acid to visualize the separated enzyme (Appendix 1)

### 3.13 Discoloration of textile dyes

Degradation of 3 dyes (Reactive Black 5, Reactive Blue and Bromophenol Blue) was evaluated incubating free or immobilized peroxidase on mMWCNT in solutions of each one of the dyes in test, for 24 h. More details about these dyes can be consulted in Appendix 1.

The reaction solutions (10 mL) were prepared dissolving a stock solution of the dye in citrate/phosphate buffer (50/100 mM, pH 4,5). Absorbance of all solutions was measured spectrophotometrically, before ( $Abs_{initial}$ ) and after ( $Abs_{final}$ ) the incubation period, at the maximum absorption wavelength of each dye: RB5 (590 nm), BPB (594 nm) and RB (590 nm). Controls with mMWCNT without peroxidase and with inactivated peroxidase (5 min, 100 °C) were made to evaluate the dye elimination by adsorption.

For each dye solution, the discoloration efficiency is defined as:

$$\%_{dye\ remotion} = \frac{Abs_{initial} - Abs_{final}}{Abs_{initial}} \times 100 \quad (3.13)$$



## 4 Results and Discussion

### 4.1 Characterization of MWCNT

The development of an efficient functionalized nanotubes support for peroxidase immobilization, using a non-covalent binding technique for investigating its influence on the biocatalyst structure function relationships, was one of the objectives of this work. In this way, multi-walled carbon nanotubes (MWCNTs) represent ideal nanoscale supports due to their easy acid oxidation to produce hydrophilic carboxylic acid and hydroxyl groups along their sidewalls. Moreover, their high surface areas may lead to high functional enzyme loadings, while their high thermal and mechanical stability make them amenable for use as robust supports for protein attachment (Asuri et al., 2006). Thus, in order to study the interaction of peroxidase with the surface of MWCNT and assess its importance on peroxidase immobilization yield and respective activity, oxygen containing groups were selectively introduced or removed on MWCNTs side walls by liquid-phase oxidation and thermal treatments, as described in the experimental section.

#### 4.1.1 N<sub>2</sub> adsorption-desorption isotherms

Nitrogen adsorption isotherms were carried out for the obtained samples and the results are presented in Fig. A1. The characterization of these materials is summarized on Table 7.

Table 7 - Specific surface area  $S_{BET}$ , pore volume  $V_p$  and pore diameter  $d_p$  for the different MWCNT samples.

Sample	$S_{BET}$ (m <sup>2</sup> .g <sup>-1</sup> )	$V_p$ (cm <sup>3</sup> .g <sup>-1</sup> )	$d_p$ (nm)	$pH_{PZC}$	CO (μmol.g <sup>-1</sup> )	CO <sub>2</sub> (μmol.g <sup>-1</sup> )	CO+ CO <sub>2</sub> (μmol.g <sup>-1</sup> )	CO/ CO <sub>2</sub>
MWCNT	255	0,944	3,2	7,2	348	70	418	5,0
MWCNTox	276	1,073	15	3,0	800	412	1212	1,9
MWCNTox -400	291	1,154	20	4,0	623	223	846	2,8
MWCNTox -900	301	1,247	25	6,9	176	37	213	4,8

Two ranges of different behavior can be observed in Fig. A1 as relative pressure ( $p/p_0$ ) increases. For low pressures ( $0 < p/p_0 < 0,4$ ) adsorbed volume increases slowly, indicating monolayer completion. The absence of a steep increase at very low  $p/p_0$  reflects the absence

of micropores with sizes in the order of magnitude of the nitrogen molecule (Vicente et al., 2011). For pressures corresponding to  $(0,4 < p/p_0 < 1,0)$ , hysteresis loop can be observed, which can be related to capillary condensation, which is known to occur in mesopores (2-50 nm) (Gregg, 1982), precisely the order of magnitude of the inner cavities of these MWCNTs samples, as shown in Table 7. The  $N_2$  adsorption uptake near  $p/p_0=1,0$  is explained by the presence of larger pores on the surface of MWCNT as a result of acid oxidation and thermal treatments. Aggregates of CNT were found to cause such effect in previous studies (Yang et al., 2001).

The surface areas of the samples, calculated by the BET method ( $S_{BET}$ ) revealed that the oxidation treatment lead to an increase of the surface area of the resulting material. After the reflux of pristine MWCNT in  $HNO_3$ , the surface area increased approximately 8% (MWCNTox, Table 7). The total pore volume ( $V_p$ ) and respective diameter ( $d_p$ ) were also increased, wherein the pore diameter of MWCNTox was around 4.7 times higher than that of pristine MWCNT. This happens because this oxidative process occurs under strong acidic conditions, creating defect sites ends and/or holes on CNTs sidewall. These findings are in line with published works for nitric acid oxidation (Silva et al., 2014) and for ozone oxidation pre-treatment (Liu et al., 2009).

#### **4.1.2 Temperature programmed desorption (TPD)**

TPD was used to analyze the oxygen functional groups of carbon nanotubes material. This investigation could offer valuable detailed information about the chemical nature of catalyst surface, since the different surface oxygenated groups could be thermally decomposed by at specific temperatures (desorption temperature) turning possible its identification from the TPD spectra. The main possible functionalities in an individual graphene sheet are schematically summarized in Fig. A2. It should be noticed that the difference of desorption temperatures of some functional groups in literature could be high, as shown in Table A1. Carboxylic groups are decomposing at low temperatures, anhydrides at intermediate temperatures and lactones at high temperatures.

As mentioned before, oxidation is an easy method to improve the oxygen amount on the surface of CNTs. The TPD profiles of purified MWCNTs, oxidized MWCNTox and calcined MWCNTox-400 and MWCNTox-900 are displayed in Fig. 10. The total amounts of CO and  $CO_2$  evolved from the samples are also presented in Table 7.



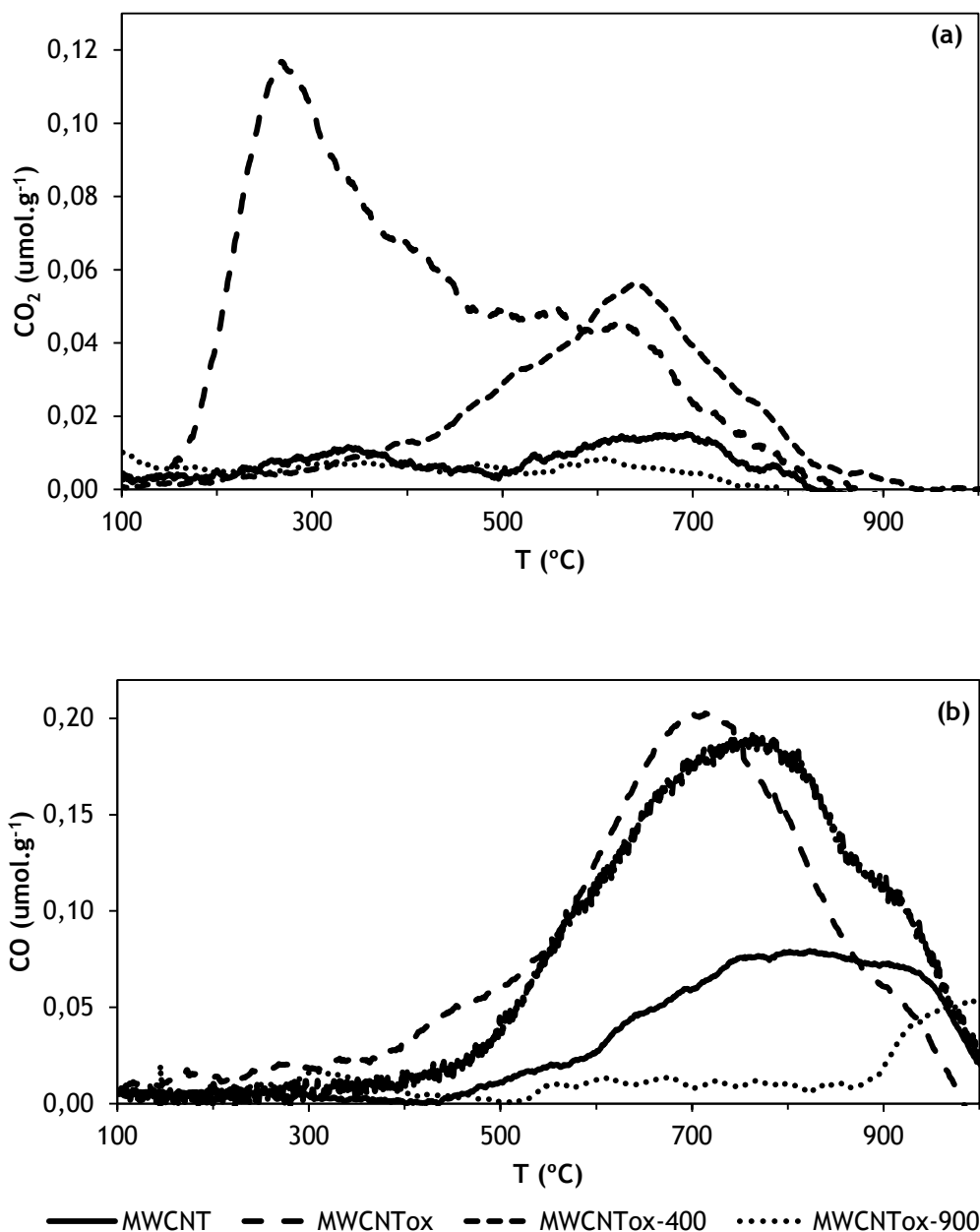


Fig. 10 - CO<sub>2</sub> (a) and CO (b) TPD profiles of pristine and functionalized MWCNTs.

As expected, the surface of MWCNTox was highly functionalized. In the TPD CO<sub>2</sub> profile, a larger peak at 300 °C and others at 500 °C and 650 °C were identified, assigned to the decomposition of carboxylic acid, anhydride and lactone, respectively (Liu, 2008). The peak observed at 750 °C on CO profile of this sample corresponded to the decomposition of quinone groups. After calcination at 400 °C, a CO<sub>2</sub> desorption peak at about 650 °C was observed which indicates that the thermal treatment at 400 °C remove part of carboxylic acids, but some carbonyl/quinones remains on the surface of the MWCNTox-400. When further treatment at 900 °C, few oxygenated surface groups were anchored in carbon nanotubes. It

should be noted that the thermal treatment significantly decreased the percentage area of peaks at lower and medium temperatures in CO<sub>2</sub> desorption profile.

The CO/CO<sub>2</sub> ratio (Table 7) indicates the acidic character of the functionalized samples. According to the  $pH_{PZC}$  results, MWCNTox is the most acidic sample, and thus it presents the lowest ratio. The thermal treated samples are less acidic character, since the acid groups are removed at lower temperatures than neutral and basic groups (Figueiredo et al., 2006).

#### **4.1.3 Fourier transform infrared (FTIR)**

The FT-IR analysis of treated MWCNTs was carried out to confirm the presence of functional groups and to investigate carbon nanotube-peroxidase interactions. Fig. A3 shows the FTIR-ATR spectra of these four samples before and after peroxidase immobilization.

The appearance of a peak at 1530-1560 cm<sup>-1</sup> confirmed the integrity of hexagonal structure on the pristine MWCNT (Fig. A3a), elucidating existence of carbon double bonding C=C (Naseh et al., 2009). The decreasing the transmittance of the band corresponding to C=C indicates oxidation of carbon with remarkably emerging of a peak at 1800 cm<sup>-1</sup> attributed to C=O stretching vibration in lactones, carboxylic acids and anhydrides (Matsuura et al., 2006), and indicating the expansion of carboxylation on the surfaces of purified and functionalized MWCNTs (Fig. A3b). As shown by TPD analysis, the amount of functional groups increases after the oxidation treatment. Nitric acid solution attack double bonding of carbon, resulting in a decrease in the intensity of the peak at the region 1530-1560 cm<sup>-1</sup>, and the hexagonal carbon at the region 650 -1000cm<sup>-1</sup>. Reducing the intensity of peak elucidates the presence of large number of asymmetrical hexagonal carbon (Yudianti et al., 2011). Other bands could be identified: a broad band assigned to O-H bending in phenols and carbonyls centered at 1400 cm<sup>-1</sup> and at 1020 cm<sup>-1</sup> assigned to the C-O stretching vibration in ethers and phenols. Other band at 880 cm<sup>-1</sup> ascribed to isolated aromatic C-H out-of-plane bending mode vibration (Chen et al., 2012).

The FTIR spectra of the samples with thermal treatments (Fig. A3c and Fig. A3d) shown a significantly reduction of the intensity of the band at 1800 cm<sup>-1</sup>. It should be attributed to desorption of oxygen functional groups with low thermal stability, such as carboxylic acid groups (see TPD analysis Fig. 10). Moreover, the band at 1050 cm<sup>-1</sup> became more intense probably due to the decrease in the electronic and spatial interactions between ether and phenol groups with carboxylic acid groups. Finally, the aromatic out-of-plane C-H bending band appears deviated peaking at 785 cm<sup>-1</sup> (Silva et al., 2014).

As we can see in Fig. A3, the infrared spectrum has changed after peroxidase immobilization on all MWCNTs. When MWCNTox was used as support, two new bands at 1650 and 1320 cm<sup>-1</sup> has been recorded. This corresponds to N-H bending and C-N stretching vibration of amines,

respectively. It was also detected an expressive decrease in the intensity of the bands attributed to O-H bending and C=O stretching. These results suggest that, the main interaction mechanism for peroxidase immobilization on MWCNTox is through physical adsorption on carboxylic acid sites.

In the case of peroxidase immobilized on MWCNTox-400 (Fig. A3c), an increase in the intensity of the NH bending band can be observed ( $1650\text{ cm}^{-1}$ ). It can be said that peroxidase is immobilized onto this carrier by different interaction, namely the formation of hydrogen bonds between OH groups at the surface of the nanotubes and amine terminal groups of the enzyme.

#### **4.1.4 Scanning electron microscope (SEM)**

The peroxidase immobilized on MWCNTox-900 was characterized by scanning electron microscope (SEM). From Fig. A4, the globular structures on the carbon nanotubes are suggestive of peroxidase immobilization onto MWCNTox-900 in the form of sphere-like particles. It can be observed peroxidase aggregates, which is in agreement with other reported SEM images (Hu et al., 2011), showing analogous structure of enzymes wrapped onto the nanotubes.

#### **4.1.5 X-ray diffraction (XDR)**

Fig. A5 shows the XRD patterns of the samples, where the reflections of the  $\text{Fe}_3\text{O}_4$  nanoparticles and mMWCNTs are reliably identified. The planes of pure  $\text{Fe}_3\text{O}_4$  are observed at  $2\theta=30,06^\circ$ ,  $37,31^\circ$ ,  $43,46^\circ$ ,  $57,33^\circ$  and  $63,03^\circ$ , which correspond well to the reported values for  $\text{Fe}_3\text{O}_4$  and are well indexed to the inverse cubic spinel phase of  $\text{Fe}_3\text{O}_4$  (Hong et al., 2006). From the XRD of mMWCNTs, approximately the same planes of  $\text{Fe}_3\text{O}_4$  are observed, in which the values of  $2\theta$  is less than those of pure  $\text{Fe}_3\text{O}_4$  due to the interaction of the magnetite nanoparticles and MWCNTs. In the case of the hybrid material, the presence of a diffraction peak in the range of  $2\theta = 20\text{-}30^\circ$  is also observed, attributed to the presence of the carbon phase. These results confirm the presence of magnetite in mMWCNTs. The composition of both materials and the dimension of the respective particles are presented in Table A2.

#### **4.1.6 Transmission electron microscopy TEM**

Magnetic MWCNTs were analyzed by TEM to evaluate the presence of  $\text{Fe}_3\text{O}_4$  nanoparticle on mMWCNTs (Fig. A7).  $\text{Fe}_3\text{O}_4$  material is constituted by magnetite crystallites of around 15-20 nm, which aggregate to form bigger particles (Fig. A7a). The dimensions of the crystallite are in accordance to the determined by XRD analysis (Table A2). In the case of the hybrid material, it can be observed that in general  $\text{Fe}_3\text{O}_4$  particles are attached to the surface of the carbon nanotubes (Fig. A7b and Fig. A7c), but the presence of magnetite particles inside of

CNT was also observed (Fig. A7d). This important to notice that there is plenty of CNT surface available for enzyme immobilization.

## **4.2 Optimization of peroxidase immobilization on MWCNTs**

In this section, the optimal peroxidase concentration and the effect of contact time between peroxidase and purified MWCNT were studied. The optimal immobilization pH was also analyzed and the results were discussed in following section.

According to the results obtained from Fig. 11a, for peroxidase solutions (pH 6,0 and contact time 1h) with concentrations under  $8 \mu\text{L}/\text{mL}_{\text{buffer}}$ , the enzymatic activity of the immobilized peroxidase rises gradually with the enzyme load, while for concentrations above it, enzymatic activity do not differ significantly. These suggest two patterns of enzyme immobilization on MWCNT surface.

Increasing peroxidase concentration up to  $8 \mu\text{L}/\text{mL}_{\text{buffer}}$ , more enzyme molecules can adsorb as a monolayer onto the free space still available in the nanotubes surface. For concentrations above  $8 \mu\text{L}/\text{mL}_{\text{buffer}}$ , the surface of MWCNTs must be fully occupied by peroxidase molecules, and so, despite an increase in the concentration of enzymatic solution, fewer biomolecules are capable to attach to the carrier.

The influence of time interval during which peroxidase and MWCNTs are in contact was also evaluated ( $8 \mu\text{L}/\text{mL}_{\text{buffer}}$  and pH 6,0). According to Fig. 11b, after 30 min of the immobilization process the maximum enzyme activity was reached. This time interval was enough to enzyme reach adsorption equilibrium onto the carrier. Long contact times don't mean more immobilization yield and more enzyme activity because the high surface area of MWCNTs was completely filled. In other works, the contact time for maximum immobilization of peroxidase on other carriers was much higher: overnight for porous silica nanoparticles (Voss et al., 2007) and for ion-beam-treated polyethylene (Kondyurin et al., 2012); 48 h for chitosan (Bindhu and Abraham, 2003) and for macroporous of glycidyl methacrylate GMA (Prokopijevic et al., 2014); 20 h for nanoporous copper (Qiu et al., 2010).

To finish, it is possible to conclude that the optimum conditions for peroxidase immobilization on MWCNTs are acid pH (4,5), peroxidase concentration of  $8 \mu\text{L}/\text{mL}_{\text{buffer}}$  and contact time of 30 min.

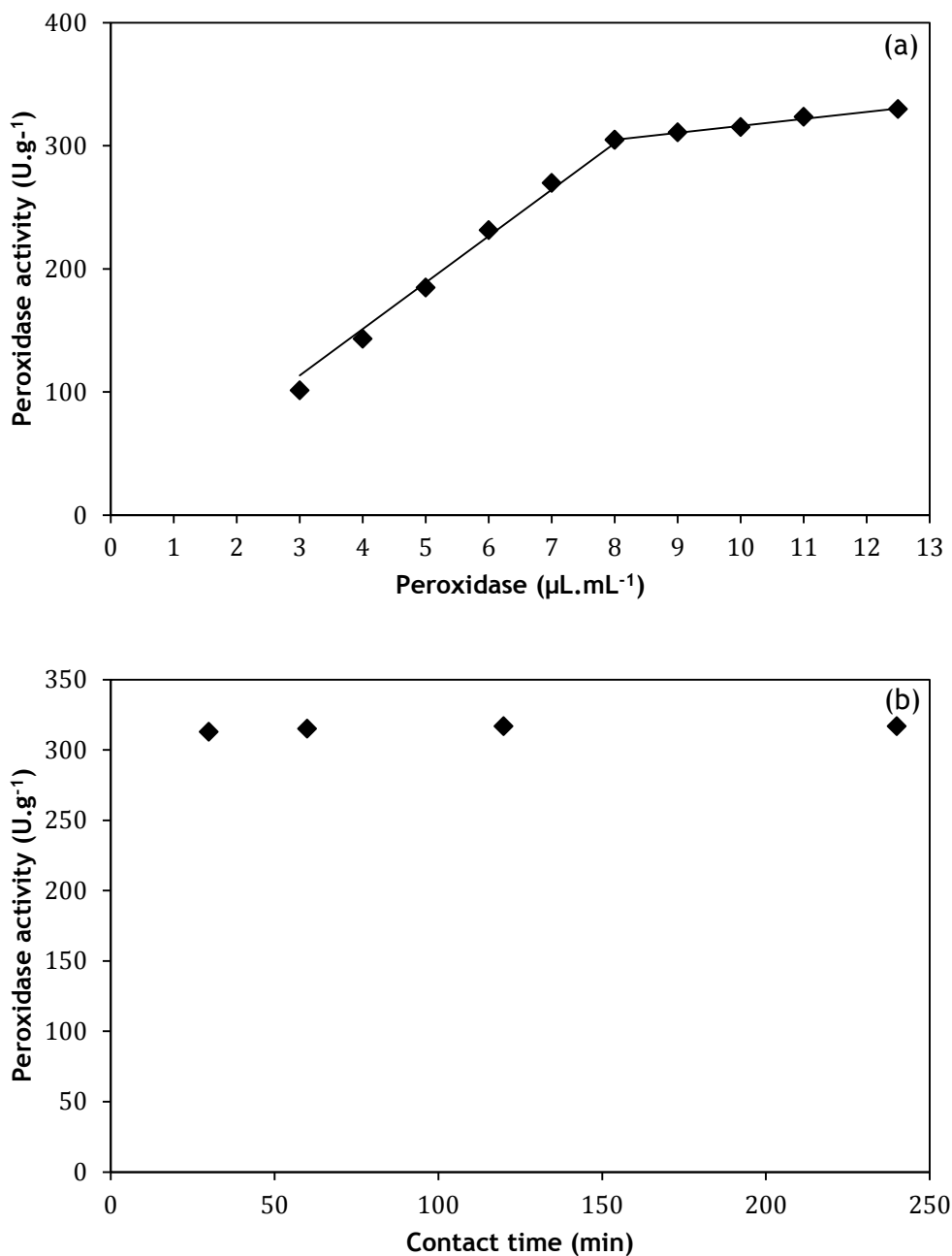


Fig. 11 - Enzymatic activity registered in the catalysis using MWCNT with immobilized peroxidase when immobilization was performed with peroxidase solutions of different concentrations (a) and for different periods of contact time (b).

### 4.3 Effect of MWCNT surface chemistry on peroxidase immobilization

As described above, MWCNTs have been demonstrated to have the ability to adsorb many types of enzymes. This adsorption is a commonly used non-covalent technique and it involves both hydrophobic and electrostatic interaction (Karajanagi et al., 2004). Apart from these two types of interactions, hydrogen bonds and nonspecific adsorption ( $\pi$ - $\pi$  interactions) can also play an important role for enzyme adsorption onto CNTs (Matsuura et al., 2006).

Adsorption capacity and activity of bound protein depends on several factors, mainly the CNT surface properties and enzyme side chain functional groups.

In this section, the influences of pH and carrier treatment in immobilization of peroxidase were studied.

As depicted in Fig. 12, the maximum peroxidase activity was obtained when immobilization was performed at pH 6. This is the optimal pH value for maximizing the rate of reaction of this enzyme (Heinzkill et al., 1998). The results show that when immobilization was performed in acidic media and neutral, peroxidase activity was higher than alkaline media. So it can be concluded that the immobilized peroxidase is stable at acid pH. This may be explained by the maintenance of the native structure of the immobilized peroxidase and by the interactions between enzyme and MWCNTs which was more favorable at this pH. Reports found in literature on peroxidase immobilization in other supports, show that the optimum pH for the peroxidase immobilization on magnetite-modified polyaniline was in the range between 4.0 and 6.0 (Barbosa et al., 2012) and on calcium alginate gel beads was 7,4 (Nahakpam et al., 2008).

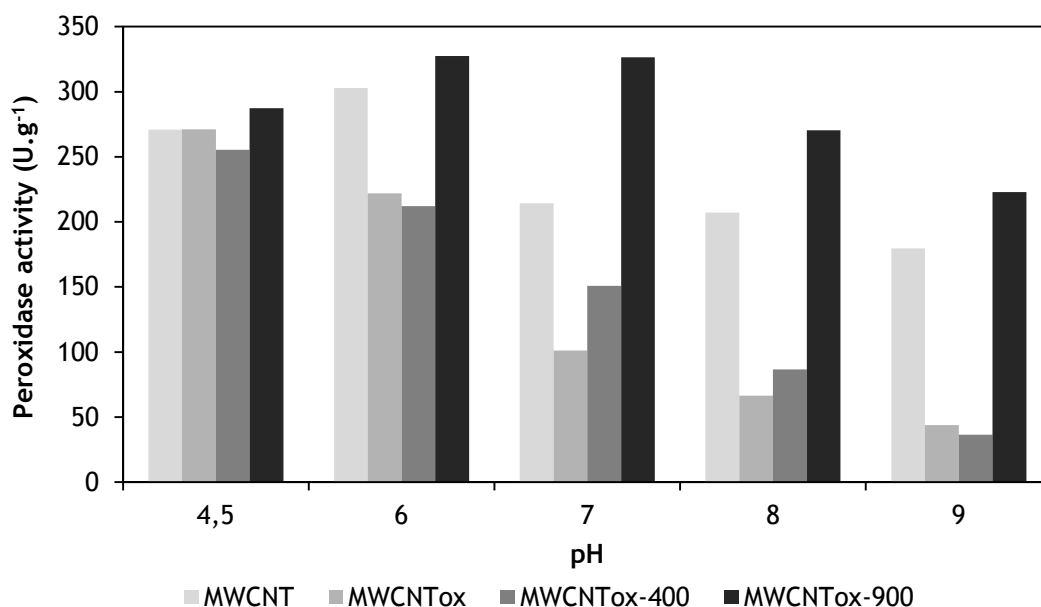


Fig. 12 - Immobilized peroxidase activity on treated MWCNTs at different pH values

The influence of pre-treatment of the carrier is also represented in Fig. 12. Different types of MWCNTs were compared. As already mentioned, the oxidation process with  $H_2SO_4$  and/or  $HNO_3$  results on the oxidation of CNTs. Specifically, the treatment with  $HNO_3$  (sample MWCNTox) leads to the introduction of carboxylic acid, phenol, carbonyl and quinone groups on the nanotube's surface. These groups represent useful sites for further modifications. They enable the covalent coupling of molecules through the creation of amide and ester bonds. By this method the nanotubes can be provided with a wide range of functional moieties, for

which purpose bifunctional molecules are often utilized as linkers. The thermal treatment at 400 °C selectively removes carboxylic acid groups and by treating the MWCNT oxidized with HNO<sub>3</sub> at 900 °C it is expected that most of the surface groups be removed from the surface of the material (Figueiredo and Pereira, 2010). This has been demonstrated earlier in the material's characterization section.

Analyzing the Fig. 12, it can be concluded that the different MWCNT materials presented different behavior along the immobilization pH range tested. The results can be mostly rationalized in terms of the electric charge properties of both the enzyme and the support. The isoelectric point of peroxidase is around 3,5 (Fig. A17), which means that, at this pH, it is in its neutral state. Oxidized materials have generally points of zero charge ( $pH_{PZC}$ ) at very low pH (around 3); as carboxylic acid groups are removed at 400 °C, the  $pH_{PZC}$  increases normally to values around 4 and when treated at 900 °C,  $pH_{PZC}$  is normally neutral, since most of the surface groups are removed from the surface of the nanotubes (Gonçalves et al., 2013). For example, in the materials oxidized with HNO<sub>3</sub> and treated at 400 °C, the maximum immobilized activity corresponded to pH 4,5. For higher pH values both enzyme and support are negatively charged and therefore repulsive interactions may occur. At low pH, the interaction of the available protons in the medium may change the ionization state of some aminoacids and, consequently, the structure of the enzymes immobilized, affecting their function.

The highest enzymatic activity value obtained was 327,4 U.g<sup>-1</sup>, at pH 6,0, for a CNTs treated at 900 °C. At these pH conditions, the enzyme is negatively charged and the carbon nanotube's surface is positively charged, thus the main driving force between enzyme and carrier is electrostatic attraction mechanism. In this way, analyzing the immobilized peroxidase activity, it can be said that the best support for the peroxidase immobilization was the one that was treated at 900 °C, where the highest activities were obtained. This can be explained by the higher and stronger interactions that may have increased the amount of immobilized peroxidase.

Comparing the pristine MWCNT with the oxidized MWCNT, it can be conclude that nanotubes purified with sulfuric acid allowed a better enzymatic activity than those oxidized with nitric acid. This can be explained by the fact that the use of sulfuric acid in the purification process causes both, purity improvement as well as partial oxidation of carbon. However, the longer oxidation reaction of nanotubes with HNO<sub>3</sub> should increase the number of carboxyl groups influencing the stabilization of peroxidase. A higher dependence of enzyme activity on solution pH was observed for this case. This effect becomes more obvious when solid supports with polar or ionic groups on their surfaces are used for the immobilization of enzymes. MWCNT oxidized with HNO<sub>3</sub> have carboxylic groups on the surface. Therefore, the

dependence of the activity of the immobilized peroxidase on solution pH is expected to be different from that of the free peroxidase.

The immobilization yield (%) and the recovered activity (%) are shown in Table 8 and Table 9, respectively. These two parameters allow us to analyze the effectiveness of each type of support for the immobilization of peroxidase at different pH values.

*Table 8 - Peroxidase immobilization yield on the MWCNT materials for the different pH*

Immobilization Yield %				
pH	MWCNT	MWCNTox	MWCNTox-400	MWCNTox-900
4,5	99,8	87,9	83,7	94,0
6	96,4	75,5	73,2	85,1
7	98,4	68,7	67,2	83,4
8	90,8	68,8	65,3	80,3
9	95,4	73,3	47,8	84,8

*Table 9 - Recovered activity of the immobilization process for the different pH of the medium used to perform immobilization*

Activity Recovered %				
pH	MWCNT	MWCNTox	MWCNTox-400	MWCNTox-900
4,5	2,0	2,3	3,0	2,3
6	2,3	1,8	2,9	2,3
7	1,2	0,9	1,6	2,4
8	1,8	0,7	1,0	2,2
9	1,4	0,4	0,8	1,6

It can be observed that even without any further treatment, purified MWCNT shows higher immobilization capacities (90-100%) over the range of pH tested. This value was also obtained for laccase immobilization (Silva et al., 2014). In this purification treatment, no defects were created at the surface of CNTs. So, peroxidase is immobilized on MWCNT by physical adsorption, where hydrophobic and  $\pi$ - $\pi$  stacking interactions (with peroxidase hydrophobic regions and aromatic rings, respectively) are the most probable interactions.

In other way, the peroxidase immobilization on functionalized MWCNT results from specific electrostatic interactions between carboxyl groups and proper polar or ionic groups of peroxidase. This should result in much higher immobilization yield, but this did not occur. It



can be related to the creation of covalent bonds between the COOH groups and the enzyme, which is not likely to occur in this case; being necessary a mediator such as carbodiimide for carboxylic acid activation (Asuri et al., 2006).

Among the modified materials, MWCNTox-900, which has a  $pH_{PZC}$  normally neutral, presents the highest immobilization capacity. In this case, more intense electrostatic interactions are expected for acid-neutral pH values, conditions at which the carbon support is positively charged and the enzyme is negatively charged. On the other hand, MWCNTox-400 shows the lowest immobilization efficiency, which may be related to the proximity between the  $pH_{PZC}$  of the carbon materials (4,0) and the  $pI$  of peroxidase (3,5). The same happens with MWCNTox, which has a  $pH_{PZC}$  of 3,0. However, it shows higher immobilization yield than MWCNTox-400. These results can be explained by the fact of MWCNTox surface being negatively charged while peroxidase is positively charged, leading to the existence of stronger electrostatic interactions between the enzyme and this materials, rather than with MWCNTox-400.

It must be noticed that even if the immobilization efficiency is high, that doesn't mean that all enzymes immobilized are available to react, since they can attach to enzymes previously attached to the carrier or in an orientation that block the active site of the enzyme or too close to other enzyme molecules, generating allosteric hindrances that difficult/prevent the access to the substrates. Then, according to Table 9, considering the values between the optimal range of pH 4,5-7, the maximal recovery of activity is registered on carrier with a thermal treatment at 400 °C (3,02%), despite the immobilization efficiency has not been the best. This may be due to the arrangement of the enzymes on the nanotubes surface, where the density and the orientation of the enzymes optimize their activity. An example that can support this explanation is the case of purification with H<sub>2</sub>SO<sub>4</sub>. In this case, the immobilization yield is higher, but the activity recovered was one of the lowest. Possible allosteric changes in enzyme may have happened. It is worth noticing that the percentage of recovery of activity is also low. In consequence, the majority of the enzymes immobilized on the different carriers are not able to perform catalysis.

Considering all the results, we can say that the best pH value to perform the enzymatic immobilization is 4.5. Regarding the choice of support, if we want a better enzyme activity we should choose the treatment at 900 °C. On the other hand, if we want perform immobilization without wasting much enzyme, we should choose the nanotubes purified with H<sub>2</sub>SO<sub>4</sub>.

#### **4.4 Thermal stability of free and immobilized peroxidase**

The temperature influences the speed of an enzymatic reaction such as with any chemical reaction. However, in the case of enzymes, the effect produced is more complex due to external factors such as the effect of temperature on enzyme structure and on complex enzyme-substrate, ionization of aminoacids, etc. The reaction rate typically reaches a maximum temperature, and for higher temperature values, there is a rapid loss of enzymatic activity resulting from protein denaturation. The enzyme deactivation during reaction and storage (section 4.6) is often a critical limitation to commercial use. Therefore, the thermal stability of free and immobilized peroxidase (MWCNTox-400) was evaluated. The samples were incubated in buffer solution at different temperatures from 30 to 50°C. The thermal parameters for immobilized peroxidase on purified and functionalized MWCNTs were also investigated at 40 and 50°C. It was considered that the pattern of thermal deactivation of this enzyme follows an exponential decay, so, the experimental points for both free and immobilized peroxidase could be adequately represented by Equation (3.7. In this model the enzyme was inactivated in only one phase (a one-step transition between the active and denatured state) considering the possibility of the existence of remaining activity, which is represented by the  $\alpha$  parameter.

As can be seen in Fig. 13, it is evident that the thermal stability of the peroxidase immobilized on CNTs was improved. The free peroxidase lost its activity after 40 min of incubation at 50°C and it was nearly zero after 2 h at 35-40°C, whereas the immobilized peroxidase retained almost 44% of its initial activity after 2 h of incubation at highest temperature. This result is in agreement with thermal stabilization shown in Table 6 for other fungal peroxidase. This inactivation is probably due to a higher vibration of the peroxidase structure that may break some chemical bonds inside the molecule and, as consequence, change its 3D structure (Silva et al., 2014). Thus, the enzyme acquires a conformation which doesn't allow them to maintain their catalytic capacity. For higher temperatures, (Asuri et al., 2006) shown that the native SBP has a half-life of 9 min at 90 °C and this is increased sevenfold for the MWCNT-SBP conjugates.

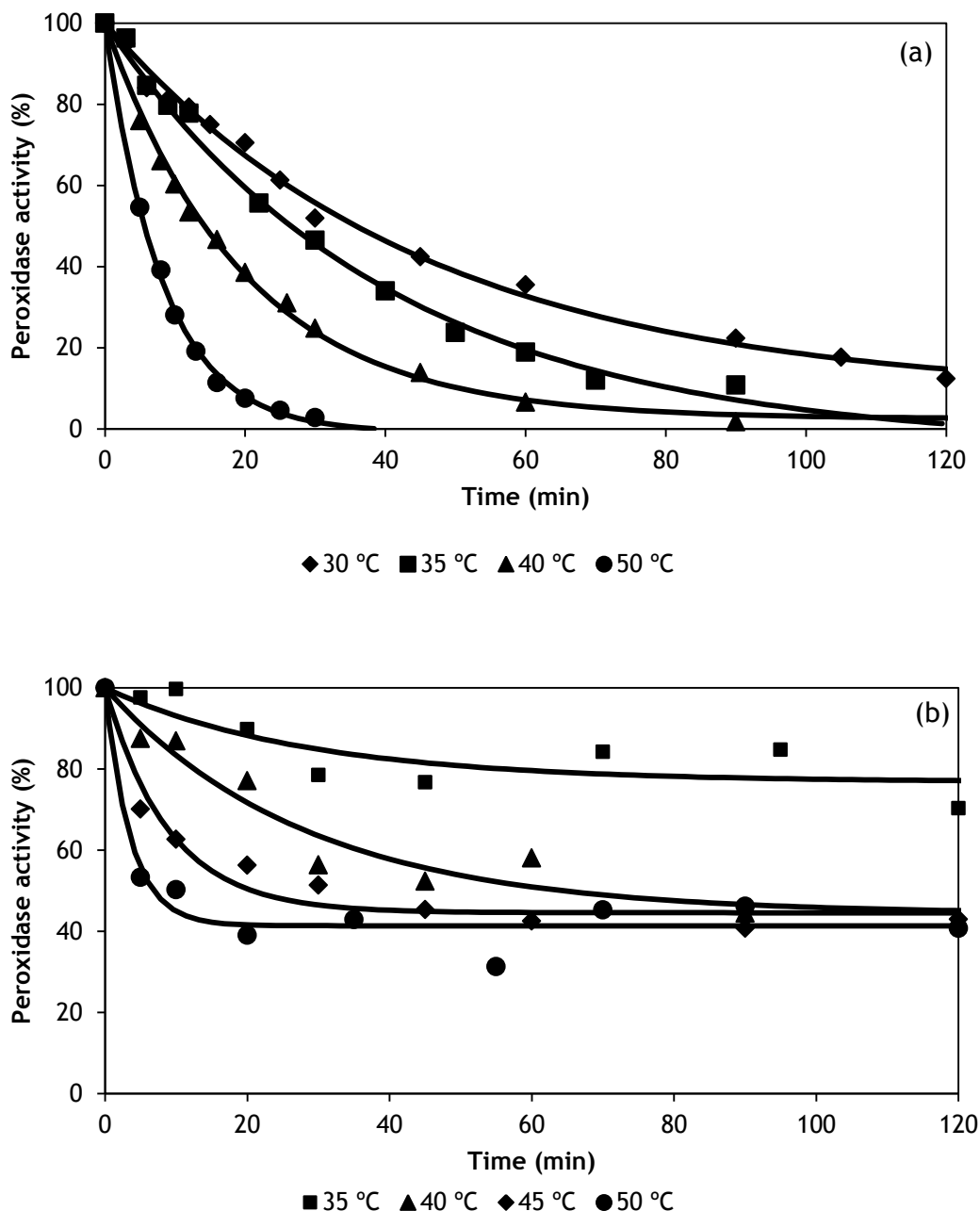


Fig. 13 - Thermal inactivation of (a) free peroxidase and (b) immobilized on MWCNTox-400

The increase thermal stability observed for the immobilized enzyme observed may be attributed to a reduction in the protein structure mobility, due to anchorage to the support and subsequent translation of the rigidity at each anchorage point to the whole enzyme structure, thus protecting it from the denaturing effects of the environment (Verma et al., 2013). Specifically, the native enzyme has a half-life of 5.6 min at 50 °C (Table 10). The stabilization of peroxidase upon conjugation onto the MWCNTs is not surprising given the well-known stabilization of enzymes on solid supports. The increased stabilization can be due to multi-point attachment of the enzyme to the support and/or because of decreased

protein-protein interactions on the highly curved surface of carbon nanotubes (Asuri et al., 2006).

The thermal parameters  $\alpha$ ,  $k$  and  $t_{1/2}$  for free and immobilized peroxidase are presented in Table 10.

*Table 10 - Thermal parameters and thermal stabilities obtained for the thermal inactivation of free and immobilized peroxidase*

**Free peroxidase**

T (°C)	k (h <sup>-1</sup> )	$\alpha$	$t_{1/2}$ (h)	$\Delta G^0$ (kJ.mol <sup>-1</sup> )	$\Delta H$ (kJ.mol <sup>-1</sup> )	$\Delta S$ (J.mol <sup>-1</sup> )	Ea (kJ.mol <sup>-1</sup> )
30	1,316±0,081	8,135±2,617	0,597	94,239	71,661	-74,477	74
35	1,479±0,117	4,162±4,039	0,442	95,536	71,620	-77,612	
40	3,039±0,094	2,480±1,264	0,237	95,254	71,578	-75,605	
50	7,323±0,228	0,867±1,099	0,093	96,017	71,495	-75,883	

**Immobilized peroxidase**

T (°C)	k (h <sup>-1</sup> )	$\alpha$	$t_{1/2}$ (h)	$\Delta G^0$ (kJ.mol <sup>-1</sup> )	$\Delta H$ (kJ.mol <sup>-1</sup> )	$\Delta S$ (J.mol <sup>-1</sup> )	Ea (kJ.mol <sup>-1</sup> )
35	2,115±1,204	76,824±4,598	-	94,620	119,129	79,535	122
40	2,124±0,580	44,290±6,238	1,072	96,187	119,087	73,131	
45	6,733±1,061	44,569±1,921	0,345	94,712	119,046	76,485	
50	16,848±4,217	41,366±2,070	0,114	93,778	119,004	78,063	

The stabilization of peroxidase through this immobilization method can be also confirmed by these results. After the immobilization, higher enzyme half-life time ( $t_{1/2}$ ) was obtained, which means that a longer period of time is necessary to denaturate/deactivate the

peroxidase. For example, comparing at 40 °C, the  $t_{1/2}$  was 4.5 times higher for immobilized peroxidase than for the free form. Although in some cases initial inactivation is faster for immobilized peroxidase 50 °C, which results in a higher  $k$  parameter, the remaining activity,  $\alpha$  parameter, increases after 2 hours. This fact is rapidly confirmed by the Fig. 13, where the remaining enzyme activity was considerably higher for immobilized peroxidase at all temperatures. As previously stated, the CNTs adsorb the enzyme and protected it from the denaturing effects of the environment.

The Arrhenius activation energy ( $E_a$ ) is best regarded as an experimentally determined parameter that indicates the sensitivity of the reaction rate to temperature. Thus, the activation energies, for the thermal enzymatic deactivation, were obtained by Equation (3.8). As a non-linear equation, the  $E_a$  parameter was estimated by an Arrhenius plots ( $\ln k$  vs  $T^{-1}$ ). The results are shown in Fig. A8. The activation energies of free and immobilized peroxidase were 74 and 122  $\text{kJ}\cdot\text{mol}^{-1}$ , respectively. These results confirm what was been said so far, as more energy is required to deactivate the immobilized peroxidase.

The thermodynamic parameters presented in Table 10 can be helpful in predicting enzyme stability. Protein unfolding is followed by the rupture of several links, generating a disorganized system. This increase in entropy ( $\Delta S$ ) (Eq. (3.11)) is compensated by a decrease in Gibbs free energy (Eq. (3.9)), making it easier for denaturation to occur, meaning that, when the susceptibility to denaturation is higher, the enzyme is in a less energetic state and in greater disorder, since its original structure has been destroyed (Aguiar-Oliveira and Maugeri, 2011).

In relation of free peroxidase, the values of enthalpy of denaturation ( $\Delta H$ ) and free energy of denaturation ( $\Delta G$ ) were 71,578  $\text{kJ}\cdot\text{mol}^{-1}$  and 95,254  $\text{kJ}\cdot\text{mol}^{-1}$  while that of entropy of deactivation ( $\Delta S$ ) was -75,605  $\text{J}\cdot\text{mol}^{-1}\cdot\text{K}^{-1}$  at 40 °C. At this temperature, for immobilized enzyme, the value of  $\Delta G$  was slightly higher 96,187  $\text{kJ}\cdot\text{mol}^{-1}$ . This increase in  $\Delta G$  revealed that the thermal stabilization of peroxidase was due to the higher free energy (functional energy) which enabled the enzyme to resist against unfolding of its transition state. It should be noted that all  $\Delta G$  values was positive and in the same order of magnitude, which indicates that the thermal inactivation process is thermodynamically nonspontaneous and slightly decreases with the temperature.

The large value of  $\Delta H$  is associated with increased enzyme stability unless coupled with a large compensatory increase in the value of  $\Delta S$ , which is destabilizing. Hence, stability of enzyme is enhanced with moderately high levels of  $\Delta H$  and low levels of  $\Delta S$ . When a protein molecule is deactivated the randomness of the system increases which is a direct measure of entropy. By second law of thermodynamics, the entropy of the system is positive but the negative values of entropy are often encountered in the case of enzymes. As shown in Table

10, a large values of  $\Delta H$  were obtained for immobilized peroxidase, which indicates more stability. However, positive  $\Delta S$  values were obtained for immobilized peroxidase. The positive values of  $\Delta S$  indicates protein unfolding reaction as the rate-limiting step during thermal deactivation under the studied conditions (Owusu et al., 1992). Thus, the negative  $\Delta S$  for free peroxidase suggests that the rate-limiting reaction probably involves the aggregation of partially unfolded enzyme molecules which are predominant during the exposure of protein to high temperatures.

Finally, in order to evaluate the influence of carbon nanotubes functionalization in the thermal stability of peroxidase, the thermal deactivation parameters were estimated at 40 °C and 50 °C, represented in Table A4 and Table 11, respectively..

*Table 11 - Thermal parameters (50 °C) for free and immobilized peroxidase on purified and functionalized MWCNT*

Enzyme	Thermal parameters (50°C)		$t_{1/2}$ (h)
	$\alpha$	$k$ (h <sup>-1</sup> )	
Free	-0,867±1,099	7,323± 0,228	0,093
MWCNT	16,028±3,133	7,691±1,263	0,118
MWCNTox	29,876±3,027	13,777±3,691	0,091
MWCNTox-400	41,366±2,070	16,848±4,217	0,114
MWCNTox-900	28,686±2,850	10,097±2,146	0,120

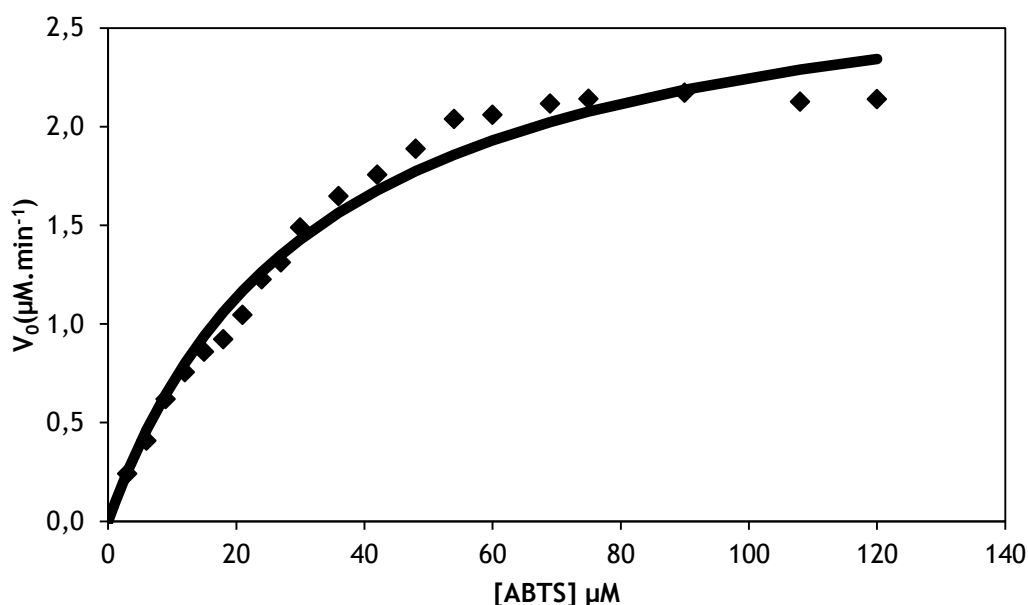
The data show that the peroxidase is thermally more stable when it is immobilized on MWCNTox-400, at 50 °C. In this case, the parameters  $\alpha$  and  $k$  are higher compared to other samples, (41,366 and 16,848 h<sup>-1</sup>) which means that despite the faster initial inactivation, after 2 h of incubation period, peroxidase maintains higher residual activity (41,37%). This indicates that the adsorption of peroxidase is more stable in this support due to the availability of OH groups on the surface of the CNTs, which allows the creation of hydrogen bonds with the enzyme.

Comparing the purified MWCNTs with the sample MWCNTox, it can be said that the oxidation treatment can promote the stabilization of immobilized enzyme. The  $\alpha$  value was almost 2

times higher for MWCNTox. A sample with same treatment was used to immobilize the laccase enzyme, and it was obtained a  $\alpha$  value 1.3 times higher than purified MWCNTs. This can be explained by the presence of carboxylic acid and phenol groups on the nanotube's surface, which provides a more stable peroxidase immobilization. On the other hand, MWCNTs have negligible amounts of surface groups, so the interactions between this support and the peroxidase are weaker. The value of this parameter should also be lower for nanotubes treated at 900 °C, almost equal to that of the purified nanotubes, but this was not observed. This is probably due to intense electrostatic interactions and to the higher surface area and higher porous diameter than pristine MWCNTs, which may protect the enzyme from denaturing effects of the environment.

#### 4.5 Kinetic parameters of free and immobilized peroxidase

A more accurate assessment of the changes in the peroxidase enzyme after immobilization would be to examine the difference in enzyme kinetics, i.e. the affinity of ABTS oxidation. To obtain the kinetic parameters  $K_M$  and  $v_{max}$ , the initial reaction rates of the ABTS oxidation by both free and immobilized peroxidase were measured at a predetermined range of substrate concentrations. The parameters for free and immobilized peroxidase were calculated using the Michaelis-Menten equation as shown in Eq. (3.12) and are summarized in Table 12.



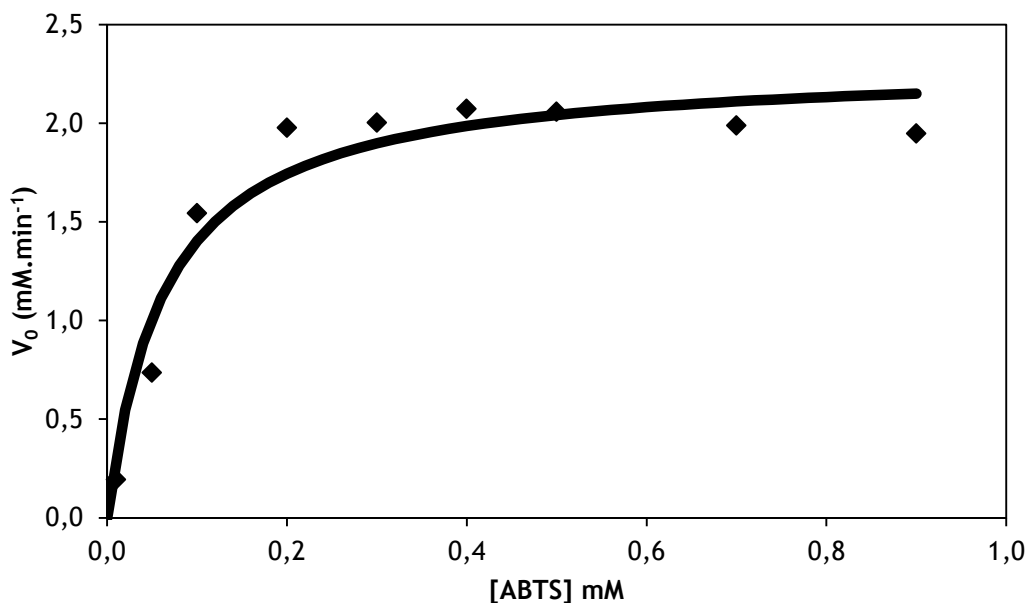


Fig. 14 - Michaelis-Menten plot for peroxidase catalysis. Effect of substrate concentration on the initial rate of oxidation of ABTS catalyzed by (a) free peroxidase and (b) MWCNT-peroxidase.

The behavior of free and immobilized peroxidase was different. Free peroxidase followed conventional Michaelis-Menten kinetics for ABTS as substrate (Fig. 14a) with a  $K_M$  of  $0,033 \pm 0,004$  mM and a  $v_{max}$  of  $2,979 \pm 0,130$  mM.min<sup>-1</sup>. This value of  $K_M$  obtained is in accordance with data on Table 6 for *Coprinus cinereus* peroxidase. On the other hand, for MWCNT-peroxidase conjugates (Fig. 14b), the kinetic parameters  $K_M$  and  $v_{max}$  were  $0,064 \pm 0,018$  mM and  $2,303 \pm 0,137$  mM.min<sup>-1</sup>, respectively. The constant  $K_M$  measures the affinity of enzyme-substrate complex and it is specific for each enzyme. Thus, the higher  $K_M$ , the more amount of substrate is necessary, for the reaction, to reach half of  $v_{max}$ , that is, the affinity of the enzyme for the substrate is smaller. Then, it can be concluded that the immobilization diminishes the affinity of peroxidase to ABTS, however diffusional limitation should also be considered. As seen in Table 12, the catalytic efficiency, as given by the  $v_{max}/K_M$  ratio, has decreased after immobilization onto purified MWCNTs. This is expected, as immobilization of the peroxidase enzyme would induce changes in the enzyme conformation that, directly or indirectly, affect the active site, thus reducing the enzyme activity. In the same way, the immobilization process induces some limitations of mass transfer of the substrate to the surface of MWCNTs. In other works, the catalytic efficiency of SBP covalently immobilized on MWCNTs was nearly 40% of that for native SBP in aqueous solution (Asuri et al., 2007) and up to 57% for amyloglucosidase (AMG) immobilized non-covalently on SWCNTs (Goh et al., 2012). The enzyme activity after covalent immobilization is much lower than physical adsorption. (Goh et al., 2012) deduce that that the increased



enzyme loading in covalent immobilization is offset by a greater change in the enzyme conformation, therefore resulting in reduced catalytic activity.

Table 12 - Kinetic parameters of ABTS oxidation for free and immobilized peroxidase on purified MWCNTs

Peroxidase	$v_{max}$ (mM.min <sup>-1</sup> )	$K_M$ (mM)	$v_{max}/K_M$ (s <sup>-1</sup> )
Free	2,979±0,130	0,033±0,004	1,505
Immobilized	2,303±0,137	0,064±0,018	0,600

Several methods have been used to determine the changes on secondary structure of enzymes after immobilization on carbon nanotubes, e.g. circular dichroism spectroscopy CD<sup>1</sup> and FT-IR spectra (amide I region 1600-1700 cm<sup>-1</sup>). This region, which consists mainly of the C=O stretching vibration of the backbone peptide bonds in proteins, has been used to estimate quantitatively the secondary structural features of proteins (Dong et al., 1990; Vedantham et al., 2000). This spectrum can be used to obtain the  $\alpha$ -helix and  $\beta$ -sheet contents of peroxidase. Karajanagi et al., (2004) reported that the differences in secondary structure between the soluble and adsorbed SBP, as represented by the simple sum of magnitudes of changes in  $\alpha$ -helix and  $\beta$ -sheet contents, were 13% and, relatively to the 3D shape, the SBP retains its native three-dimensional shape on the nanotube surface. Other case, when HRP is attached covalently to SWCNTs retains 68% of its native  $\alpha$ -helix (Asuri et al., 2007); this value is similar to that for the previous case, where SBP retains 77% of its native  $\alpha$ -helix content when noncovalently adsorbed onto SWCNTs (Karajanagi et al., 2004). Goh et al., (2012) studied the role of the surface chemistry of carbon nanotubes on the enzyme conformation change. They concluded that the structural changes by physical adsorption and covalent approach are similar probably because both surfaces involve carboxylic groups in the enzyme immobilization, thus resulting in similar structural changes (Goh et al., 2012).

#### 4.6 Storage and operational stability of immobilized peroxidase

The stability of a product is an important consideration in the estimation of its shelf life and can affect its feasibility for apply in the industry or other commercial use. The activity of the immobilized peroxidase should be stable for a reasonable period of time, before any application. Hence, the storage stability of free and MWCNT-peroxidase conjugates was

<sup>1</sup> CD analysis is considered more accurate, as the protein remains in its aqueous environment during the analysis, and thus can be used to correlate to its activity

evaluated by incubating the conjugates for extend periods in aqueous buffer pH 6 at 4 °C ( $T_{\text{refrigerator}}$ ) and the results are presented in Fig. 15

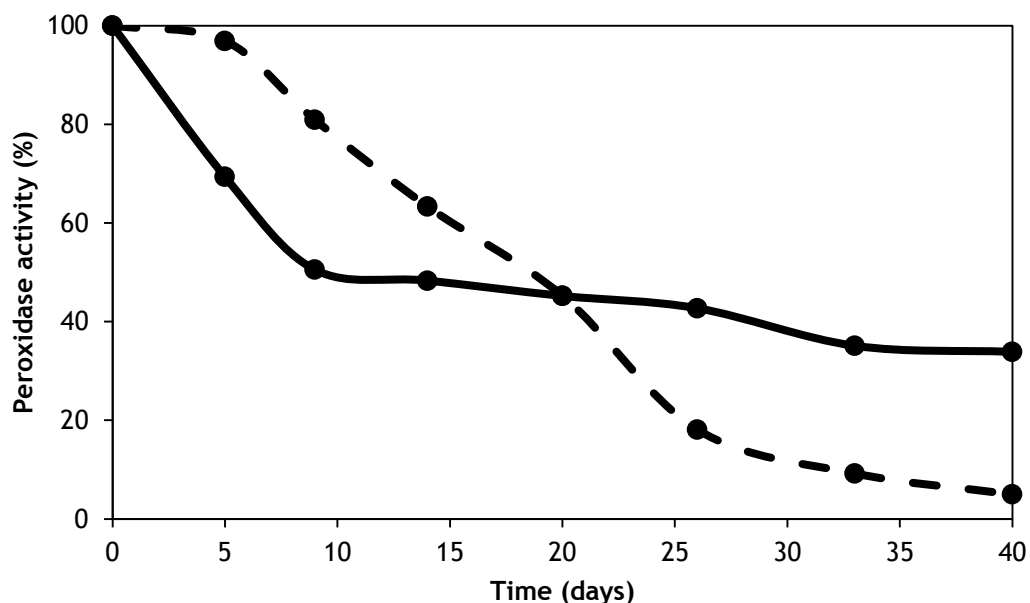


*Fig. 15 - Storage stability of the free (dashed line) and immobilized (solid line) peroxidase by physical adsorption at 4 °C over 40 days.*

From Fig. 15, it is evident that the activity of the peroxidase was more stable when stored at immobilized form than at free form. Even after 40 days the MWCNT-peroxidase conjugates retained ca. 34% of its initial activity, whereas native peroxidase retained only 5% of its activity. It can be considered that peroxidase immobilized on purified MWCNTs is stable when stored at 4 °C for a large period of time.

Reuse of immobilized enzymes is a highly relevant to the industry, as enzymes incur fixed costs in production lines. To that end, the reusability of the MWCNT-MNP-peroxidase conjugates was examined (Fig. 16). This was carried out by repeatedly incubating the magnetic conjugates in an ABTS solution, measuring the catalytic activity, and then recovering the immobilized peroxidase by a simple magnet and its subsequent reuse in a new fresh substrate solution. This stability can provide essential information about the biocatalyst resistance and effectiveness of this support. It should be noted that these MWCNTs were magnetic as can be seen in Fig. A6 and could be easily collected from the dark green solution after repeated usage which suggests that the adopted and adapted protocol proposed by (Xu et al., 2008) was appropriate for our MWCNTs.

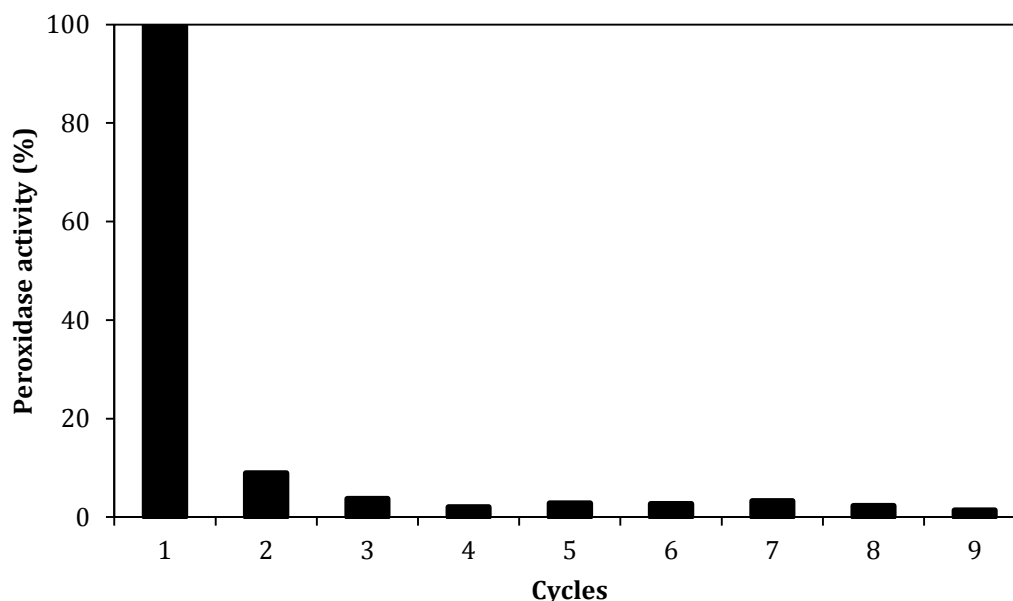


*Fig. 16 - Reusability of complex mMWCNT-Peroxidase*

Analyzing Fig. 16, it can be immediately concluded that this magnetic complex is not useful for peroxidase reusability. Although the mMWCNT-peroxidase conjugates can be easily recovered with a simple magnet, the peroxidase loses almost all of its activity after the first cycle. This can be explained by several factors that lead to the loss of peroxidase activity. First, the peroxidase can be desorbed from the magnetic nanotubes after each cycle. This should not be the main reason because after immobilization process and before the first cycle, this complex is washed several times, which does not justify the large difference observed. However, it is an aspect to take into account because, as the MNPs are covalently linked to the carboxyl groups of the MWCNTox and some MNPs are also adsorbed on the surface, the peroxidase may not have space to adsorb strongly to the carbon nanotube, binding, possibly, to MNPs. Another aspect is the change in peroxidase conformation after reaction with ABTS. The change on the structure of an enzyme and, specially, the availability of the active site are important to define the enzyme activity. After oxidation of ABTS, the active site of peroxidase can be structurally altered or occupied with product, or even the compound I cannot be formed by the hydrogen peroxide oxidation, stopping the reaction process.

The same behavior was observed with peroxidase immobilized on MWCNTox-400 (Fig. A14) and immobilized on a MWCNTs membrane (Fig. A15). This corroborates the last aspect mentioned above.

These results were not expected. In order to understand the influence of the immobilization method and the influence of the functionalization of MWCNTs, it can be made in future the covalent immobilization of peroxidase on MWCNTs with MNPs adsorbed. Asuri et al., (2007)

reported, for SBP immobilized covalently in MWCNTs that after 20 cycles the activity recovered was about 60%. A circular dichroism spectroscopy and a quantification of protein after each cycle may also be important.

#### 4.7 Discoloration of textile dyes

Dyes used for paper printing, colour photography, textile dyeing and as an additive in petroleum products have a synthetic origin and complex aromatic molecular structure (Hamid and Khalil ur, 2009). About 10-15% of the synthetic dyes produced are discharged into industrial effluents (Spadaro et al., 1992), causing environmental problems. Recently, the enzymatic approach has attracted much interest in the discoloration/degradation of these dyes from wastewater as an alternative strategy to conventional chemical and physical treatments, which pose serious limitations such as high cost, limited applicability and high energy input, and usually these treatments may result in the production of toxic by-products. As mentioned before, soluble enzymes have limitations such as stability and reusability and cannot be exploited at the large scale. Therefore, the use of immobilized enzymes has significant advantages over free form enzymes.

With this approach, discoloration of 3 synthetic dyes (RB5, RB and BR) was evaluated by free and immobilized peroxidase. Magnetic nanotubes were used to perform peroxidase immobilization, and thus, in addition to the advantages of immobilization on carbon nanotubes, the easy recover of the immobilized enzyme is added. The results are summarized in Table 13.

*Table 13 - Dye discoloration % of RB5, RB and BR by free and immobilized peroxidase on mMWCNTs. (1) 1<sup>st</sup> cycle, (2) 2<sup>nd</sup> cycle*

Dye	Peroxidase	mMWCNT-Px		mMWCNT		mMWCNT-Inactive	
		1	2	1	2	1	2
RB5	27	4	-	3	-	3	-
RB	91	87	38	64	35	84	36
BR	98	80	13	12	8	85	15

The percentages of discoloration were different for the three dyes, which indicates that the peroxidase specificity obtained depends on the molecular structure and redox properties of each dye. As it can be seen, the dyes RB and BR were more susceptible to enzymatic treatment, obtaining a dye discoloration of 91% and 98%, respectively. It is important to note that it was a quick reaction with the free peroxidase. On the other hand, for RB5 dye only

27% degradation was observed, this was a result of the low affinity between this dye and peroxidase.

The mMWCNT-Peroxidase conjugate was also evaluated. A decrease in dye discoloration % was observed in all samples. This was expected due to diffusional limitations. For the dye RB5, practically no interaction occurred with the enzyme immobilized on the nanotube, and thus it was not analyzed its reusability. For the control samples, it was found that only with magnetic carbon nanotubes can absorb dye, especially RB dye. These results were expected due to the high surface area and porosity of this material. In other studies, the absorption percentage of dyes on MWCNT was almost 96%. Comparatively, this obtained result was not so high because, in this case, it was used oxidized MWCNT with MNPs adsorbed into its surface. However, it should be taking into account the possibility of Fenton reaction ( $H_2O_2/Fe^{2+}$ ). (Lucas and Peres, (2006) reported that RB5 can be effectively decolorized using Fenton process for optimal conditions. The best degradation % was obtained for dye BR, with 68% of immobilized enzymatic discoloration, followed by 23% for dye RB. Hence, this complex mMWCNT-peroxidase was used in another cycle. It was observed the loss of peroxidase activity, as previously happened when the reusability of immobilized enzyme was tested. The dye discoloration (%) of the control samples (mMWCNT with peroxidase and with inactive peroxidase) were the same in all samples. Thus, this enzyme was not in inactive form and 5 minutes at 100 °C was not enough to disable peroxidase. Finally, it can be said that degradation of dyes is a potential application of peroxidase and the use of this magnetic support may be advantageous due to its easy and inexpensive reuse. However, further testing to optimize the reaction conditions is needed.



## 5 Concluding remarks and research needs

### 5.1 General conclusions

As it has been said, the main goal of this thesis was to develop MWCNT-peroxidase conjugates for applications relevant to biocatalysis. Also, this work aimed to elucidate about the influence of the nanoscale environment on structure and function of this enzyme. To achieve this aim, MWCNTs were produced, functionalized through selective introduction or removal of oxygen-containing groups and finally characterized. Another objective was to evaluate the structure, function, and stability of peroxidase on different MWCNTs with the overall aim of synthesis being the development of biocatalysts with high performance. Finally, the biocatalytic capacity of free and immobilized peroxidase for degradation of textile dyes was studied.

Therefore, several conclusions were obtained accordingly to the aimed goals. Regarding the functionalization process:

- The treatment with nitric acid increases the pore volume and diameter of MWCNTs due to the creation of defect sites ends and/or holes on CNTs sidewall;
- This treatment also introduces carboxylic acid, anhydride, lactone and quinone groups on the MWCNTs surface, confirmed by the characterization tests;
- The pHPZC values of the samples varied according to MWCNTs > MWCNTox-900 > MWCNTox-400 > MWCNTox;
- The presence of functional groups could be confirmed through FT-IR spectra analysis;
- With the FT-IR spectra analysis, the presence of peroxidase on MWCNTox through physical adsorption on carboxylic sites was confirmed;
- For the purified MWCNTs, the main driving forces are hydrophobic interactions between the support and the enzyme;
- On MWCNTox, electrostatic interactions and hydrogen bonding are the main mechanisms involved in the immobilization process;
- For the MWCNTox-400, peroxidase is immobilized by the formation of hydrogen bonds between OH groups at the surface of the nanotubes and peroxidase's amine terminal groups;
- The magnetic characteristic of Fe<sub>3</sub>O<sub>4</sub> modified nanotubes was successfully confirmed.

Regarding the synthesis of biocatalysts with high performance:

- The maximum peroxidase activity was obtained when immobilization was performed at pH 6. It can be assumed that the immobilized peroxidase is stable at relatively acidic conditions;
- Different MWCNT materials presented different behaviors along the immobilization pH range tested. The highest enzymatic activity value obtained was  $327.4 \text{ U.g}^{-1}$ , at pH 6, for the CNTs heat treated at  $900 \text{ }^\circ\text{C}$ ;
- Purified MWCNT allows a better enzymatic activity than those oxidized with nitric acid (MWCNTox);
- Purified MWCNT shows higher immobilization capacities (90-100%) over the range of pH tested;
- Concerning the choice of the support, the carrier with better immobilized enzyme activity is the one which was treated at  $900 \text{ }^\circ\text{C}$  and the carrier with better enzyme immobilization yield is the one which was purified with  $\text{H}_2\text{SO}_4$ ;
- The optimum conditions for peroxidase immobilization on MWCNTs are acid pH (4.5), peroxidase concentration of  $8 \mu\text{L}/\text{mL}_{\text{buffer}}$  and contact time of 30 min;
- On the topic of the thermal treatment, the free peroxidase lost its activity after 40 min of incubation at  $50^\circ\text{C}$  and it was nearly zero after 2 h at  $35\text{-}40^\circ\text{C}$ , whereas the immobilized peroxidase retained almost 44% of its initial activity after 2 h of incubation at the highest temperature. For example, comparing at  $40 \text{ }^\circ\text{C}$ , the  $t_{1/2}$  was 4.5 times higher for immobilized peroxidase than for the free form;
- Peroxidase is thermally more stable when it is immobilized on MWCNTox-400 at  $50 \text{ }^\circ\text{C}$ , due to the availability of OH groups on the surface of the CNTs, which allows the creation of hydrogen bonds with the enzyme.;
- The activation energies of free and immobilized peroxidase were 74 and  $122 \text{ kJ}\cdot\text{mol}^{-1}$ , respectively. These results confirm that further energy is compulsory to deactivate the immobilized peroxidase;
- The oxidation treatment promotes the stabilization of immobilized enzyme and the  $\alpha$  parameter was almost 2 times higher for MWCNTox samples;
- The kinetic behavior of free and immobilized peroxidase was different. Free peroxidase followed conventional Michaelis-Menten kinetics for ABTS as substrate with a  $K_M$  of  $0,033\pm 0,004 \text{ mM}$  and a  $v_{max}$  of  $2,979\pm 0,130 \text{ mM}\cdot\text{min}^{-1}$  and for the immobilized, the values were  $0,064\pm 0,018 \text{ mM}$  and  $2,303\pm 0,137 \text{ mM}\cdot\text{min}^{-1}$ , respectively;



- The immobilization decreases the affinity of peroxidase with the substrate, however diffusional limitation should also be considered;
- The activity of the peroxidase was more stable when stored in the immobilized form than at free form; After 40 days, the MWCNT-peroxidase conjugates retained ca. 34% of its initial activity, whereas native peroxidase retained only 5% of its activity;
- Despite the mMWCNT-peroxidase conjugates can be effortlessly recovered with a simple magnet, the peroxidase loses almost all of its activity after the first cycle. The same behavior was observed with peroxidase immobilized on MWCNTox-400;

Regarding the biocatalyst application:

- Peroxidase can be used for dye discoloration, obtaining a dye discoloration of 23% for RB5, 91% for RB and 98% for BR;
- Immobilization process reduces the dye discoloration percentage because of diffusional limitations. However, the magnetic support may be beneficial due to its inexpensive and easy reuse;

Overall, the advantages of the using MWCNT supported were demonstrated, as well as the importance of support functionalization in the protection of peroxidase structure perspective. Therefore, the usage of this enzyme by the industries is thought to be a massive advantage.

## **5.2 Perspectives for further research**

During this work, it was noticed that more assessments and more information would be interesting about the theme addressed in this dissertation. Therefore, there are several lines of research which should be pursued.

First of all, although studies on the influence of the functionalization of MWCNTs in the peroxidase immobilization have been performed and the optimal immobilization conditions being established, it was noticed that it was difficult to reuse the MWCNTs-peroxidase complexes. Thus, the covalent immobilization of peroxidase on MWCNTs could be examined in future works. This analysis will allow the comparison of these two types of immobilization and it is expected that the peroxidase is linked more strongly to MWCNTs would facilitate its reusability.

Another aspect, which may also be related to the previous problem is to study the change of the three dimensional structure of peroxidase, after immobilization on these samples, by circular dichroism spectroscopy. This method allows determining the change in  $\alpha$  and  $\beta$  conformation of the enzyme after utilization in the immobilized form.

Regarding the magnetization process, it can be done in future works another type of insertion of MNPs on MWCNTs. In this thesis, it was used the covalent linkage between MNPs and the carboxylic groups on the surface of MWCNTs, through the use of binders such as APTS. However, it will be possible to make the insertion of MNPs inside the MWCNTs leaving the entire surface for peroxidase immobilization. This will enable any functionalization on its surface, adding the same magnetic characteristic of the carrier.

As a final point, concerning the application of this biocatalyst and due to time constrains, the conditions used for dye degradation should be optimized.

### **5.3 Final appreciation**

In brief, this project has been considered as a very successful experience, in which all the expectations were achieved. Although it has been a frankly demanding work, it is expected that the present results contribute to the advance of the scientific knowledge in the field of peroxidase based biocatalysis.

## 6 References

- Aguiar-Oliveira, E. and F. Maugeri (2011). "Thermal stability of the immobilized fructosyltransferase from *Rhodotorula* sp." Brazilian Journal of Chemical Engineering **28**: 363-372.
- Aqel, A., K. M. M. A. El-Nour, R. A. A. Ammar and A. Al-Warthan (2012). "Carbon nanotubes, science and technology part (I) structure, synthesis and characterisation." Arabian Journal of Chemistry **5**(1): 1-23.
- Aso, H., K. Matsuoka, A. Sharma and A. Tomita (2004). "Evaluation of Size of Graphene Sheet in Anthracite by a Temperature-Programmed Oxidation Method." Energy & Fuels **18**(5): 1309-1314.
- Asuri, P., S. S. Bale, R. C. Pangule, D. A. Shah, R. S. Kane and J. S. Dordick (2007). "Structure, Function, and Stability of Enzymes Covalently Attached to Single-Walled Carbon Nanotubes." Langmuir **23**(24): 12318-12321.
- Asuri, P., S. S. Karajanagi, E. Sellitto, D.-Y. Kim, R. S. Kane and J. S. Dordick (2006). "Water-soluble carbon nanotube-enzyme conjugates as functional biocatalytic formulations." Biotechnology and Bioengineering **95**(5): 804-811.
- Balasubramanian, K. and M. Burghard (2005). "Chemically functionalized carbon nanotubes." Small **1**(2): 180-192.
- Balasubramanian, K. a. B., M. (2006). "Biosensors based on carbon nanotubes." Anal Bioanal Chem **385**: 452-468.
- Barbosa, E. F., F. J. Molina, F. M. Lopes, (2012). Immobilization of peroxidase onto magnetite modified polyaniline.
- Bindhu, L. V. and E. T. Abraham (2003). "Immobilization of horseradish peroxidase on chitosan for use in nonaqueous media." Journal of Applied Polymer Science **88**(6): 1456-1464.
- Bommarius, A. S. and B. R. Riebel-Bommarius (2007). Biocatalysis: Fundamentals and Applications, Wiley.
- Bower, C., O. Zhou, W. Zhu, D. J. Werder and S. Jin (2000). "Nucleation and growth of carbon nanotubes by microwave plasma chemical vapor deposition." Applied Physics Letters **77**(17): 2767-2769.
- Brady, D. and J. Jordaan (2009). "Advances in enzyme immobilisation." Biotechnology Letters **31**(11): 1639-1650.

- Brena, B. M. and F. Batista-Viera (2006). "Immobilization of Enzymes". Immobilization of Enzymes and Cells. **22**: 15-30.
- Bruns, N. and J. C. Tiller (2004). "Amphiphilic Network as Nanoreactor for Enzymes in Organic Solvents." Nano Letters **5**(1): 45-48.
- Cabral, J. M. and J. F. Kennedy (1991). "Covalent and coordination immobilization of proteins".
- Chen, J., Q. Chen and Q. Ma (2012). "Influence of surface functionalization via chemical oxidation on the properties of carbon nanotubes." Journal of Colloid and Interface Science **370**(1): 32-38.
- Chen, J., M. A. Hamon, H. Hu, Y. Chen, A. M. Rao, P. C. Eklund and R. C. Haddon (1998). "Solution properties of single-walled carbon nanotubes." Science **282**(5386): 95-98.
- Chen, Q., S. Ai, X. Zhu, H. Yin, Q. Ma and Y. Qiu (2009). "A nitrite biosensor based on the immobilization of Cytochrome c on multi-walled carbon nanotubes-PAMAM-chitosan nanocomposite modified glass carbon electrode." Biosensors and Bioelectronics **24**(10): 2991-2996.
- Chu, Y., J. Hu, W. Yang, C. Wang and J. Z. Zhang (2006). "Growth and characterization of highly branched nanostructures of magnetic nanoparticles." Journal of Physical Chemistry B **110**(7): 3135-3139.
- Chung, K.-T., L. Kirkovsky, A. Kirkovsky and W. P. Purcell (1997). "Review of mutagenicity of monocyclic aromatic amines: quantitative structure-activity relationships." Mutation Research/Reviews in Mutation Research **387**(1): 1-16.
- Coleman, J. N., U. Khan and Y. K. Gun'ko (2006). "Mechanical reinforcement of polymers using carbon nanotubes." Advanced Materials **18**(6): 689-706.
- Dalboge H., E.B. Jensen and K. G. Welinder (1992). "A process for producing heme proteins". **WO 92/16634**.
- Dong, A., P. Huang and W. S. Caughey (1990). "Protein secondary structures in water from second-derivative amide I infrared spectra." Biochemistry **29**(13): 3303-3308.
- Dresselhaus, M. S., G. Dresselhaus and A. Jorio (2004). "Unusual properties and structure of carbon nanotubes." Annual Review of Materials Research **34**(1): 247-278.
- Drexler, K. E. (1996). Engines of Creation, Fourth Estate Limited.
- Du, P., S. Liu, P. Wu and C. Cai (2007). "Preparation and characterization of room temperature ionic liquid/single-walled carbon nanotube nanocomposites and their

- application to the direct electrochemistry of heme-containing proteins/enzymes." Electrochimica Acta **52**(23): 6534-6547.
- Esumi, K., M. Ishigami, A. Nakajima, K. Sawada and H. Honda (1996). "Chemical treatment of carbon nanotubes." Carbon **34**(2): 279-281.
- Fan, S., M. G. Chapline, N. R. Franklin, T. W. Tombler, A. M. Cassell and H. Dai (1999). "Self-Oriented Regular Arrays of Carbon Nanotubes and Their Field Emission Properties." Science **283**(5401): 512-514.
- Fawal, N., Q. Li, B. Savelli, M. Brette, G. Passaia, M. Fabre, C. Mathé and C. Dunand (2013). "PeroxiBase: a database for large-scale evolutionary analysis of peroxidases." Nucleic Acids Research **41**(D1): D441-D444.
- Figueiredo, J. L. and M. F. R. Pereira (2010). "The role of surface chemistry in catalysis with carbons." Catalysis Today **150**(1-2): 2-7.
- Figueiredo, J. L., M. F. R. Pereira, M. M. A. Freitas and J. J. M. Órfão (1999). "Modification of the surface chemistry of activated carbons." Carbon **37**(9): 1379-1389.
- Figueiredo, J. L., M. F. R. Pereira, M. M. A. Freitas and J. J. M. Órfão (2006). "Characterization of Active Sites on Carbon Catalysts." Industrial & Engineering Chemistry Research **46**(12): 4110-4115.
- Finzel, B. C., T. L. Poulos and J. Kraut (1984). "Crystal structure of yeast cytochrome c peroxidase refined at 1.7-Å resolution." Journal of Biological Chemistry **259**(21): 13027-13036.
- Fukuyama, K. and T. Okada (2007). "Structures of cyanide, nitric oxide and hydroxylamine complexes of *Arthromyces ramosus* peroxidase at 100 K refined to 1.3 Å resolution: coordination geometries of the ligands to the haem iron." Acta Crystallographica Section D **63**(4): 472-477.
- Gao, Y. and I. Kyratzis (2008). "Covalent Immobilization of Proteins on Carbon Nanotubes Using the Cross-Linker 1-Ethyl-3-(3-dimethylaminopropyl)carbodiimide—a Critical Assessment." Bioconjugate Chemistry **19**(10): 1945-1950.
- Georgakilas, V., D. Gournis, V. Tzitzios, L. Pasquato, D. M. Guldi and M. Prato (2007). "Decorating carbon nanotubes with metal or semiconductor nanoparticles." Journal of Materials Chemistry **17**(26): 2679-2694.
- Goel, M. K. (1994). "Immobilized Enzymes." Retrieved 10-Jan, 2014, from <http://www.rpi.edu/dept/chem-eng/Biotech-Environ/IMMOB/goel2nd.htm>.

- Goh, W. J., V. S. Makam, J. Hu, L. Kang, M. Zheng, S. L. Yoong, C. N. B. Udalagama and G. Pastorin (2012). "Iron Oxide Filled Magnetic Carbon Nanotube-Enzyme Conjugates for Recycling of Amyloglucosidase: Toward Useful Applications in Biofuel Production Process." Langmuir **28**(49): 16864-16873.
- Gómez, J. M., M. D. Romero and T. M. Fernández (2005). "Immobilization of  $\beta$ -Glucosidase on carbon nanotubes." Catalysis Letters **101**(3-4): 275-278.
- Gonçalves, A. G., J. J. M. Órfão and M. F. R. Pereira (2013). "Ozonation of sulfamethoxazole promoted by MWCNT." Catalysis Communications **35**(0): 82-87.
- Gong K.P., Y. Y. M., Zhang M.N., Su L., Xiong S.X., Mao L.Q. (2005). Anal. Sci. **21**: 1383-1392.
- Gong, X., J. Liu, S. Baskaran, R. D. Voise and J. S. Young (2000). "Surfactant-assisted processing of carbon nanotube/polymer composites." Chemistry of Materials **12**(4): 1049-1052.
- Gregg, S. J. S. K. S. W. (1982). Adsorption, surface area, and porosity. London; New York, Academic Press.
- H.W., K., Ed. (1991). "Peroxidase: An important enzyme for diagnostic test kits".
- Hamid, M. and R. Khalil ur (2009). "Potential applications of peroxidases." Food Chemistry **115**(4): 1177-1186.
- Hamon, M. A., H. Hui, P. Bhowmik, H. M. E. Itkis and R. C. Haddon (2002). "Ester-functionalized soluble single-walled carbon nanotubes." Applied Physics A: Materials Science and Processing **74**(3): 333-338.
- Heinzkill, M., L. Bech, T. Halkier, P. Schneider and T. Anke (1998). "Characterization of Laccases and Peroxidases from Wood-Rotting Fungi (Family Coprinaceae)." Applied and Environmental Microbiology **64**(5): 1601-1606.
- Henley, J. P. and A. Sadana (1985). "Categorization of enzyme deactivations using a series-type mechanism." Enzyme and Microbial Technology **7**(2): 50-60.
- Hill, D. E., Y. Lin, A. M. Rao, L. F. Allard and Y. P. Sun (2002). "Functionalization of carbon nanotubes with polystyrene." Macromolecules **35**(25): 9466-9471.
- Hirsch, A. (2002). "Functionalization of single-walled carbon nanotubes." Angewandte Chemie - International Edition **41**(11): 1853-1859.
- Hirsch, A. and O. Vostrowsky (2007). "Functionalization of Carbon Nanotubes". Functional Organic Materials, 1-57.
- Holzinger, M., J. Steinmetz, D. Samaille, M. Glerup, M. Paillet, P. Bernier, L. Ley and R. Graupner (2004). "Cycloaddition for cross-linking SWCNTs." Carbon **42**(5-6): 941-947.

- Hong, R. Y., T. T. Pan and H. Z. Li (2006). "Microwave synthesis of magnetic Fe<sub>3</sub>O<sub>4</sub> nanoparticles used as a precursor of nanocomposites and ferrofluids." Journal of Magnetism and Magnetic Materials **303**(1): 60-68.
- Hu, F., S. Chen, C. Wang, R. Yuan, Y. Chai, Y. Xiang and C. Wang (2011). "ZnO nanoparticle and multiwalled carbon nanotubes for glucose oxidase direct electron transfer and electrocatalytic activity investigation." Journal of Molecular Catalysis B: Enzymatic **72**(3-4): 298-304.
- Hu, H., B. Zhao, M. A. Hamon, K. Kamaras, M. E. Itkis and R. C. Haddon (2003). "Sidewall Functionalization of Single-Walled Carbon Nanotubes by Addition of Dichlorocarbene." Journal of the American Chemical Society **125**(48): 14893-14900.
- Huang, J.-L. and Y.-C. Tsai (2009). "Direct electrochemistry and biosensing of hydrogen peroxide of horseradish peroxidase immobilized at multiwalled carbon nanotube/alumina-coated silica nanocomposite modified glassy carbon electrode." Sensors and Actuators B: Chemical **140**(1): 267-272.
- Iijima, S. (1991). "Helical microtubules of graphitic carbon." Nature **354**(6348): 56-58.
- Ito, A., M. Shinkai, H. Honda and T. Kobayashi (2005). "Medical application of functionalized magnetic nanoparticles." Journal of Bioscience and Bioengineering **100**(1): 1-11.
- Ivnitski, D., K. Artyushkova, R. A. Rincón, P. Atanassov, H. R. Luckarift and G. R. Johnson (2008). "Entrapment of Enzymes and Carbon Nanotubes in Biologically Synthesized Silica: Glucose Oxidase-Catalyzed Direct Electron Transfer." Small **4**(3): 357-364.
- Jeykumari, D. R. S. and S. S. Narayanan (2008). "Fabrication of bienzyme nanobiocomposite electrode using functionalized carbon nanotubes for biosensing applications." Biosensors and Bioelectronics **23**(11): 1686-1693.
- Jeykumari, D. R. S. and S. S. Narayanan (2009). "Functionalized carbon nanotube-bienzyme biocomposite for amperometric sensing." Carbon **47**(4): 957-966.
- Jiang, H., C. Du, Z. Zou, X. Li, D. Akins and H. Yang (2009). "A biosensing platform based on horseradish peroxidase immobilized onto chitosan-wrapped single-walled carbon nanotubes." Journal of Solid State Electrochemistry **13**(5): 791-798.
- Johannes Everse, Matthew B. Grisham and K. E. Everse (1990). "Peroxidases in Chemistry and Biology", CRC Press.
- Journet, C., W. K. Maser, P. Bernier, A. Loiseau, M. L. de la Chapelle, S. Lefrant, P. Deniard, R. Lee and J. E. Fischer (1997). "Large-scale production of single-walled carbon nanotubes by the electric-arc technique." Nature **388**(6644): 756-758.

- Kang, X., J. Wang, Z. Tang, H. Wu and Y. Lin (2009). "Direct electrochemistry and electrocatalysis of horseradish peroxidase immobilized in hybrid organic-inorganic film of chitosan/sol-gel/carbon nanotubes." Talanta **78**(1): 120-125.
- Kaput, J., S. Goltz and G. Blobel (1982). "Nucleotide sequence of the yeast nuclear gene for cytochrome c peroxidase precursor. Functional implications of the pre sequence for protein transport into mitochondria." Journal of Biological Chemistry **257**(24): 15054-15058.
- Karajanagi, S. S., A. A. Vertegel, R. S. Kane and J. S. Dordick (2004). "Structure and Function of Enzymes Adsorbed onto Single-Walled Carbon Nanotubes." Langmuir **20**(26): 11594-11599.
- Katchalski-Katzir, E. (1993). "Immobilized enzymes – learning from past successes and failures." Trends in Biotechnology **11**(11): 471-478.
- Khan, A. A. and M. A. Alzohairy (2010). "Recent Advances and Applications of Immobilized Enzyme Technologies: A Review." Research Journal of Biological Sciences **5**(8): 565-575.
- Kim, B. J., B. K. Kang, Y. Y. Bahk, K. H. Yoo and K. J. Lim (2009). "Immobilization of horseradish peroxidase on multi-walled carbon nanotubes and its enzymatic stability." Current Applied Physics **9**: 263-265.
- Kim, J., J. W. Grate and P. Wang (2006). "Nanostructures for enzyme stabilization." Chemical Engineering Science **61**(3): 1017-1026.
- Kim, K. S., D. J. Bae, J. R. Kim, K. A. Park, S. C. Lim, J. J. Kim, W. B. Choi, C. Y. Park and Y. H. Lee (2002). "Modification of electronic structures of a carbon nanotube by hydrogen functionalization." Advanced Materials **14**(24): 1818-1821.
- Kim, T. H., C. Doe, S. R. Kline and S. M. Choi (2007). "Water-redispersible isolated single-walled carbon nanotubes fabricated by in situ polymerization of micelles." Advanced Materials **19**(7): 929-933.
- Kimura, Y., Y. Asada, T. Oka and M. Kuwahara (1991). "Molecular analysis of a Bjerkandera adusta lignin peroxidase gene." Applied Microbiology and Biotechnology **35**(4): 510-514.
- Kondyurin, A. V., P. Naseri, J. M. R. Tilley, N. J. Nosworthy, M. M. M. Bilek and D. R. McKenzie (2012). "Mechanisms for Covalent Immobilization of Horseradish Peroxidase on Ion-Beam-Treated Polyethylene." Scientifica **2012**: 28.
- Kong, J., A. M. Cassell and H. Dai (1998). "Chemical vapor deposition of methane for single-walled carbon nanotubes." Chemical Physics Letters **292**(4-6): 567-574.



- Kunishima, N., K. Fukuyama, H. Matsubara, H. Hatanaka, Y. Shibano and T. Amachi (1994). "Crystal structure of the fungal peroxidase from *Arthromyces ramosus* at 1.9 Å resolution: Structural comparisons with the lignin and cytochrome c peroxidases." Journal of Molecular Biology **235**(1): 331-344.
- Lalonde, J. and A. Margolin (2008). Immobilization of Enzymes. Enzyme Catalysis in Organic Synthesis, Wiley: 163-184.
- Lee, H., E. Lee, D. K. Kim, N. K. Jang, Y. Y. Jeong and S. Jon (2006). "Antibiofouling polymer-coated superparamagnetic iron oxide nanoparticles as potential magnetic resonance contrast agents for in vivo cancer imaging." Journal of the American Chemical Society **128**(22): 7383-7389.
- Lin, Z. F., L. H. Chen and W. Q. Zhang (1996). "Peroxidase from *Ipomoea cairica* (L) SW. Isolation, purification and some properties." Process Biochemistry **31**(5): 443-448.
- Liu, J., A. G. Rinzler, H. Dai, J. H. Hafner, R. Kelley Bradley, P. J. Boul, A. Lu, T. Iverson, K. Shelimov, C. B. Huffman, F. Rodriguez-Macias, Y. S. Shon, T. R. Lee, D. T. Colbert and R. E. Smalley (1998). Science **280**(5367): 1253-1256.
- Liu, S. and C. Cai (2007). "Immobilization and characterization of alcohol dehydrogenase on single-walled carbon nanotubes and its application in sensing ethanol." Journal of Electroanalytical Chemistry **602**(1): 103-114.
- Liu, X. (2008). "Carbon Nanotubes as Catalysts in the Catalytic Oxidation of C4 Hydrocarbons". phd, Technische Universität Berlin.
- Liu, Y., X. Qu, H. Guo, H. Chen, B. Liu and S. Dong (2006). "Facile preparation of amperometric laccase biosensor with multifunction based on the matrix of carbon nanotubes-chitosan composite." Biosensors and Bioelectronics **21**(12): 2195-2201.
- Liu, Z.-Q., J. Ma, Y.-H. Cui and B.-P. Zhang (2009). "Effect of ozonation pretreatment on the surface properties and catalytic activity of multi-walled carbon nanotube." Applied Catalysis B: Environmental **92**(3-4): 301-306.
- Longo, M. A. and D. Combes (1999). "Thermostability of modified enzymes: a detailed study." Journal of Chemical Technology & Biotechnology **74**(1): 25-32.
- Lucas, M. S. and J. A. Peres (2006). "Decolorization of the azo dye Reactive Black 5 by Fenton and photo-Fenton oxidation." Dyes and Pigments **71**(3): 236-244.
- Ma, P.-C., N. A. Siddiqui, G. Marom and J.-K. Kim (2010). "Dispersion and functionalization of carbon nanotubes for polymer-based nanocomposites: A review." Composites Part A: Applied Science and Manufacturing **41**(10): 1345-1367.

- Ma, P. C., J. K. Kim and B. Z. Tang (2006). "Functionalization of carbon nanotubes using a silane coupling agent." Carbon **44**(15): 3232-3238.
- Maier, K. (2014). "What is peroxidase?" Retrieved 10, Jan, 2014, from <http://www.wisegeek.org/what-is-a-peroxidase.htm>.
- Mantha, R., N. Biswas, K. E. Taylor and J. K. Bewtra (2002). "Removal of Nitroaromatics from Synthetic Wastewater Using Two-Step Zero-Valent Iron Reduction and Peroxidase-Catalyzed Oxidative Polymerization." Water Environment Research **74**(3): 280-287.
- Marchon, B., J. Carrazza, H. Heinemann and G. A. Somorjai (1988). "TPD and XPS studies of O<sub>2</sub>, CO<sub>2</sub>, and H<sub>2</sub>O adsorption on clean polycrystalline graphite." Carbon **26**(4): 507-514.
- Matsuura, K., T. Saito, T. Okazaki, S. Ohshima, M. Yumura and S. Iijima (2006). "Selectivity of water-soluble proteins in single-walled carbon nanotube dispersions." Chemical Physics Letters **429**(4-6): 497-502.
- McCarthy, B., J. N. Coleman, R. Czerw, A. B. Dalton, D. L. Carroll and W. J. Blau (2001). "Microscopy studies of nanotube-conjugated polymer interactions." Synthetic Metals **121**(1-3): 1225-1226.
- Mickelson, E. T., C. B. Huffman, A. G. Rinzler, R. E. Smalley, R. H. Hauge and J. L. Margrave (1998). "Fluorination of single-wall carbon nanotubes." Chemical Physics Letters **296**(1-2): 188-194.
- Morançais, A., B. Caussat, Y. Kihn, P. Kalck, D. Plee, P. Gaillard, D. Bernard and P. Serp (2007). "A parametric study of the large scale production of multi-walled carbon nanotubes by fluidized bed catalytic chemical vapor deposition." Carbon **45**(3): 624-635.
- Morita, Y., H. Yamashita, B. Mikami, H. Iwamoto, S. Aibara, M. Terada and J. Minami (1988). "Purification, crystallization, and characterization of peroxidase from *Coprinus cinereus*." Journal of Biochemistry **103**(4): 693-699.
- Moyo, M., J. O. Okonkwo and N. M. Agyei (2014). "An amperometric biosensor based on horseradish peroxidase immobilized onto maize tassel-multi-walled carbon nanotubes modified glassy carbon electrode for determination of heavy metal ions in aqueous solution." Enzyme and Microbial Technology **56**(0): 28-34.
- Nahakpam, S., P. Singh and K. Shah (2008). "Effect of calcium on immobilization of rice (*Oryza sativa* L.) peroxidase for bioassays in sodium alginate and Agarose gel." Biotechnology and Bioprocess Engineering **13**(5): 632-638.

- Nakayama, T. and T. Amachi (1999). "Fungal peroxidase: its structure, function, and application." Journal of Molecular Catalysis B: Enzymatic **6**(3): 185-198.
- Naseh, M. V., A. A. Khodadadi, Y. Mortazavi, O. A. Sahraei, F. Pourfayaz and S. M. Sedghi (2009). "Functionalization of Carbon Nanotubes Using Nitric Acid Oxidation and DBD Plasma." World Academy of Science, Engineering and Technology **25**: 151 - 153.
- Neves, L. F. F. (2007). "Attachment of Annexin V and Horseradish Peroxidase to SWCNTs". Bachelor of Science, University of Oklahoma.
- Otake, Y. and R. G. Jenkins (1993). "Characterization of oxygen-containing surface complexes created on a microporous carbon by air and nitric acid treatment." Carbon **31**(1): 109-121.
- Owusu, R. K., A. Makhzoum and J. S. Knapp (1992). "Heat inactivation of lipase from psychrotrophic *Pseudomonas fluorescens* P38: Activation parameters and enzyme stability at low or ultra-high temperatures." Food Chemistry **44**(4): 261-268.
- Pan, B. F., F. Gao and H. C. Gu (2005). "Dendrimer modified magnetite nanoparticles for protein immobilization." Journal of Colloid and Interface Science **284**(1): 1-6.
- Pang, Y., G.-m. Zeng, L. Tang, Y. Zhang, Z. Li and L.-j. Chen (2011). "Laccase biosensor using magnetic multiwalled carbon nanotubes and chitosan/silica hybrid membrane modified magnetic carbon paste electrode." Journal of Central South University of Technology **18**(6): 1849-1856.
- Patterson, W. R. and T. L. Poulos (1995). "Crystal structure of recombinant pea cytosolic ascorbate peroxidase." Biochemistry **34**(13): 4331-4341.
- Petersen, J. F. W., A. Kadziola and S. Larsen (1994). "Three-dimensional structure of a recombinant peroxidase from *Coprinus cinereus* at 2.6 Å resolution." FEBS Letters **339**(3): 291-296.
- Piontek, K., T. Glumoff and K. Winterhalter (1993). "Low pH crystal structure of glycosylated lignin peroxidase from *Phanerochaete chrysosporium* at 2.5 Å resolution." FEBS Letters **315**(2): 119-124.
- Poulos, T. L., S. L. Edwards, H. Wariishi and M. H. Gold (1993). "Crystallographic refinement of lignin peroxidase at 2 Å." Journal of Biological Chemistry **268**(6): 4429-4440.
- Poulos, T. L., Patterson W. R. and S. M. (1995). "The crystal structure of ascorbate and manganese peroxidases: the role of non-haem metal in the catalytic mechanism." Biochem Soc Trans. **23**: 228-232.

- Prokopijevic, M., O. Prodanovic, D. Spasojevic, Z. Stojanovic, K. Radotic and R. Prodanovic (2014). "Soybean hull peroxidase immobilization on macroporous glycidyl methacrylates with different surface characteristics." Bioprocess and Biosystems Engineering **37**(5): 799-804.
- Qiu, H., L. Lu, X. Huang, Z. Zhang and Y. Qu (2010). "Immobilization of horseradish peroxidase on nanoporous copper and its potential applications." Bioresource Technology **101**(24): 9415-9420.
- Qu, S., F. Huang, S. Yu, G. Chen and J. Kong (2008). "Magnetic removal of dyes from aqueous solution using multi-walled carbon nanotubes filled with Fe<sub>2</sub>O<sub>3</sub> particles." Journal of Hazardous Materials **160**(2-3): 643-647.
- Roco, M. C. (2003). "Nanotechnology: convergence with modern biology and medicine." Current Opinion in Biotechnology **14**(3): 337-346.
- Saifuddin, N., A. Z. Raziah and A. R. Junizah (2013). "Carbon Nanotubes: A Review on Structure and Their Interaction with Proteins." Journal of Chemistry **2013**: 18.
- Sawai-Hatanaka, H., T. Ashikari, Y. Tanaka, Y. Asada, T. Nakayama, H. Minakata, N. Kunishima, K. Fukuyama, H. Yamada, Y. Shibano and T. Amachi (1995). "Cloning, sequencing, and heterologous expression of a gene coding for *Arthromyces ramosus* peroxidase." Bioscience, Biotechnology and Biochemistry **59**(7): 1221-1228.
- Sham, M. L. and J. K. Kim (2006). "Surface functionalities of multi-wall carbon nanotubes after UV/Ozone and TETA treatments." Carbon **44**(4): 768-777.
- Shi, Q., D. Yang, Y. Su, J. Li, Z. Jiang, Y. Jiang and W. Yuan (2007). "Covalent functionalization of multi-walled carbon nanotubes by lipase." Journal of Nanoparticle Research **9**(6): 1205-1210.
- Shim, M., N. W. Shi Kam, R. J. Chen, Y. Li and H. Dai (2002). "Functionalization of Carbon Nanotubes for Biocompatibility and Biomolecular Recognition." Nano Letters **2**(4): 285-288.
- Shinmen, Y., S. Asami, T. Amachi, S. Shimizu and H. Yamada (1986). "Crystallization and Characterization of an Extracellular Fungal Peroxidase." Agricultural and Biological Chemistry **50**(1): 247-249.
- Silva, C. G., A. P. M. Tavares, G. Dražić, A. M. T. Silva, J. M. Loureiro and J. L. Faria (2014). "Controlling the Surface Chemistry of Multiwalled Carbon Nanotubes for the Production of Highly Efficient and Stable Laccase-Based Biocatalysts." ChemPlusChem

- Smolander, M., H. Boer, M. Valkiainen, R. Roozeman, M. Bergelin, J.-E. Eriksson, X.-C. Zhang, A. Koivula and L. Viikari (2008). "Development of a printable laccase-based biocathode for fuel cell applications." Enzyme and Microbial Technology **43**(2): 93-102.
- Spadaro, J. T., M. H. Gold and V. Renganathan (1992). "Degradation of azo dyes by the lignin-degrading fungus *Phanerochaete chrysosporium*." Applied and Environmental Microbiology **58**(8): 2397-2401.
- Steevensz, A., M. M. Al-Ansari, K. E. Taylor, J. K. Bewtra and N. Biswas (2009). "Comparison of soybean peroxidase with laccase in the removal of phenol from synthetic and refinery wastewater samples." Journal of Chemical Technology & Biotechnology **84**(5): 761-769.
- Stephenson, J. J., A. K. Sadana, A. L. Higginbotham and J. M. Tour (2006). "Highly functionalized and soluble multiwalled carbon nanotubes by reductive alkylation and arylation: The billups reaction." Chemistry of Materials **18**(19): 4658-4661.
- Stolarczyk, K., E. Nazaruk, J. Rogalski and R. Bilewicz (2008). "Nanostructured carbon electrodes for laccase-catalyzed oxygen reduction without added mediators." Electrochimica Acta **53**(11): 3983-3990.
- Tasis, D., N. Tagmatarchis, A. Bianco and M. Prato (2006). "Chemistry of carbon nanotubes." Chemical Reviews **106**(3): 1105-1136.
- Thess, A., R. Lee, P. Nikolaev, H. Dai, P. Petit, J. Robert, C. Xu, Y. H. Lee, S. G. Kim, A. G. Rinzler, D. T. Colbert, G. E. Scuseria, D. Tománek, J. E. Fischer and R. E. Smalley (1996). "Crystalline Ropes of Metallic Carbon Nanotubes." Science **273**(5274): 483-487.
- Thordarson, P., B. Le Droumaguet and K. Velonia (2006). "Well-defined protein-polymer conjugates—synthesis and potential applications." Applied Microbiology and Biotechnology **73**(2): 243-254.
- Tien, M. and C. P. D. Tu (1987). "Cloning and sequencing of a cDNA for a ligninase from *Phanerochaete chrysosporium*." Nature **326**(6112): 520-523.
- Tischer, W. and F. Wedekind (1999). "Immobilized Enzymes: Methods and Applications. Biocatalysis - From Discovery to Application". Springer Berlin Heidelberg. **200**: 95-126.
- Toma, F. M. (2009). Covalently functionalized carbon nanotubes and their biological applications. PhD, International school for advanced studies.
- Trojanowicz, M. (2006). "Analytical applications of carbon nanotubes: a review." TrAC Trends in Analytical Chemistry **25**(5): 480-489.

- Tsang, S. C., Z. Guo, Y. K. Chen, M. L. H. Green, H. A. O. Hill, T. W. Hambley and P. J. Sadler (1997). "Immobilization of Platinated and Iodinated Oligonucleotides on Carbon Nanotubes." Angewandte Chemie International Edition in English **36**(20): 2198-2200.
- Unger, E., A. Graham, F. Kreupl, M. Liebau and W. Hoenlein (2002). "Electrochemical functionalization of multi-walled carbon nanotubes for solvation and purification." Current Applied Physics **2**(1): 107-111.
- Valderrama, B., M. Ayala and R. Vazquez-Duhalt (2002). "Suicide Inactivation of Peroxidases and the Challenge of Engineering More Robust Enzymes." Chemistry & Biology **9**(5): 555-565.
- Vámos-Vigyázó, L. and N. F. Haard (1981). "Polyphenol oxidases and peroxidases in fruits and vegetables." C R C Critical Reviews in Food Science and Nutrition **15**(1): 49-127.
- Vedantham, G., H. G. Sparks, S. U. Sane, S. Tzannis and T. M. Przybycien (2000). "A Holistic Approach for Protein Secondary Structure Estimation from Infrared Spectra in H<sub>2</sub>O Solutions." Analytical Biochemistry **285**(1): 33-49.
- Verma, M. L., M. Naebe, C. J. Barrow and M. Puri (2013). "Enzyme Immobilisation on Amino-Functionalised Multi-Walled Carbon Nanotubes: Structural and Biocatalytic Characterisation." PLoS ONE **8**(9).
- Vicente, J., A. Albesa, J. Lianos, E. Flores, A. Fertitta, D. Soria, M. Moreno and M. Rafti (2011). "Effect of acid oxidation treatment on adsorption properties of arc-discharge synthesized multiwall carbon nanotubes." J Argent Chem Soc **98**: 29-38.
- Voss, R., M. A. Brook, J. Thompson, Y. Chen, R. H. Pelton and J. D. Brennan (2007). "Non-destructive horseradish peroxidase immobilization in porous silica nanoparticles." Journal of Materials Chemistry **17**(46): 4854-4863.
- Wei, W., A. Sethuraman, C. Jin, N. A. Monteiro-Riviere and R. J. Narayan (2007). "Biological Properties of Carbon Nanotubes." Journal of Nanoscience and Nanotechnology **7**(4-1): 1284-1297.
- Welinder, K. G. (1976). "Covalent structure of the glycoprotein horseradish peroxidase (EC 1.11.1.7)." FEBS Letters **72**(1): 19-23.
- Welinder, K. G. (1992). "Superfamily of plant, fungal and bacterial peroxidases." Current Opinion in Structural Biology **2**(3): 388-393.
- Welinder, K. G. and M. Gajhede (1993). "Structure and evolution of peroxidases." Plant peroxidases: biochemistry and physiology 35-42.

- Welinder, K. G. and G. Mazza (1977). "Amino acid sequences of heme linked, histidine containing peptides of five peroxidases from horseradish and turnip." European Journal of Biochemistry **73**(2): 353-358.
- Won, J., M. Kim, Y. W. Yi, Y. H. Kim, N. Jung and T. K. Kim (2005). "Cell biology: A magnetic nanoprobe technology for detecting molecular interactions in live cells." Science **309**(5731): 121-125.
- Xu, P., D. Cui, B. Pan, F. Gao, R. He, Q. Li, T. Huang, C. Bao and H. Yang (2008). "A facile strategy for covalent binding of nanoparticles onto carbon nanotubes." Applied Surface Science **254**(16): 5236-5240.
- Yamamoto, K., G. Shi, T. Zhou, F. Xu, J. Xu, T. Kato, J.-Y. Jin and L. Jin (2003). "Study of carbon nanotubes-HRP modified electrode and its application for novel on-line biosensors." Analyst **128**(3): 249-254.
- Yang, Q.-H., P.-X. Hou, S. Bai, M.-Z. Wang and H.-M. Cheng (2001). "Adsorption and capillarity of nitrogen in aggregated multi-walled carbon nanotubes." Chemical Physics Letters **345**(1-2): 18-24.
- Yoza, B., A. Arakaki and T. Matsunaga (2003). "DNA extraction using bacterial magnetic particles modified with hyperbranched polyamidoamine dendrimer." Journal of Biotechnology **101**(3): 219-228.
- Yu, J., N. Grossiord, C. E. Koning and J. Loos (2007). "Controlling the dispersion of multi-wall carbon nanotubes in aqueous surfactant solution." Carbon **45**(3): 618-623.
- Yu, M.-F., B. S. Files, S. Arepalli and R. S. Ruoff (2000). "Tensile Loading of Ropes of Single Wall Carbon Nanotubes and their Mechanical Properties." Physical Review Letters **84**(24): 5552-5555.
- Yu, R., L. Chen, Q. Liu, J. Lin, K. L. Tan, S. C. Ng, H. S. O. Chan, G. Q. Xu and T. S. A. Hor (1998). "Platinum Deposition on Carbon Nanotubes via Chemical Modification." Chemistry of Materials **10**(3): 718-722.
- Yudianti, R., H. Onggo, Y. Saito, T. Iwata and J.-i. Azuma (2011). "Analysis of Functional Group Sited on Multi-Wall Carbon Nanotube Surface." Open Materials Science Journal **5**: 242.
- Zhang, Y. and J. Zhang (2005). "Surface modification of monodisperse magnetite nanoparticles for improved intracellular uptake to breast cancer cells." Journal of Colloid and Interface Science **283**(2): 352-357.

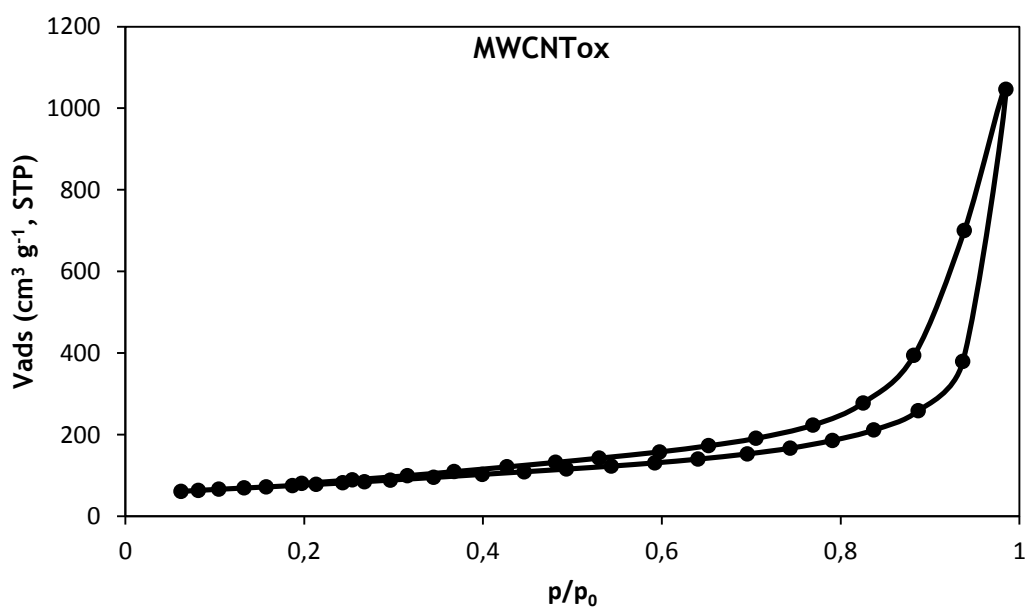
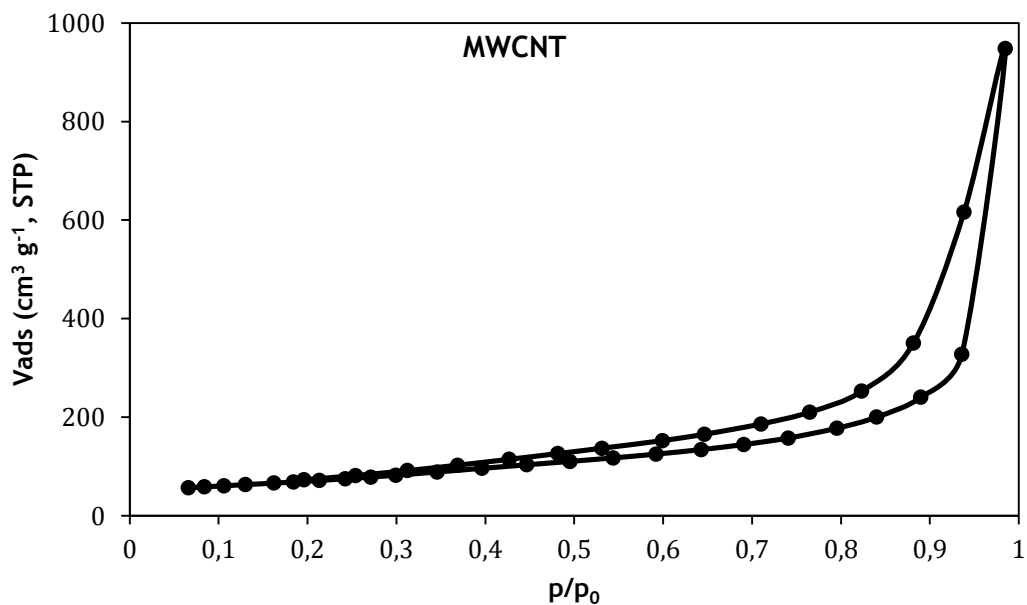
- Zhang, Y. and J. Zheng (2008). "Direct electrochemistry and electrocatalysis of cytochrome c based on chitosan-room temperature ionic liquid-carbon nanotubes composite." Electrochimica Acta **54**(2): 749-754.
- Zhuang, Q. L., T. Kyotani and A. Tomita (1994). "DRIFT and TK/TPD Analyses of Surface Oxygen Complexes Formed during Carbon Gasification." Energy & Fuels **8**(3): 714-718.
- Zielke, U., K. J. Hüttinger and W. P. Hoffman (1996). "Surface-oxidized carbon fibers: I. Surface structure and chemistry." Carbon **34**(8): 983-998.



# Appendix 1

## 1.1 Characterization of MWCNT

### 1.1.1 N<sub>2</sub> adsorption-desorption isotherms



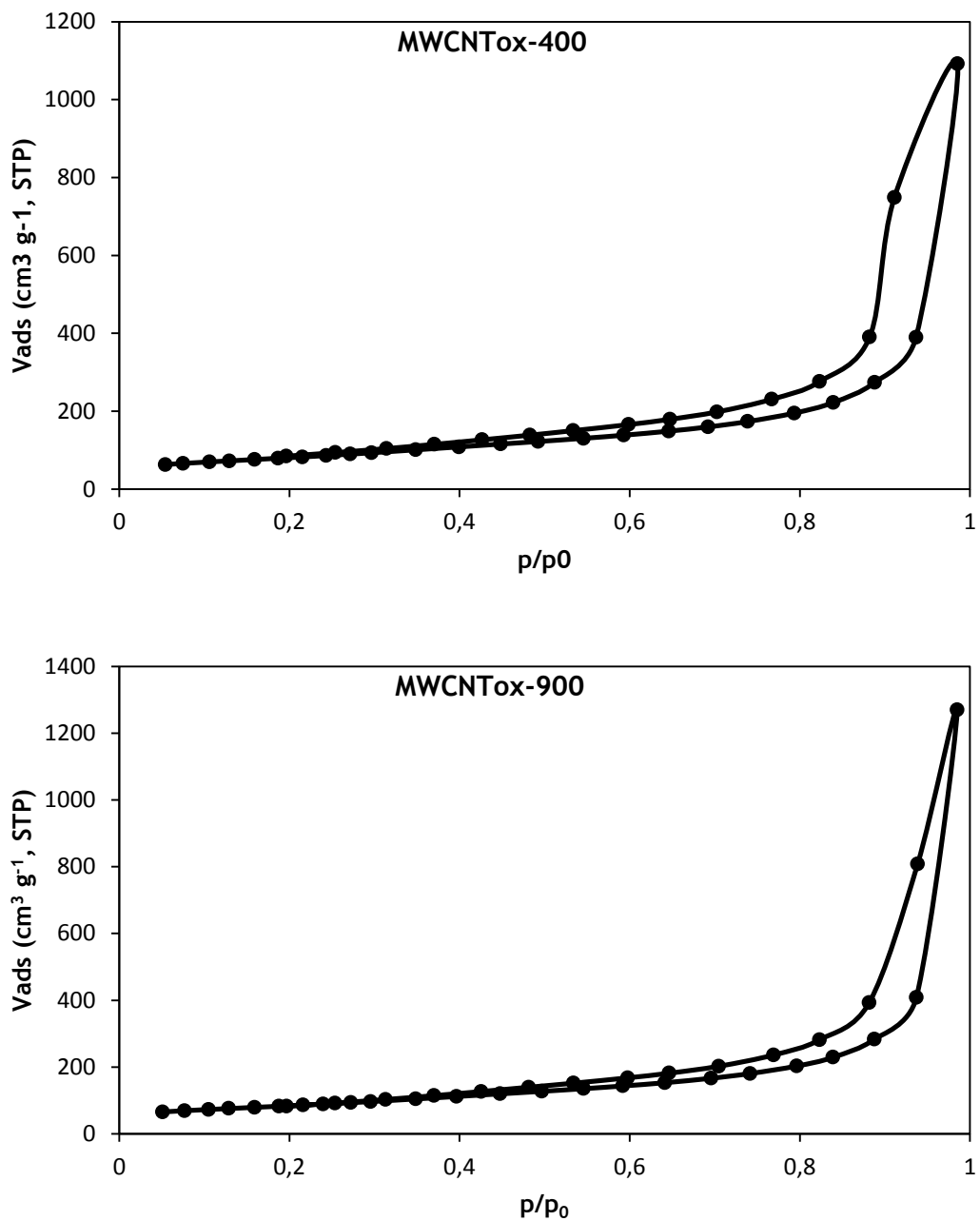


Fig. A1 - Nitrogen adsorption-desorption isotherm of obtained samples. Temperature was fixed at -196 °C.

### 1.1.2 Temperature programmed desorption (TPD)

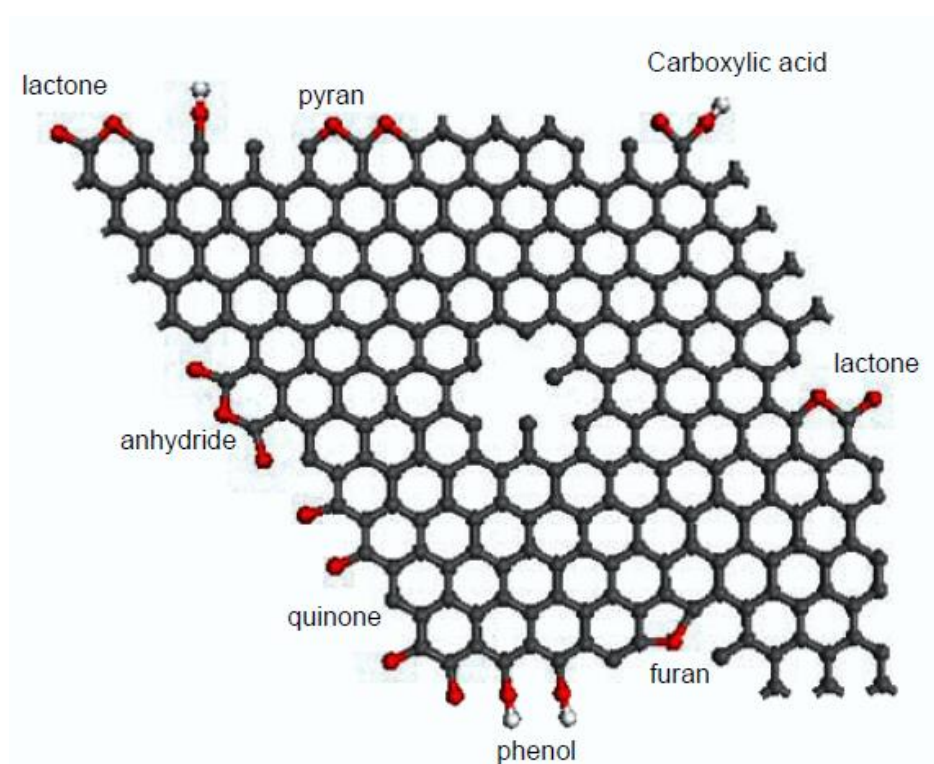


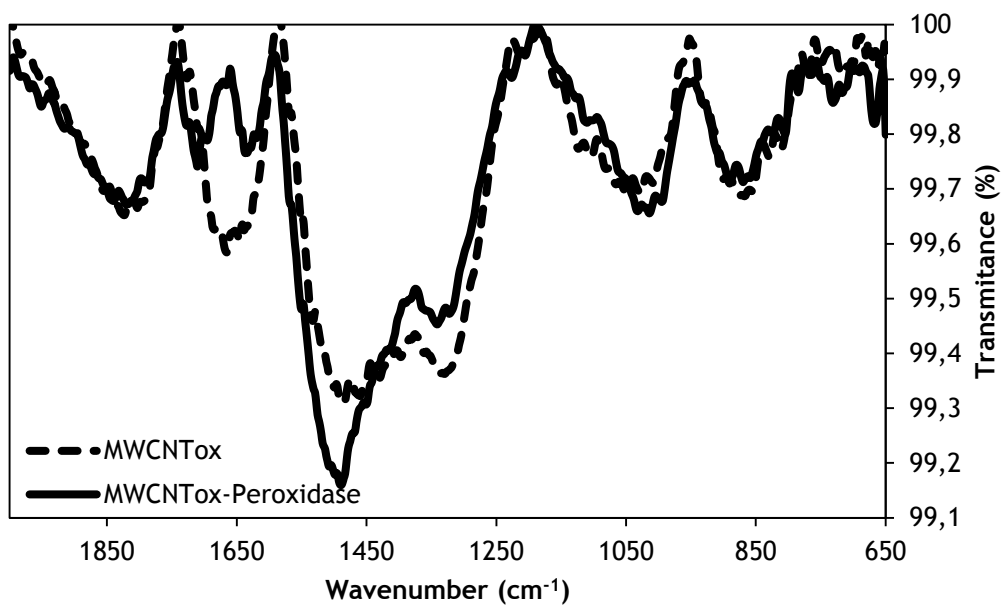
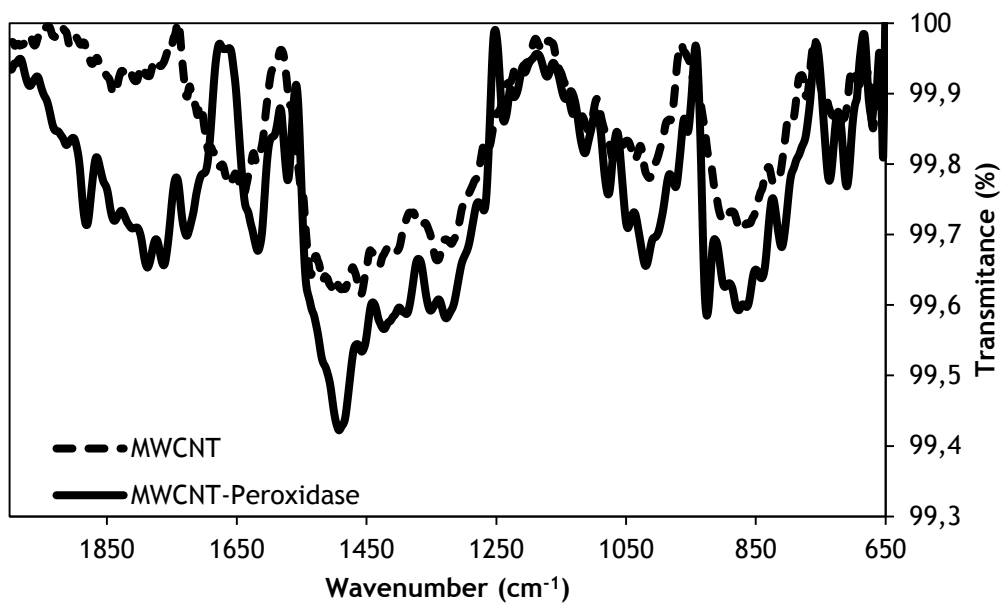
Fig. A2 - Schematic representation of the main chemical features in a graphene sheet, with its typical surface functionalities (Liu, 2008)

Table A1 - Desorption temperature of oxygen functional groups in carbon materials

Oxygen functional groups	Desorption products	Desorption temperature (°C)
Carboxylic acid	CO <sub>2</sub>	350 <sup>2</sup> , 100-300 <sup>3</sup> , 200-250 <sup>4</sup> ,
Anhydride	CO <sub>2</sub> +CO	627 <sup>5</sup> , 550 <sup>3</sup> , 250-500 <sup>4</sup> ,
Lactone	CO <sub>2</sub>	627 <sup>5</sup> , 660 <sup>3</sup> , 350-400 <sup>4</sup> ,
Phenol	CO	630 <sup>3</sup> , 600-700 <sup>4</sup>
Ether	CO	600 <sup>5</sup>
Quinone and half quinone		800 <sup>3</sup> , 800-900 <sup>4</sup> , 600-950 <sup>6</sup>

<sup>1</sup> (Aso et al., 2004); <sup>2</sup> (Otake and Jenkins, 1993) <sup>3</sup> (Figueiredo et al., 1999) <sup>4</sup> (Zielke et al., 1996) <sup>5</sup> (Zhuang et al., 1994) <sup>6</sup> (Marchon et al., 1988)

### 1.1.3 Fourier transform infrared (FTIR)



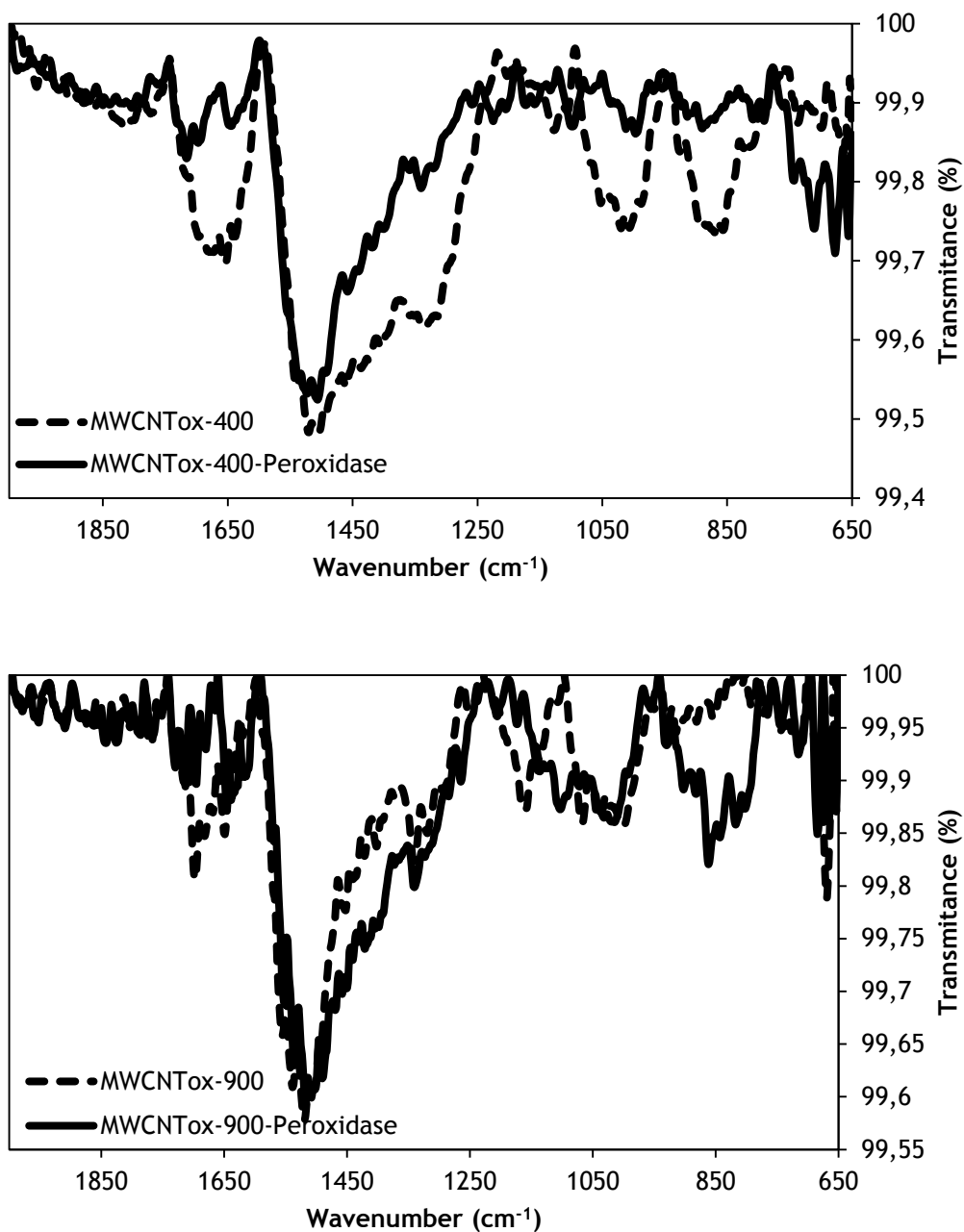


Fig. A3 - FTIR-ATR spectra of MWCNT, MWCNTox, MWCNTox-400 and MWCNTox-900, before (dash line) and after peroxidase immobilization (solid line)

### 1.1.4 Scanning electron microscope (SEM)

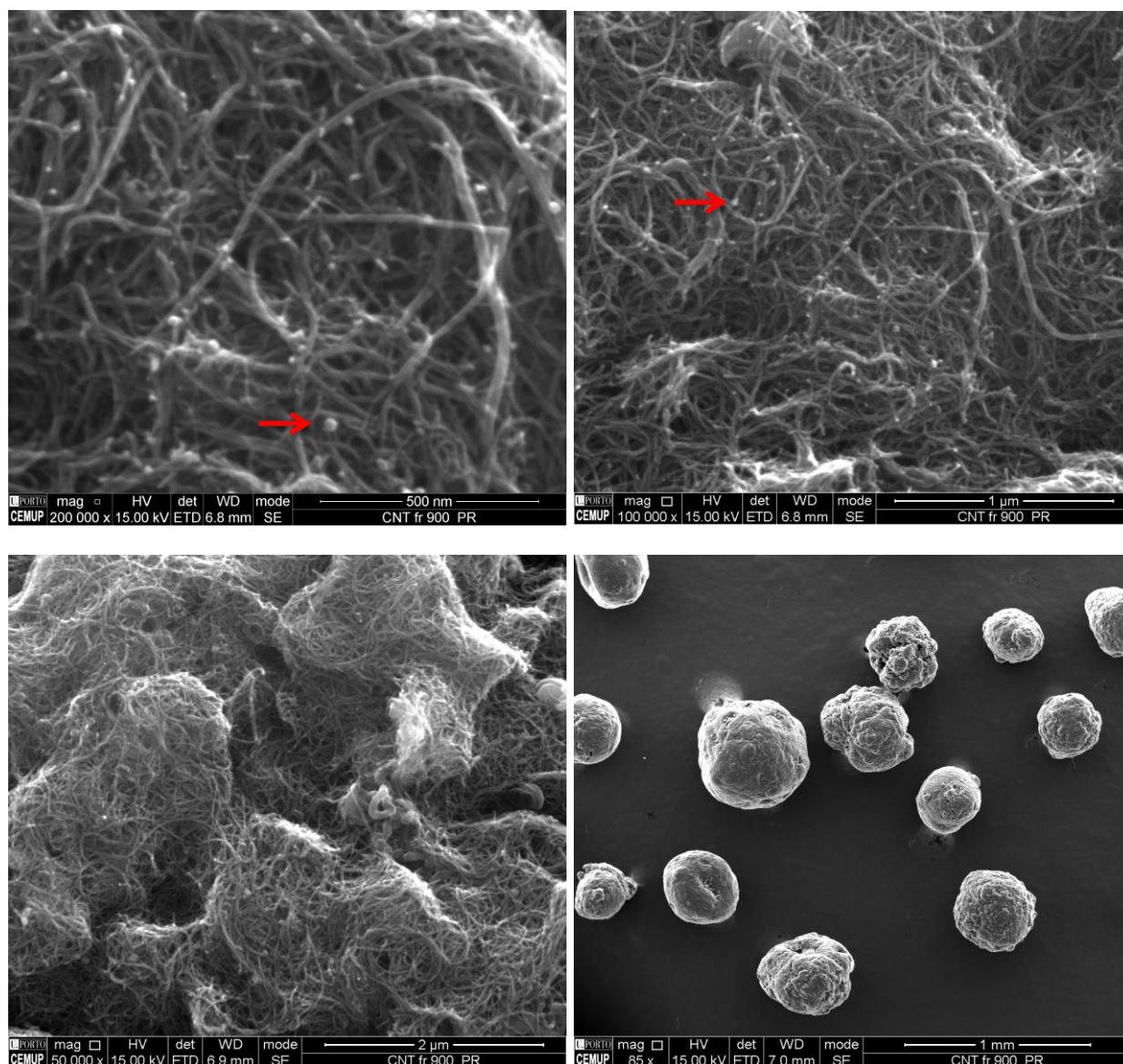


Fig. A4 - SEM images of peroxidase adsorbed in MWCNTox-900 on different resolution.

### 1.1.5 X-ray diffraction (XDR)

Fig. A5 shows the X-ray diffraction (XRD) analysis of  $\text{Fe}_3\text{O}_4$  and MWCNTs filled with  $\text{Fe}_3\text{O}_4$ . The composition of both materials and the dimension of the respective particles are also presented in Table A2.

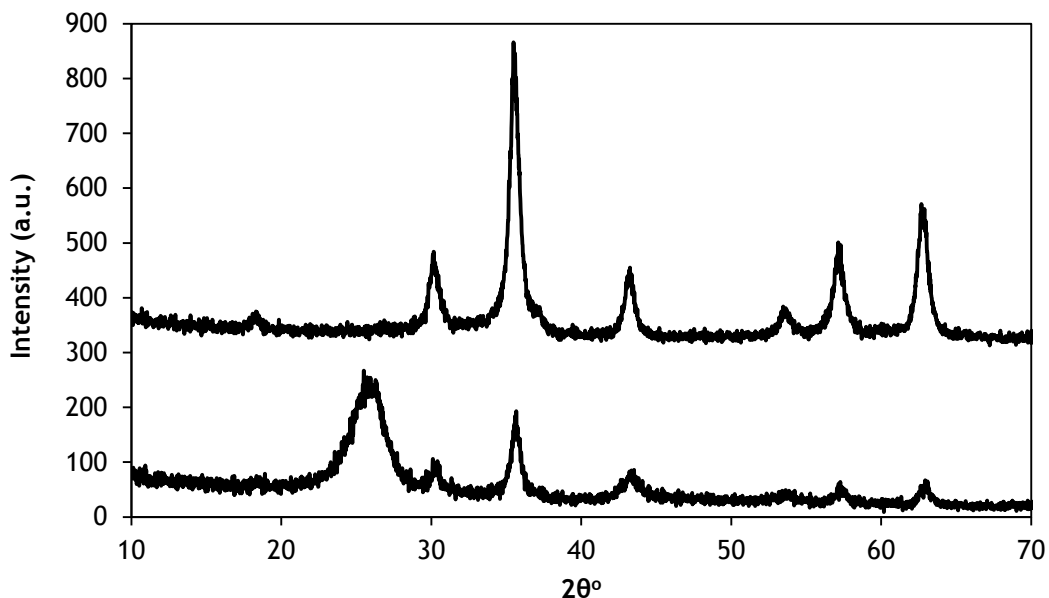
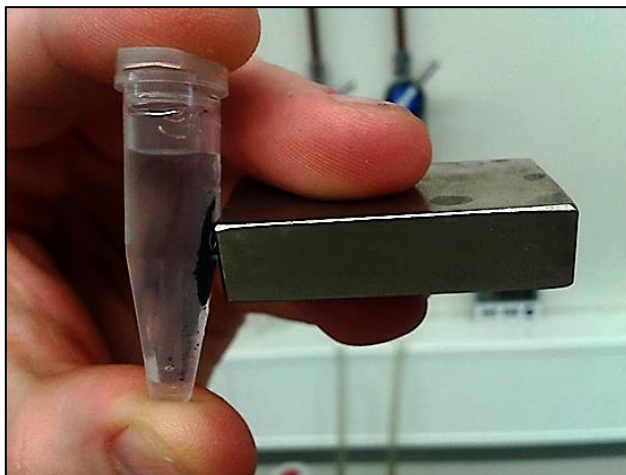


Fig. A5 - XRD diffractogram of magnetite ( $\text{Fe}_3\text{O}_4$ ) (Fawal et al.) and CNT- $\text{Fe}_3\text{O}_4$  hybrid materials.

Table A2 - Characterization of  $\text{Fe}_3\text{O}_4$  and CNT- $\text{Fe}_3\text{O}_4$  hybrid material.

Material	Composition (% vol.)	Particle dimention (nm)
Magnetite	$\text{Fe}_3\text{O}_4$ 100%	$14,54 \pm 0,5$
mMWCNTs	Graphite 97%	$7,8 \pm 3$
	$\text{Fe}_3\text{O}_4$ 3%	$18,9 \pm 4$



*Fig. A6 - m-MWCNT attracted by a simple magnet*



### 1.1.6 Transmission electron microscopy (TEM)

TEM images of  $\text{Fe}_3\text{O}_4$  nanoparticles and MWCNTs filled with  $\text{Fe}_3\text{O}_4$  nanoparticles are shown in Fig. A7.

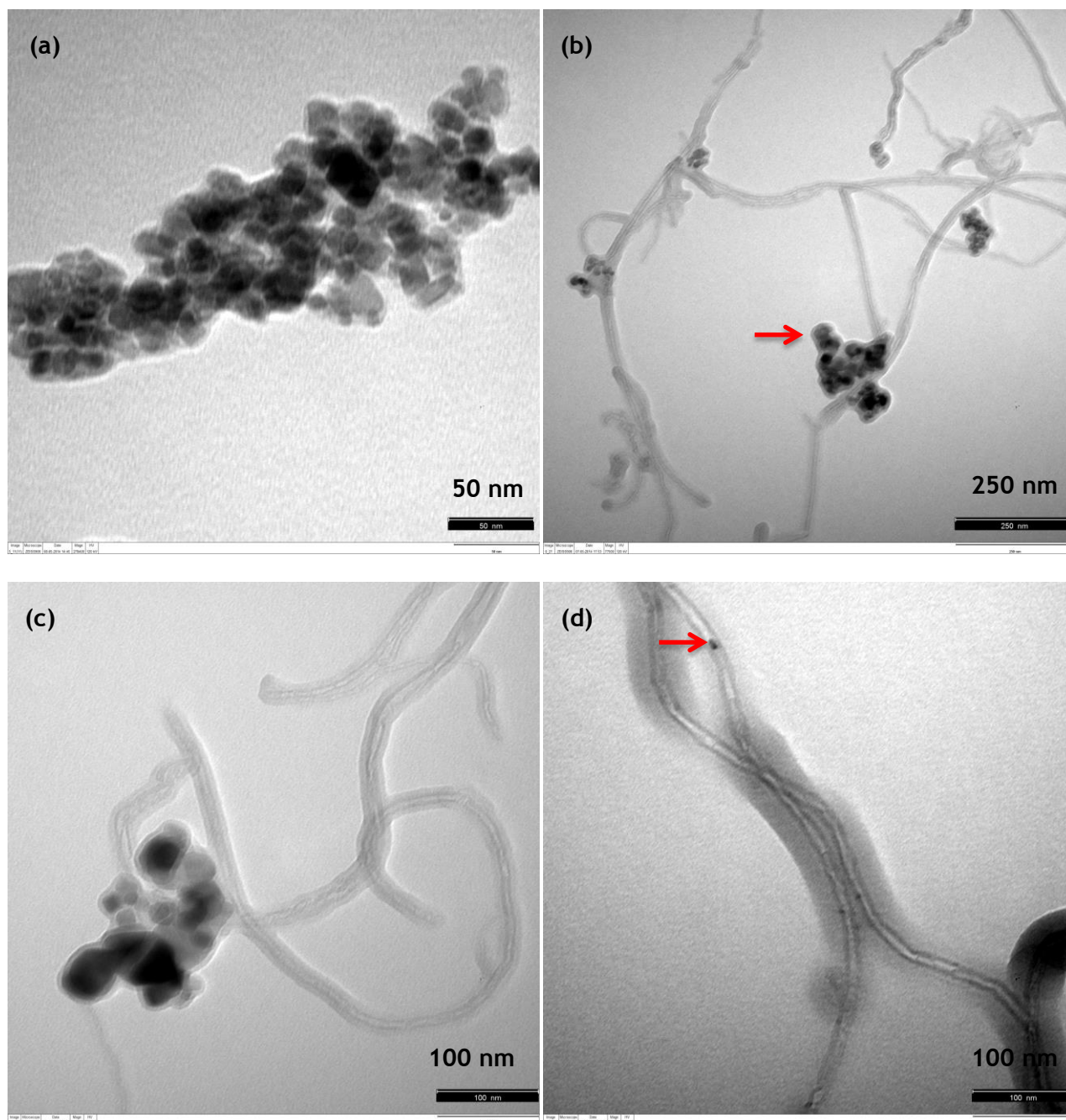


Fig. A7 - TEM images of  $\text{Fe}_3\text{O}_4$  (a) and mMWCNTs (b, c and d).

## 1.2 Effect of MWCNT surface chemistry on peroxidase immobilization

Table A3 -shows a summary of all experimental results obtained during these tests.

Table A3 - Summary table for test at pH range 4.5-9

Suporte	pH	Initial Activity (U/L)	Residual Activity (U/L)	Immobilized activity (U/g)	Immobilization efficiency (%)	Activity recovered (%)
<b>MWCNT</b>	4,5	5762500	14375	270,8	99,75	1,96
	6	5790000	206063	303,0	96,44	2,26
	7	7447500	117813	214,4	98,42	1,22
	8	5360000	491250	207,1	90,83	1,77
	9	5522500	256250	179,5	95,36	1,42
<b>MWCNTox</b>	4,5	5622500	682500	271,0	87,86	2,29
	6	6960000	1708750	222,0	75,45	1,76
	7	6920000	2163750	101,2	68,73	0,89
	8	6277500	1960000	66,5	68,78	0,64
	9	6812500	1818750	43,8	73,30	0,37
<b>MWCNTox-400</b>	4,5	4217500	690000	255,5	83,64	3,02
	6	4200000	1127500	212,1	73,15	2,88
	7	5772500	1891250	150,8	67,24	1,62
	8	5837500	2023750	86,7	65,33	0,95
	9	3932500	2053750	36,5	47,77	0,81
<b>MWCNTox-900</b>	4,5	5622500	336250	287,4	94,02	2,27
	6	6960000	1038750	327,4	85,08	2,30
	7	6920000	1150000	326,3	83,38	2,36
	8	6277500	1236250	270,4	80,31	2,24
	9	6812500	1035000	222,9	84,81	1,61

### 1.3 Thermal stability of free and immobilized peroxidase

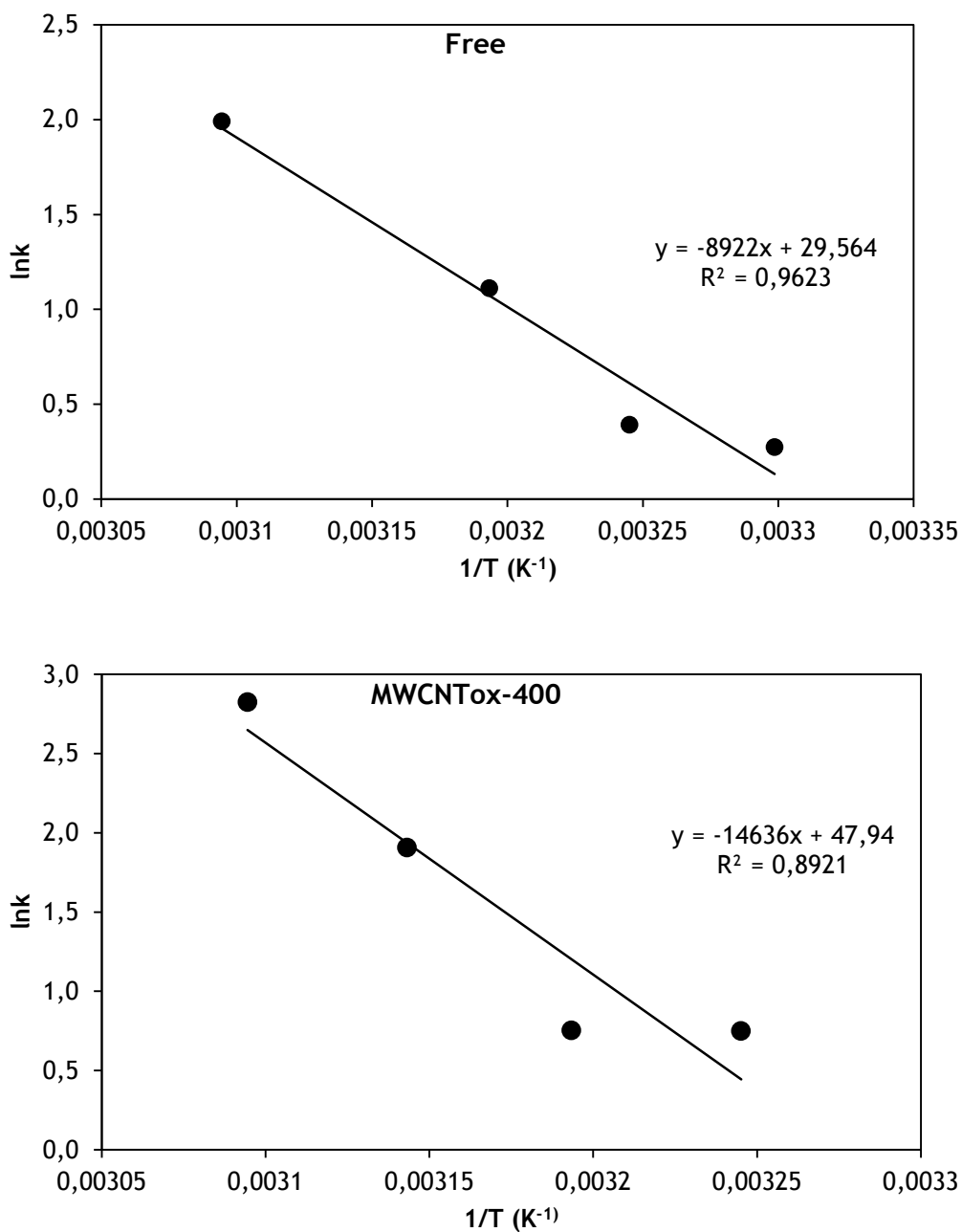


Fig. A8 - Arrhenius plot for free and immobilized peroxidase on MWCNTox-400.

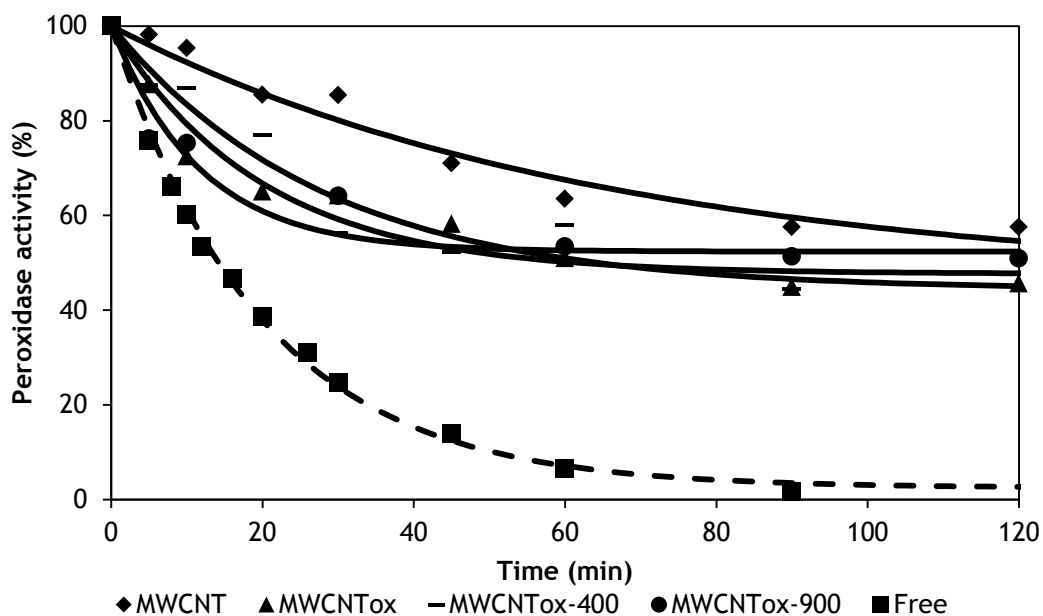


Fig. A9 - Thermal deactivation of free peroxidase and immobilized on purified and functionalized MWCNT at 40 °C

Table A4 - Thermal parameters (40 °C) for free and immobilized peroxidase on purified and functionalized MWCNT

Enzyme	Thermal parameters (40°C)		t <sub>1/2</sub> (h)
	α	k (h <sup>-1</sup> )	
Free	2,480±1,264	3,039± 0,094	0,093
MWCNT	45,959±7,587	0,918±0,238	0,118
MWCNTox	47,688±2,646	3,027±0,502	0,091
MWCNTox-400	44,290±6,238	2,124±0,580	0,114
MWCNTox-900	52,374±1,921	5,156±0,881	0,120

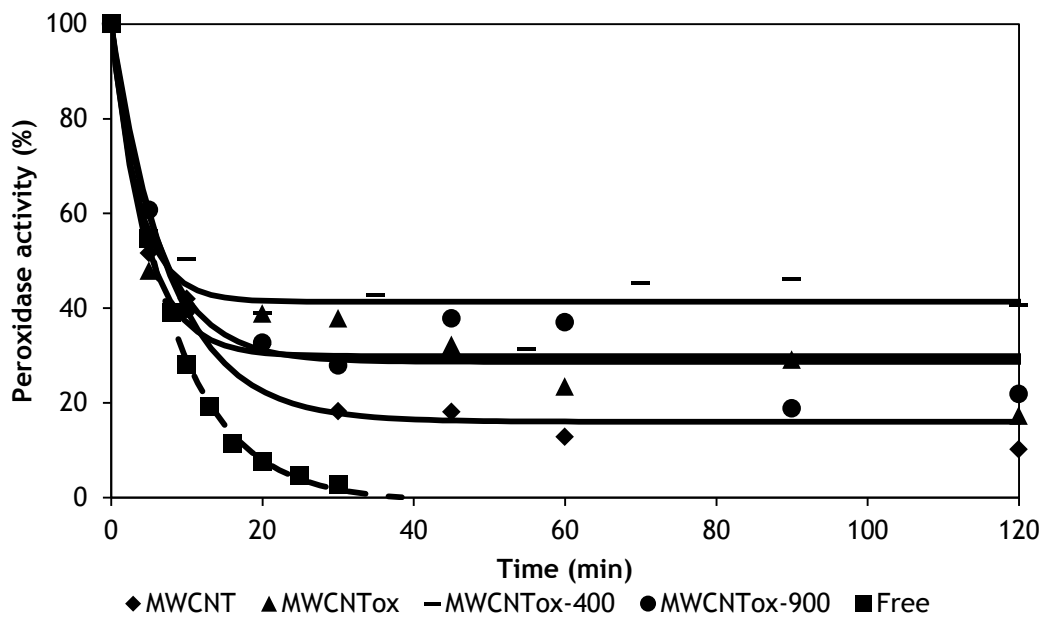


Fig. A10 - Thermal deactivation of free and immobilized peroxidase on purified and functionalized MWCNT at 50 °C

## 1.4 Kinetic parameters of free and immobilized peroxidase

The influence of the concentration of  $\text{H}_2\text{O}_2$  in the enzymatic activity of the peroxidase is shown in Fig. A11.

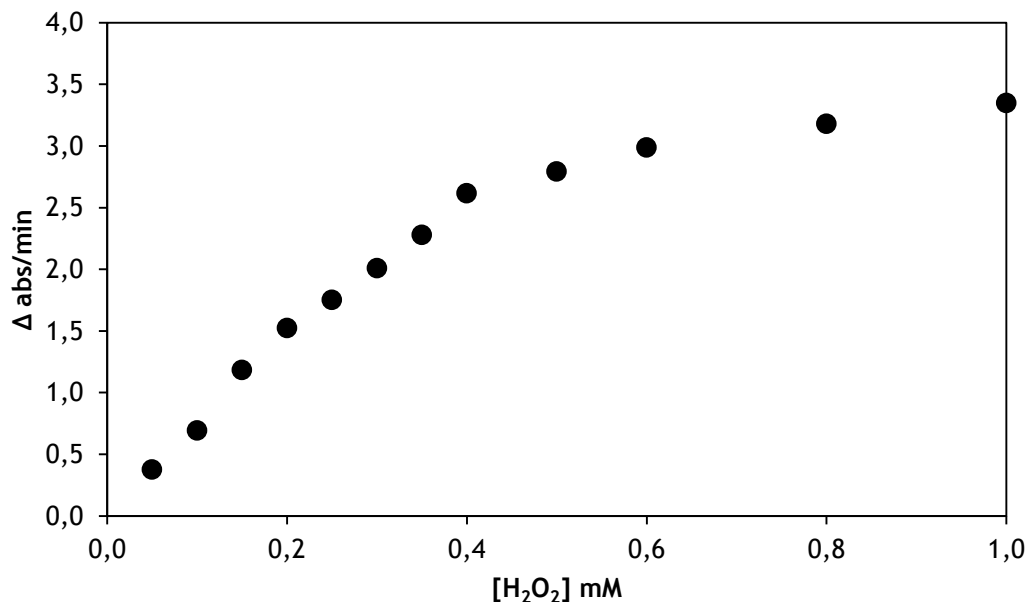


Fig. A11 - Effect of  $\text{H}_2\text{O}_2$  concentration on the initial rate of oxidation of ABTS (0.4 mM) catalyzed by free peroxidase

It should be noted that the presence of hydrogen peroxide facilitates the conversion of substrates that are poor substrates for peroxidases since they can be oxidized via redox mediation with a primary substrate that is efficiently oxidized by the peroxidase. This redox mediation involves the transfer of electrons from the primary peroxidase oxidation substrate to a secondary substrate via non-enzymatic reaction (Eq. (2.1)). As can be seen, increasing the concentration of  $\text{H}_2\text{O}_2$ , the rate of oxidation of ABTS also increases until reaching a saturation value (data not shown). After this point, when peroxidase is exposed to high concentrations of  $\text{H}_2\text{O}_2$ , it shows a kinetic behavior of a suicide inactivation. This inactivation limits the usefulness of these enzymes as reported by (Valderrama et al., 2002).

Regarding to the Michaelis-Menten constants, the velocity  $V$  tends to an asymptotic way and to accurately determine  $K_M$ , it is necessary to know  $v_{max}$  with accuracy. In this thesis, it was used the program CurveExpert to perform a non-linear fit of the experimental values, however it is common to use two linear transformations of the Michaelis-Menten equation: Lineweaver-Burk and Eadie-Hofstee. For comparative data, the Lineweaver-Burk representation of free and immobilized peroxidase are shown in Fig. A12 and Fig. A13, respectively.

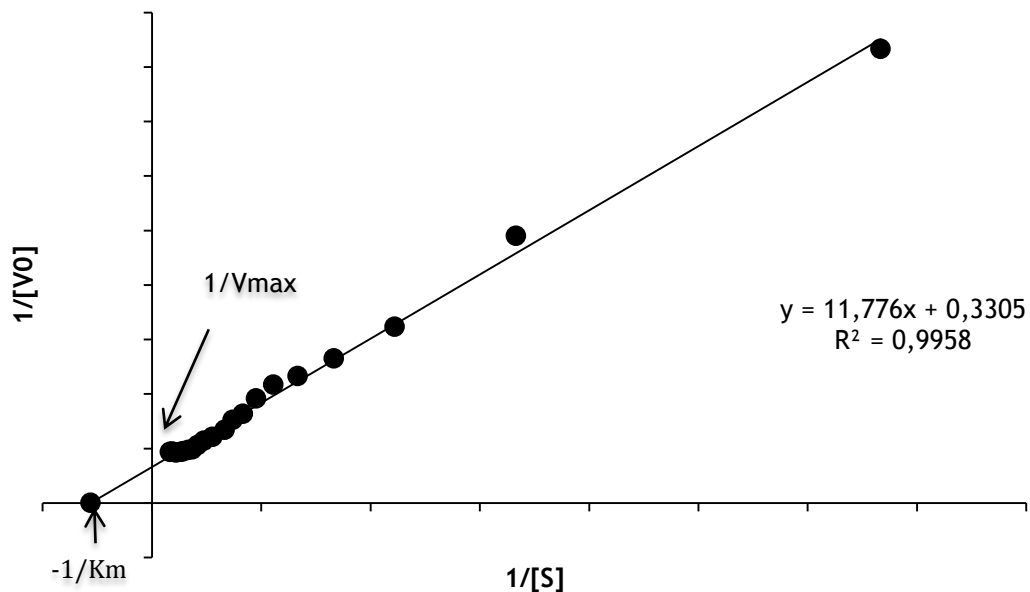


Fig. A12 - Lineweaver-Burk representation of free peroxidase

Table A5 - Comparison of Michaelis-Menten parameters obtained for free peroxidase

Michaelis-Menten	CurveExpert	Lineweaver-Burk
$v_{max}$ (mM.min <sup>-1</sup> )	2,979±0.130	3,026
$K_M$ (mM)	0,033±0,004	0,036

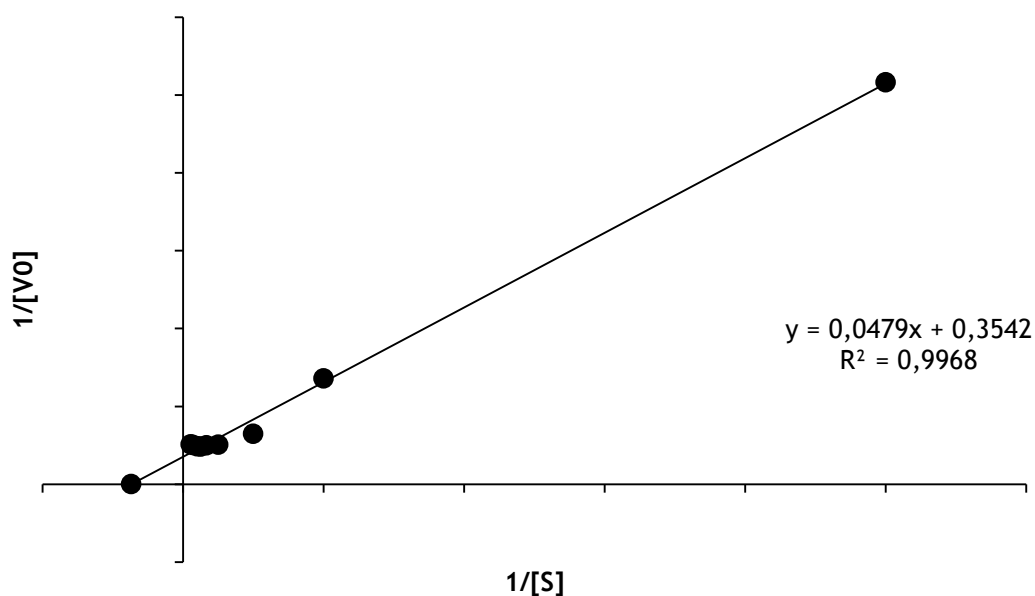


Fig. A13 - Lineweaver-Burk representation of immobilized peroxidase

*Table A6 - Comparison of Michaelis-Menten parameters obtained for immobilized peroxidase*

<b>Michaelis-Menten</b>	<b>CurveExpert</b>	<b>Lineweaver-Burk</b>
$v_{max}$ (mM.min <sup>-1</sup> )	2,303±0,137	2,824
$K_M$ (mM)	0,064±0,018	0,135



## 1.5 Storage and operational stability of immobilized peroxidase

The reusability of MWCNTox-400-peroxidase conjugates was also determined. This procedure was identical to that of magnetic carbon nanotubes. The only difference was that this conjugates was separated from the reaction solution by filtration and then resuspended in a fresh ABTS solution and the process was repeated. The results are shown in Fig. A14.

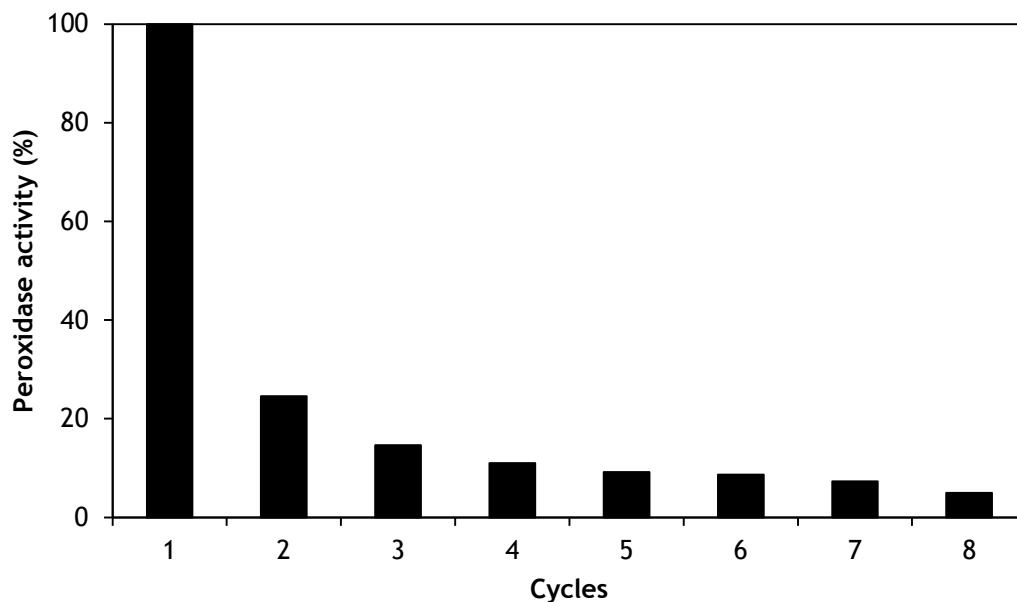


Fig. A14 - Reusability of peroxidase immobilized on MWCNTox-400

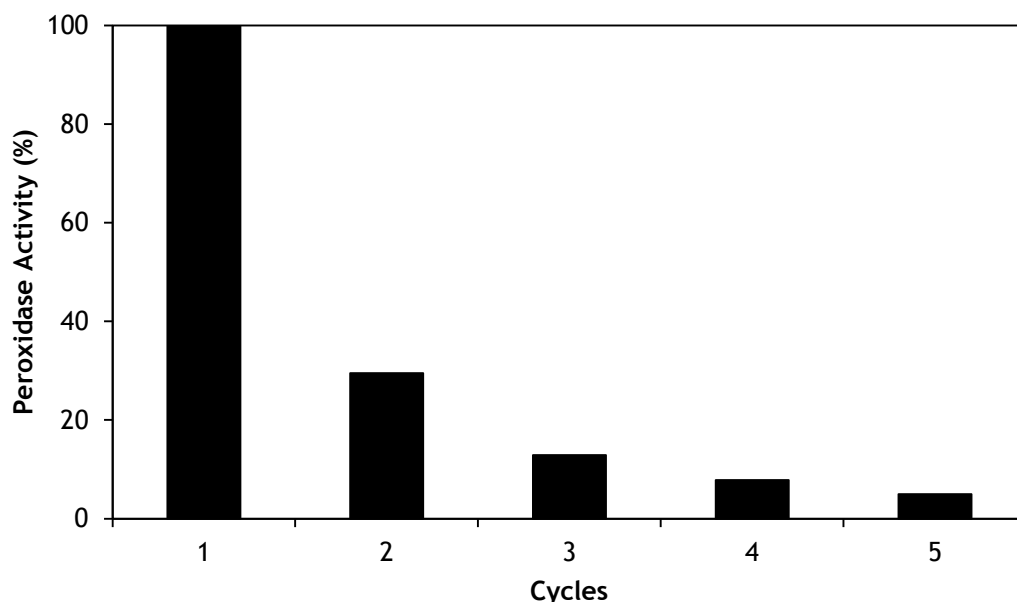


Fig. A15 - Reusability of peroxidase immobilized on a MWCNTs membrane

## 1.6 Discoloration of dyes

Table A7 - Properties of Reactive Black 5

Parameter	Value
C.I. Name	Remazol Black 5
Commercial Name	Reactive Black 5
Functional group	Azo
CAS Number	17095-24-8
EC Number	241-164-5
Mol. Mass (g.mol <sup>-1</sup> )	991,82
Mol. Formula	C <sub>26</sub> H <sub>21</sub> N <sub>5</sub> Na <sub>4</sub> O <sub>19</sub> S <sub>6</sub>
Chemical Formula	
$\lambda_{\max}$	595 nm
Purity (%)	55
Solubility	200 g.L <sup>-1</sup> in water at 80 °C
Manufacturer	Sigma-Aldrich

Table A8 - Properties of Reactive Blue 4

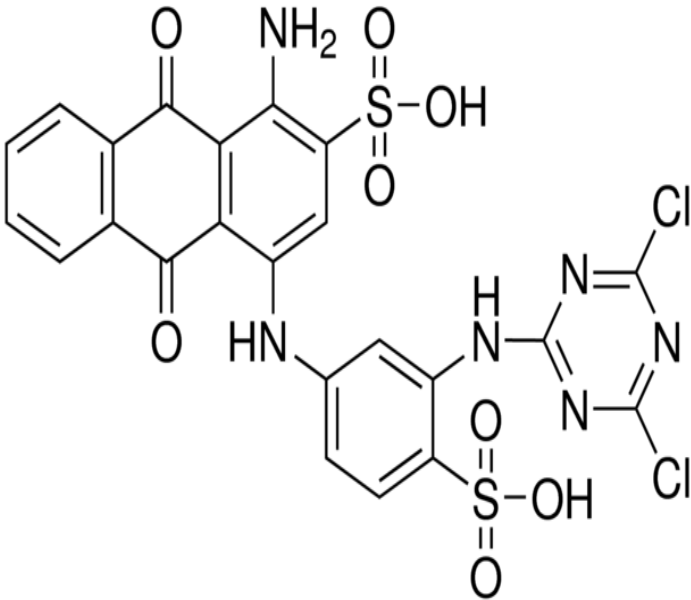
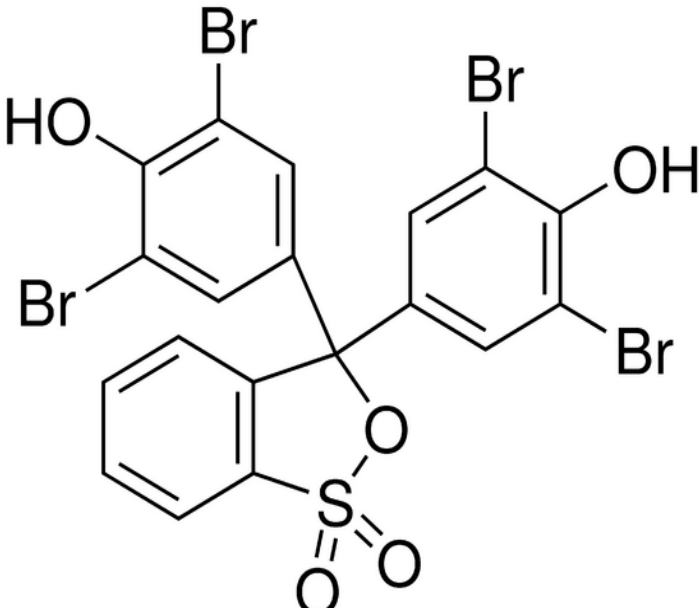
Parameter	Value
C.I. Name	Procion® blue MX-R
Commercial Name	Reactive Blue 4
Functional group	Amine
CAS Number	13324-20-4
EC Number	236-363-9
Mol. Mass (g.mol <sup>-1</sup> )	637,43
Mol. Formula	C <sub>23</sub> H <sub>14</sub> Cl <sub>2</sub> N <sub>6</sub> O <sub>8</sub> S <sub>2</sub>
Chemical Formula	
$\lambda_{\max}$	595 nm
Purity (%)	35
Manufacturer	Sigma-Aldrich

Table A9 - Properties of Bromophenol Blue

Parameter	Value
C.I. Name	Bromophenol Blue
Commercial Name	Bromophenol Blue
Functional group	Sulphonyl
CAS Number	115-39-9
EC Number	204-086-2
Mol. Mass (g.mol <sup>-1</sup> )	669,96
Mol. Formula	C <sub>19</sub> H <sub>10</sub> Br <sub>4</sub> O <sub>5</sub> S
Chemical Formula	 <p>The chemical structure of Bromophenol Blue is a triphenylmethane derivative. It consists of a central carbon atom bonded to three phenyl rings. The top-left ring is a 2,4,6-tribromophenyl group. The top-right ring is a 3,5,5'-tribromophenyl group. The bottom ring is a 2-sulphophenyl group, where the sulfur atom is double-bonded to two oxygen atoms and single-bonded to one oxygen atom that is part of the ring's fused system.</p>
$\lambda_{\max}$	595 nm
Manufacturer	Sigma-Aldrich

## **1.7 Bradford protein assay**

The protein concentration was determined using the Bradford protein assay. This method, a chromogenic assay, is based on an absorbance shift of the dye Coomassie Brilliant Blue R250 ( $C_{43}H_{44}N_3O_7S_2Na$ ), that when bound to the protein, the red form of the dye turns blue. The red form of Coomassie dye causes a disruption of the protein's native state exposing its hydrophobic regions. These regions bind via van der Waals forces to the non-polar region of the dye, causing a shift in the absorption maximum of the dye.

The increase of absorbance at 595 nm is proportional to the amount of bound dye, and thus to the concentration of protein present in the sample. In this way, a standard curve (Fig. A16) can be obtained using known protein concentrations. The obtained equation can be used to determine the protein concentration of other samples (proteins). There are other alternative methods, such as, Lowry and BCA protein assays.

### **1.7.1 Calibration curve**

The standard curves were obtained for a concentration range of  $0.01-0.1 \text{ mg.L}^{-1}$  and  $0.1-1 \text{ mg.L}^{-1}$  of a BSA solution. These results were used to obtain the peroxidase concentration in each sample. The standards were prepared mixing 1.5 mL of Coomassie Brilliant Blue with 50  $\mu\text{L}$  of the protein solution, during 5 min. After this period, the absorbance was recorded by the spectrophotometer at 595 nm. The standard curves (absorbance vs protein concentration) are represented in Fig. A16.

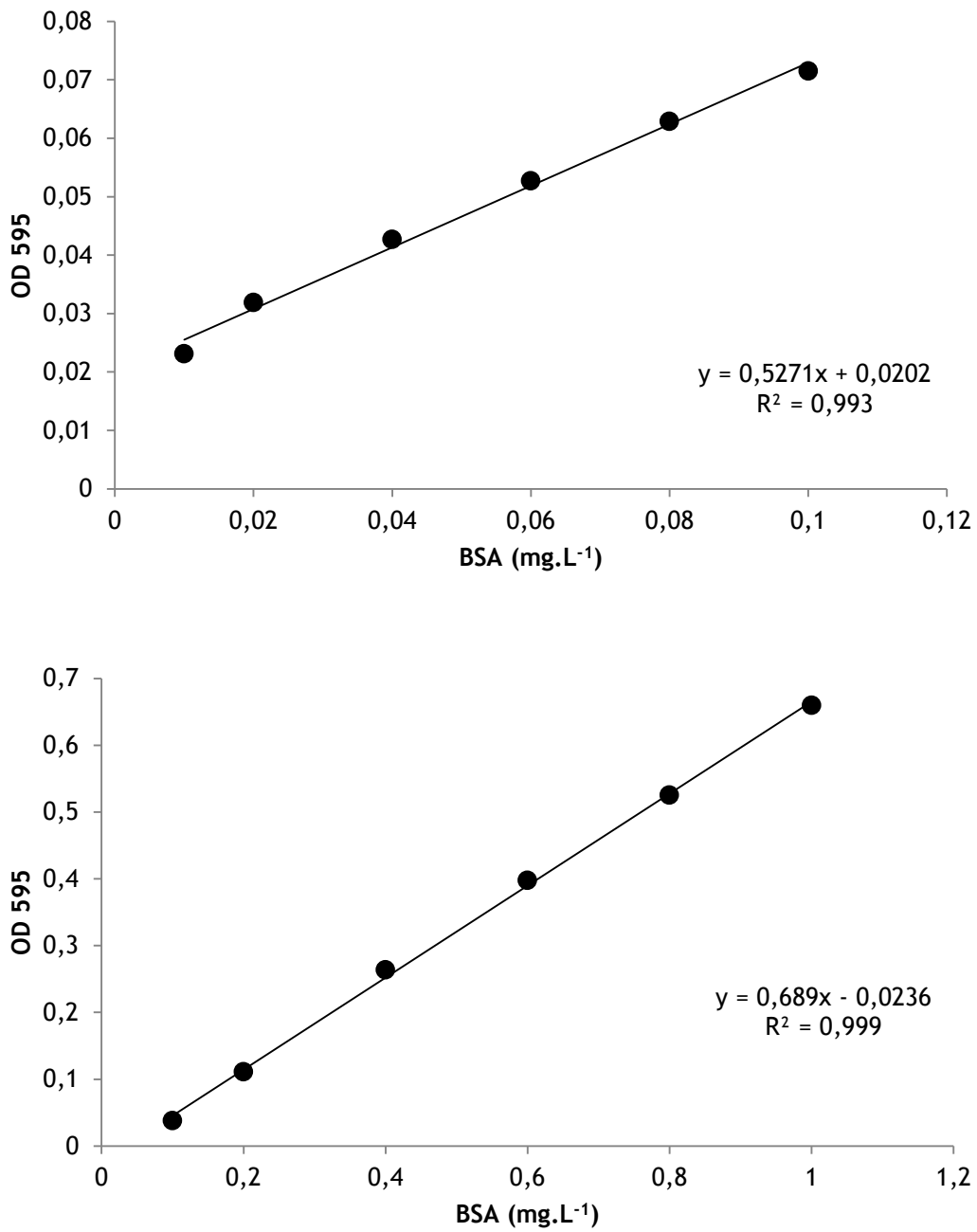


Fig. A16 - Standard curves for Bradford protein assay

*Table A10 - Protein quantification for the immobilization process*

<b>Sample</b>	<b>Abs</b>	<b>Concentration (mg.mL<sup>-1</sup>)</b>
<b>Initial</b>	0,0488	0,054
<b>W1.A</b>	0,0336	0,025
<b>W1.B</b>	0,0334	0,025
<b>W2.A</b>	0,0310	0,020
<b>10.A</b>	0,0325	0,023
<b>10.B</b>	0,0346	0,027
<b>30.A</b>	0,0211	0,002
<b>30.B</b>	0,0344	0,027
<i>W1- supernatant of the first wash</i>		
<i>W2 - supernatant of the second wash</i>		
<i>10. - supernatant of the sample after incubation at 50 °C during 10 min</i>		
<i>30. - supernatant of the sample after incubation at 50 °C during 30 min</i>		

## 1.8 Isoelectric point

The isoelectric point, or pI, is the pH at which the overall net charge on the protein is zero. It serves as a characteristic for every protein; proteins can be precipitated most easily at the pI, and similarly, charge interactions can be assessed when both the pI and pH of interest are known (Bommarius and Riebel-Bommarius, 2007). Amino acids in solution at neutral pH exist predominantly as dipolar ions called zwitterions. In this dipolar form, the amino group is protonated ( $-\text{NH}_3^+$ ) and the carboxyl group is deprotonated ( $-\text{COO}^-$ ). The pI is determined by forming a pH gradient when an electric field is applied across a solution containing the protein. At this pH value, its electrophoretic mobility is also zero. When placed on an electrical field in a pH gradient, a protein will migrate until it reaches a position in the gel at which the pH is equal to the pI of the protein (Bommarius and Riebel-Bommarius, 2007).

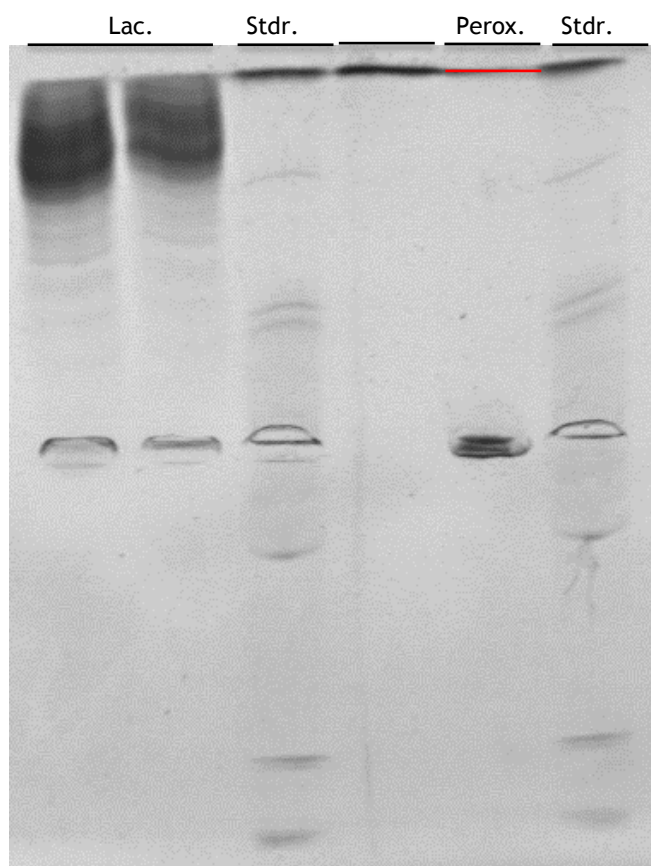


Fig. A17 - Isoelectric point focusing. Lac (Laccase), Stdr. (Standard) and Perox (Peroxidase), pH 4-6.



## 1.9 Gel Electrophoresis SDS-Page

Sodium dodecyl sulfate polyacrylamide gel electrophoresis SDS-PAGE was performed in order to evaluate the purity of commercial peroxidase solution (Fig. A18). It was used an Amersham ECL Gel Box and an Amersham ECL Gel. The following instructions contain a short protocol describing the procedure adopted.

### 1.9.1 Preparations before a run

Step	Action
1	Prepare 1X running buffer by diluting 19 mL of Amersham ECL Gel Running Buffer, 10X in 171 mL water. 190 mL buffer is sufficient for one electrophoresis gel
2	Add 90 ml of 1× running buffer to each tank of Amersham ECL Gel Box
3	Cur open the gel package and gently remove Amersham ECL Gel from the package
4	Rinse the gel cassette with distilled water. Peel off the tapes from the two legs of the cassette.
5	Place Amersham ECL Gel in Amersham ECL Gel Box so that the well side of the cassette faces toward the cathode - and the other cassette leg faces toward the anode +
6	Place the safety lid on top of Amersham ECL Gel Box
7	Connect Amersham ECL Gel Box to the power supply EPS 301 and pre-run the gel for 12 minutes in 160 V
8	Once the pre-run is finished, switch off the power
9	Remove the safety lid
10	Wiggle the comb back and forth, and bring it straight up from the cassette to make the wells available for sample loading
11	Add 6 mL of 1X running buffer to the well container

### 1.9.2 Sample loading

Step	Action
1	Prepare the samples by adding sample and 2X sample buffer in a 1:1 mixture
2	Heat the samples at 95°C for 5 minutes
3	Spin down the samples quickly in a microcentrifuge and load samples directly into the wells in the gel

- 4 Place the safety lid on top of Amersham ECL Gel Box

### 1.9.3 Running conditions

Parameter	Value
Voltage	160 V
Expected current	Start: -45 mA End: 23 to 33 mA
Run time	60 minutes

### 1.9.4 Removing the gel from the cassette

Step	Action
1	Once the run is completed, shut off the power, disconnect the electrodes, remove the safety lid and finally, remove the gel cassette from Amersham ECL Gel Box
2	Open the cassette by inserting the edge of the comb in the slot opposite the sample wells, and twist
3	Remove the top plate from the gel cassette and allow the gel to sit on the bottom plate
4	Cut the stacking gel with the end of the top plate approximately 2 cm downstream of the wells. Repeat the procedure on the other side of the gel to remove the front.
5	Hold the gel cassette bottom plate over a container with suitable buffer, with the gel facing downwards. Gently push a tweezer between the gel and the cassette bottom plate until the gel removed from the bottom plate.

### 1.9.5 Coomassie staining

Step	Action
1	<b>Fixation:</b> Immediately after electrophoresis, immerse the gel in fixing solution for 30 minutes. This solution precipitates the gel proteins and allows the SDS to diffuse out of the gel
2	<b>Staining:</b> Discard the fixing solution. Stain the gel for 10 minutes in staining solution. Cover the staining dish
3	<b>Washing:</b> Rinse the gel once in distilled water
4	<b>Destaining:</b> Destain the gel by changing the destaining solutions several times

until the stained protein bands are clearly visible against the clear background

- 5 **Preserving:** Soak the destained gel in preserving solution for 30 minutes

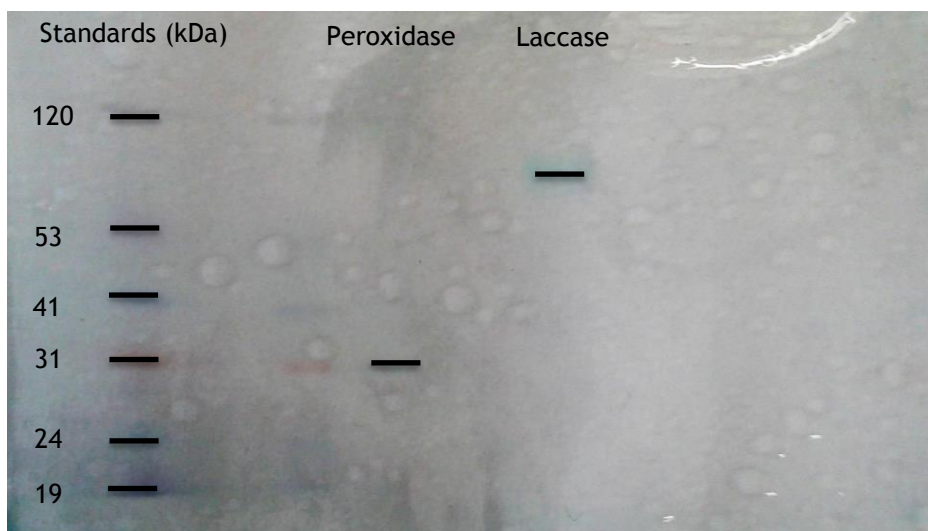


*Fig. A18 - SDS-Page image for peroxidase (~31 kDa) and for laccase (~80 kDa)*